Technical Report Documentation Page

1. Report No.	2. Government Accession No.	3. Recipients Catalog No.
FHWA/TX-91+360-2F		

4. Title and Subtitle	5. Report Date
APPROXIMATE ANALYSIS OF HORIZONTALLY CURVED GIRDER BRIDGES	November 1987
	6. Performing Organization Code

7. Author(s)	8. Performing Organization Report No.
Ann L. Fiechtl, Gregory L. Fenves, and Karl H. Frank	Research Report 360-2F

9. Performing Organization Name and Address	10. Work Unit No. (TRAIS)
Center for Transportation Research The University of Texas at Austin Austin, Texas 78712-1075	11. Contract or Grant No. Research Study 3-5-85-360
	13. Type of Report and Period Covered Final
12. Sponsoring Agency Name and Address Texas State Department of Highways and Public Transportation; Transportation Planning Division P. O. Box 5051 Austin, Texas 78763-5051	14. Sponsoring Agency Code

15. Supplementary Notes
Study conducted in cooperation with the U. S. Department of Transportation, Federal Highway Administration
Research Study Title: "Analysis of Curved Steel Girder Units"

16. Abstract

The design of multigirder bridge units with horizontal curvature is complicated by the torsional forces induced by the curvature. The proportioning of girders for preliminary design requires an approximate analysis that accounts for the curvature.

This report presents the development and an evaluation of an approximate analysis procedure for curved girder bridges. The V-load method is named because the effects of curvature are represented by self-equilibrating vertical loads acting on the girders. The V-load method, as implemented in the analysis procedure described in this report, is suitable for approximate analysis of preliminary bridge designs. The analysis procedure includes composite behavior, and allows variable radius of curvature and skew supports. Envelopes of bending moment and shear force due to moving track loads can be generated. The V-load method is evaluated by comparing the approximate response with the response from a more refined finite element analysis for a variety of bridge configurations.

17. Key Words	18. Distribution Statement
bridges, curved girder, approximate analysis, V-load method, analysis procedure, composite behavior, curvature, skew supports	No restrictions. This document is available to the public through the National Technical Information Service, Springfield, Virginia 22161.

19 Security Classif. (of this report)	20. Security Classif. (of this page)	21. No. of Pages	22. Price
Unclassified	Unclassified	96	

APPROXIMATE ANALYSIS OF HORIZONTALLY CURVED GIRDER BRIDGES

by

Ann L. Fiechtl, Gregory L. Fenves and Karl H. Frank

Research Report No. 360-2F

Research Project No. 3-5-85-360

"Analysis of Curved Steel Girder Units"

Conducted for

Texas

State Department of Highways and Public Transportation

In Cooperation with the
U.S. Department of Transportation
Federal Highway Administration

by

CENTER FOR TRANSPORTATION RESEARCH
BUREAU OF ENGINEERING RESEARCH
THE UNIVERSITY OF TEXAS AT AUSTIN

November 1987

The contents of this report reflect the views of the authors, who are responsible for the facts and the accuracy of the data presented herein. The contents do not necessarily reflect the official views or policies of the Federal Highway Administration. This report does not constitute a standard, specification, or regulation.

There was no invention or discovery conceived or first actually reduced to practice in the course of or under this contract, including any art, method, process, machine, manufacture, design or composition of matter, or any new and useful improvement thereof, or any variety of plant which is or may be patentable under the patent laws of the United States of America or any foreign country.

PREFACE

This report presents a detailed study of the V-load method for approximate analysis of horizontally curved bridge units. The V-load method is evaluated by comparison to a more refined finite element analysis method developed for curved bridge units. The finite element analysis is described in a companion report.

This work is part of Research Project 3-5-85-360, "Analysis of Curved Steel Girder Units." The studies presented in the report were conducted in the Department of Civil Engineering and Phil M. Ferguson Structural Engineering Laboratory in conjunction with the Center for Transportation Research, Bureau of Engineering Research at The University of Texas at Austin. The work was sponsored jointly with the Texas Department of Highways and Public Transportation and the Federal Highway Administration under an agreement between the University of Texas at Austin and the Texas Department of Highways and Public Transportation. Liaison with the Texas Department of Highways and Public Transportation was maintained through the contract representative, Mr. Richard Wilkison.

The project was directed by Drs. Karl H. Frank, C. Philip Johnson, and Gregory L. Fenves. The detailed work in the studies was carried out by Mr. Kristopher H. Hahn and Ms. Anne L. Fiechtl. The contribution of the staff of the Phil M. Ferguson Structural Engineering Laboratory in producing the reports, particularly Sharon Cunningham and Jean Gehrke, is gratefully acknowledged.

SUMMARY

The design of multigirder bridge units with horizontal curvature is complicated by the torsional forces induced by the curvature. The proportioning of girders for preliminary design requires an approximate analysis method that accounts for the curvature.

This report presents the development and an evaluation of an approximate analysis procedure for curved girder bridges. The V-load method is named because the effects of curvature are represented by self-equilibrating vertical loads acting on the girders. The V-load method, as implemented in the analysis procedure described in this report, is suitable for approximate analysis of preliminary bridge designs. The analysis procedure includes composite behavior, and allows variable radius of curvature and skew supports. Envelopes of bending moment and shear force due to moving track loads can be generated. The V-load method is evaluated by comparing the approximate response with the response from a more refined finite element analysis for a variety of bridge configurations.

IMPLEMENTATION

This report presents an approximate analysis procedure, the V-load method, suitable for preliminary design of curved steel girder bridge units. This report, in conjunction with the companion report on finite element analysis of curved bridges, provides a complete set of analysis procedures for the design and checking of curved steel girder bridges. The assumptions and limitations of the V-load method are documented in this report along with examples of typical applications. The examples and evaluation provide the bridge engineer using the V-load method the insight required to properly use this approximate method in design.

TABLE OF CONTENTS

TABLE OF CONTENTS (continued)

LIST OF FIGURES

LIST OF TABLES

CHAPTER 1

INTRODUCTION

1.1 Background and Objectives

The design of today's roadways has placed increasing demands on the engineer. The use of horizontally curved bridges has grown out of alignment requirements and constraints. The right of way available for the construction of a new roadway may be limited because of the expansion that many cities are experiencing. It may be impossible to build a straight bridge or overpass, so a curved bridge is necessary with the alignment adapted to suit the site. In addition, the spans can be continuous which allows shallower girders. The aesthetics of a curved, continuous bridge is also an advantage.

There are, however, disadvantages which the engineer should be aware of when designing curved bridges. The fabrication costs are generally higher, and the curved bridge segments are produced in smaller pieces which increases the erection and transportation costs. Analysis of curved bridges is different than for a straight bridge because of the twisting of the unit due to its curvature.

The objective of this study is to develop and implement an approximate method of analysis for horizontally curved bridge units. Bending and warping stresses and the envelope responses of bending moment, shear force, and reactions are computed. The effects of the design parameters on the response quantities are evaluated, and the accuracy of the approximate method is assessed by comparison of the response to those of a more exact analysis.

1.2 Review of Previous Work

One of the first presentations of an approximate analysis of horizontally curved girders was by the United States Steel Corporation in 1963 [11,13,14]. The United States Steel approximate method became known as the V-load method and was extended to analyze multigirder bridge units in 1965 [13]. A computer program implementing the V-load method was developed in 1966 for multigirder bridge units with radial supports [13]. About the same time, Dabrowski [12] developed expressions for the warping moment in a curved girder using differential equations.

Developments in curved girder analysis were also made by Gillespie and Ketchek. Gillespie [5] used an approximate analysis method where it was found that the lateral bending stress was dependent on the lateral bending moment which is related to the diaphragm spacing. Another method was developed by Ketchek [11] who, in addition to

allowing for the V-loads used in earlier reports, allowed for the direct application of uniformly distributed torsional moments to the girders.

In the 1970's, CURT, Consortium of University Research Teams [2,13], was established to develop methods of curved bridge design and analysis and determine bridge requirements. Also during this time, Weissman [18] was developing a method for analyzing curved girders using statically indeterminate analysis of plane grid systems with straight elements. The slope deflection technique was used by Heins and Siminou [9] to determine various distribution factors to relate a single straight girder to a single curved girder and then to a system of curved girders.

Culver, Brogan, and Bednar [3] utilized the flexibility method [12] to develop an approximate analysis using equivalent straight girders. They discovered that the maximum deflection of a curved girder is much larger than that of an equivalent straight girder. For small radii of curvature, a curved beam is more flexible than the equivalent straight girder, and the ratio of deflections between a curved and a straight girder increases as the radius of curvature decreases. They also found that the diaphragm spacing influenced the maximum warping stress but not the bending stress. The approximate method predicted the outer girder stress fairly well but underestimated the stress on the inner girder [3].

Heins and Spates [10] developed a computer program based on the solution of the governing differential equations with reasonable experimental correlation for the response of a single curved girder subjected to various loadings and boundary conditions.

In the 1980's the V-load method was revised to accommodate skewed bridges with the effort of US Steel Research and Richardson, Gordon, and Associates [13,15,16]. Grubb [6] found this approximate analysis method very accurate for the dead load condition. For live load he found that the V-load results were reasonable for the exterior girders but not for the interior girders. The accuracy was largely affected by the lateral distribution factors assumed in the V-load method.

Heins and Jin [8] in 1984 developed expressions for live load distribution factors for braced systems by the use of a three-dimensional space frame matrix formulation. Bottom bracing was added to their models to examine its effect on the load distribution. Bracing stiffens the system and the live load is distributed more uniformly to all the girders and the load to a given girder is decreased.

1.3 Organization of Report

This report is comprised of Chapters 1 through 6. The chapters explain the theory, use, and accuracy of the approximate V-load analysis method.

In Chapter 2 the fundamentals of the V-load analysis are described for both a two girder and multigirder bridge unit. The theory behind using equivalent straight girders to compute the bending and warping stresses is explained. Chapter 3 describes the analysis procedures used to compute the response of a bridge unit to a single load, response envelopes, and the warping stresses which develop in the flanges. Chapter 4 presents the V-load responses of a two girder and multigirder bridge units. The same bridge configurations are analyzed using the finite element method and the V- load and finite element responses are compared. The effect of the radius of curvature, diaphragm spacing, and support skew on the responses are examined. Chapter 5 presents the bending moment, shear force, and reaction envelopes due to a truck load moving along two bridge units. Lateral distribution factors for the live load are included in the response computations. Chapter 6 summarizes the approximate V-load analysis method and presents conclusions of this study.

CHAPTER 2

APPROXIMATE ANALYSIS OF HORIZONTALLY CURVED BRIDGES

2.1 Introduction

Horizontally curved bridges respond to loads differently than do straight bridges because of the torsional forces induced by the curvature of the longitudinal axis. An approximate method of analysis for horizontally curved bridges can be developed using equivalent straight girders if the torque produced by the curvature is represented by self-equilibrating loads on the girders. These additional loads are called V-loads because they are a set of vertical shears on the equivalent straight girders. The V-loads are developed from equilibrium requirements and are primarily a function of the radius of curvature, width of the bridge unit, and spacing of diaphragms between the girders.

This chapter presents the V-load method for approximate analysis of horizontally curved bridge units. The development closely follows References 5, 6, 13 and 15. The method will first be developed for a two girder bridge unit and then for a multigirder bridge unit.

2.2 Two Girder Bridge Unit

The approximate forces on two horizontally curved girders connected with radial diaphragms can be determined from equilibrium. Figure 2.1 shows a horizontally curved bridge unit with two girders spaced a distance D. The angle of curvature of the bridge is θ. The radius of the outside girder, girder 1, is R_1 and the arclength is L_1. The radius and arclength of girder 2 are R_2 and L_2, respectively. Radial diaphragms, spaced a distance d, connect girders 1 and 2.

Vertical loads on the bridge produce bending moments in both girders. Assuming the plate girder sections resist the bending moment entirely by longitudinal forces in the flanges, as shown in Fig. 2.2, the force in each flange of girder 1 is M_1/h_1, where h_1 is the depth of the girder and M_1 is the bending moment. In girder 2 the bending moment is M_2 and the flange forces are M_2/h_2. However, because the flanges of the girder are horizontally curved, the longitudinal forces due to bending are not in equilibrium. Figure 2.3 shows a section of the top flange of girder 1 centered about a diaphragm, where the longitudinal forces due to bending are not collinear. To maintain radial equilibrium of the flange, the chord of the diaphragm must develop a force.

Similar forces develop at the bottom cord of the diaphragm, for equilibrium of the bottom flange. Figure 2.4 shows a freebody diagram of a diaphragm between the girders. The force, H_1, which develops in the diaphragm is found by equilibrium along a radial line

at the diaphragm location. Referring to Fig. 2.3 the force H_1 from equilibrium is :

$$H_1 = \frac{M_1 \theta}{h_1} \qquad (2.1)$$

where θ in this context is the angle subtended by adjacent diaphragms. Substituting the geometrical relationship $\theta = d_1 / R_1$ where d_1 is the diaphragm spacing of girder 1, into Eq. 2.1 gives:

$$H_1 = \frac{M_1 d_1}{h_1 R_1} \qquad (2.2)$$

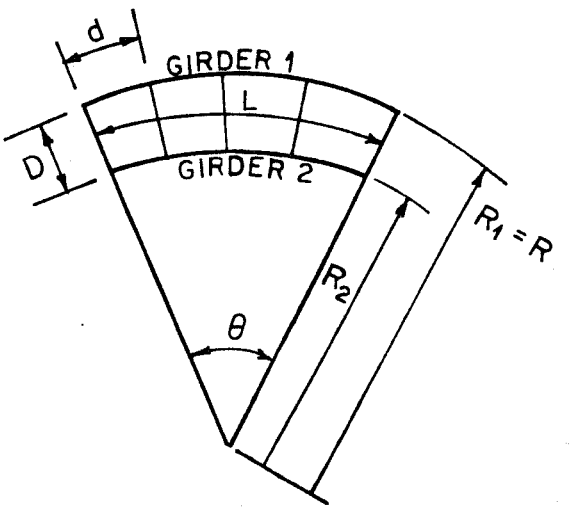

Figure 2.1 Two girder horizontally curved bridge unit.

The corresponding diaphragm force H_2 for girder 2 is computed using the same procedure as used for H_1. The direction of H_2 is opposite that of H_1 because girder 2 is on the inside of the bridge unit. Because of the forces on the chords of the diaphragm, a vertical shear is required for equilibrium of the diaphragm as shown in Fig. 2.4. For moment equilibrium of the diaphragm the vertical shear is:

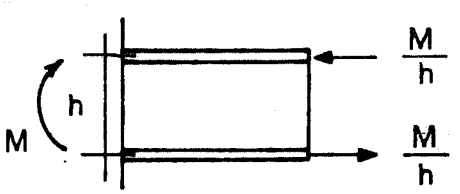

Figure 2.2 Longitudinal bending moment and flange forces in girder section.

$$V = (H_1 + H_2) \frac{h}{D} \qquad (2.3)$$

where the two girders are assumed to have the same depth h.

Substituting Eq. 2.2 for H_1 and a similar expression for H_2 into Eq. 2.3 gives:

$$V = \frac{M_1 \frac{d_1}{R_1} + M_2 \frac{d_2}{R_2}}{D}$$

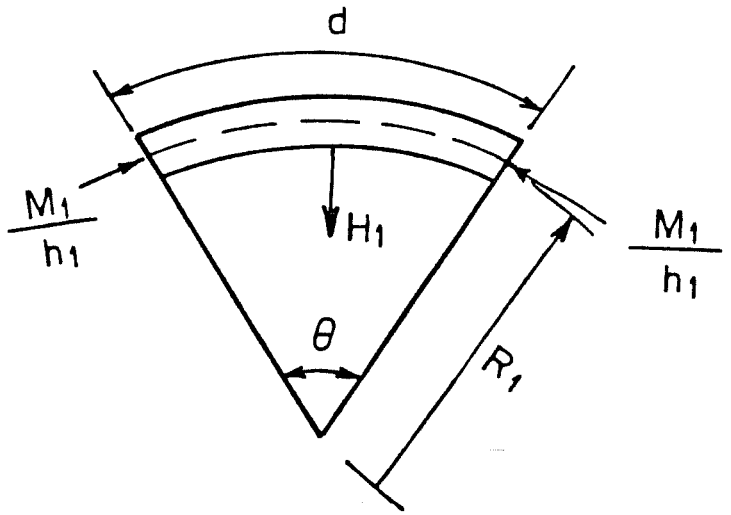

Figure 2.3 Section of top flange of girder subjected to bending moment.

But from geometry, $d_1 / R_1 = d_2 / R_2 = d / R$ so the shear force in the diaphragm is:

$$V = \frac{M_1 + M_2}{R\,D / d} \tag{2.4}$$

These shear forces in the diaphragm act in the opposite direction on girders 1 and 2 (Fig. 2.4). The shear forces, known as V-loads, are self-equilibrating forces on the bridge unit that approximate the effects of the horizontal curvature of the girders. They must be self-equilibrating forces because they are not actual loads applied to the bridge unit.

The bending moments M_1 and M_2 are the moments in girders 1 and 2 due to the applied loads and the additional forces due to curvature, as represented by the V-loads. The two contributions to the totals moment can be separated as :

$$M_1 = M_{1p} + M_{1v} \tag{2.5}$$
$$M_2 = M_{2p} + M_{2v} \tag{2.6}$$

The subscripts p and v denote responses due to the P-loads, which are applied loads, and V-loads respectively.

In common application of the V-load method (15), the bending moments produced by the concentrated V-load forces are assumed proportional to their respective girder lengths [15]:

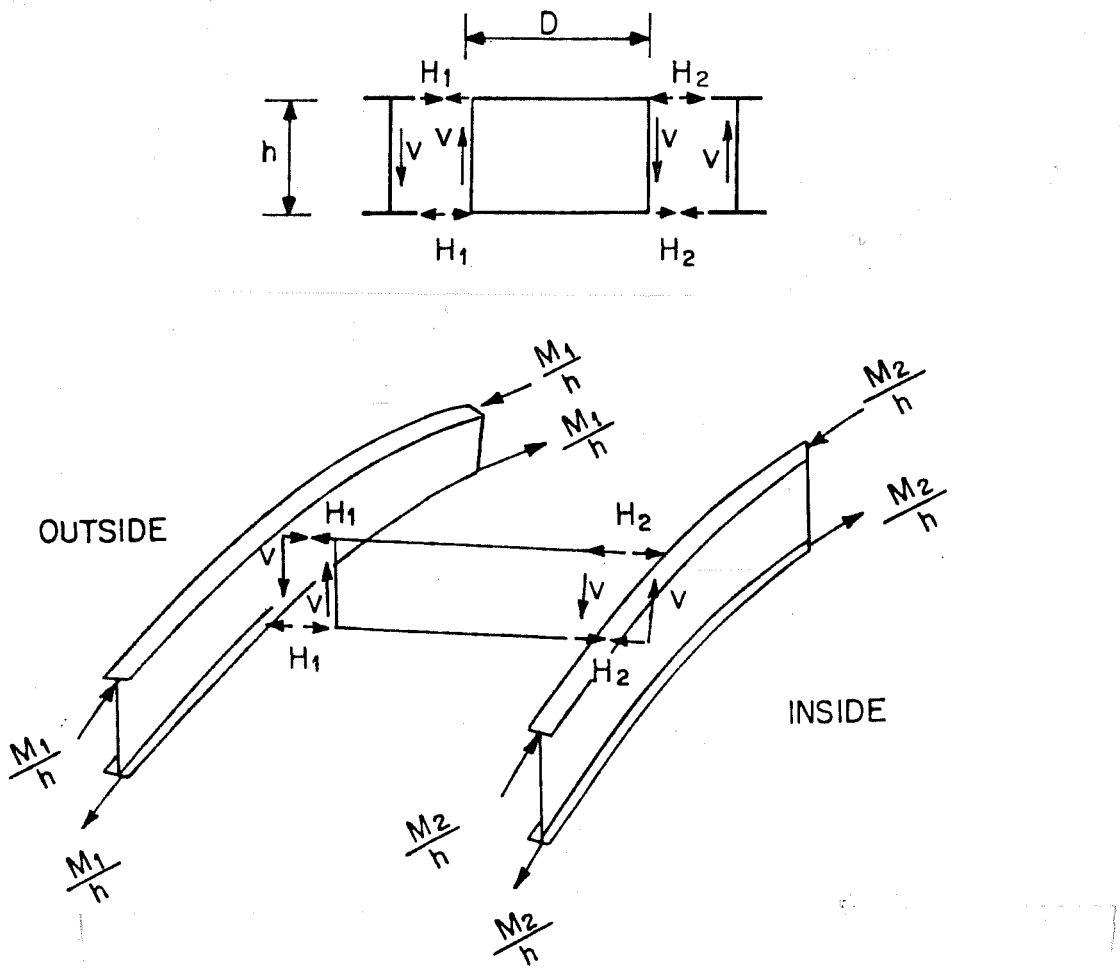

Figure 2.4 Cross section of bridge showing diaphragm and girders.

$$\frac{M_{2v}}{L_2} = \frac{-M_{1v}}{L_1}$$

where the change in sign indicates the V-loads act in opposite direction on the two girders.

Substituting this relationship into Eqs. 2.5 and 2.6 and summing M_1 and M_2 gives:

$$M_1 + M_2 = M_{1p} + M_{2p} * \left(1 - \frac{L_2}{L_1} \right) \tag{2.7}$$

In Eq. 2.7, the arclength ratio L_2/L_1 is generally close to 1 so $(1 - L_2/L_1)$ is small. Consequently, total bending moments may be approximated by P-loads only. With this

simplification, Eq. 2.4 gives the magnitude of the V-loads as a function of the P-load moments only:

$$V + \frac{M_{1p} + M_{2p}}{R\,D/d} \tag{2.8}$$

where the V-load forces act on the girders at the diaphragm location. The magnitude of the V-loads increase with decreasing radius of curvature, decreasing bridge unit width and increasing diaphragm spacing.

In summary, the V-load method involves analyzing the girders in the bridge unit as equivalent straight girders twice. The first analysis gives the response to P-loads, including M_{1p} and M_{2p}. The second analysis gives the response to the self-equilibrating V-loads applied at the diagram locations. The total response on the girders is the sum of the responses to the P-loads and V-loads.

2.3 Multiple Girder Bridges

In a curved bridge unit with two girders, the outer girder experiences an increase in load due to the curvature while the inner one experiences a decrease in load. The same phenomenon occurs in a unit with more than two girders, but the effect of curvature must also be distributed to the inner girders. A general expression for the V-loads acting on multiple girder units can be developed using a similar procedure as for the two girder bridge geometry.

Figure 2.5 shows a cross section of a bridge unit with N_g girders, where D is the distance between outer and inner girders. Due to the curvature of the unit the section is subjected to twisting. Lateral flange forces develop and produce forces in the diaphragms as described in Sec. 2.2. The V-loads are derived using equilibrium between the girders and the diaphragms. It can be shown that equilibrium of the diaphragm panels allows summation of the lateral flange forces, H_i, in terms of the shear forces in the diaphragm panels [14, 15]:

$$\sum_{i=1}^{N_g} H_i = \sum_{i=1}^{N} V_i' \left(\frac{D}{Nh}\right) \tag{2.9}$$

where V_i' is the shear in diaphragm i, H_i is the lateral flange force in girder i, h is the depth of the girders, and N is the number of diaphragm panels in the cross section, $N = N_g - 1$. As developed in Sec. 2.2, the flange force, H_i is related to the bending moment in girder i, M_i by :

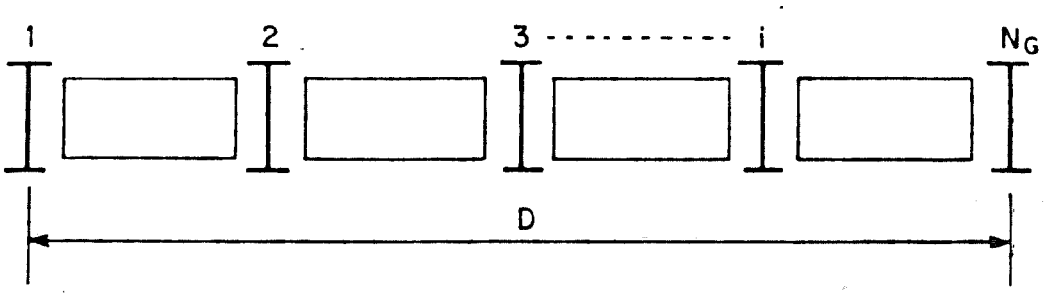

Figure 2.5 Cross section of a multi-girder bridge unit.

$$H_i = \frac{M_i\, d}{hR} \tag{2.10}$$

where d and R are the diaphragm spacing and radius of curvature, respectively, at any girder in the unit.

Substitution of Eq. 2.10 into Eq. 2.9 gives:

$$\sum_{i=1}^{N_g} M_i \frac{dN}{RD} = \sum_{i=1}^{N} v_i' \tag{2.11}$$

Considering a freebody diagram of the unit, the shear in panel j, V_j' is equal to the sum of the shear forces on girders 1 to j:

$$V_j' = \sum_{i=1}^{j} V_i \tag{2.12}$$

where V_i is the vertical force acting on girder i. Assuming a linear distribution of shear forces on the girders, the shear in girder i can be expressed as:

$$V_i = V\left[1 - \frac{2(i-1)}{N}\right] \tag{2.13}$$

where V is the shear force on the outer girder. Combining Eq. 2.12 and 2.13 gives:

$$V_j' = \sum_{i=1}^{j} V\left[1 - \frac{2(i-1)}{N}\right] \tag{2.14}$$

Substitution of Eq. 2.14 into Eq. 2.11 gives:

$$C'V = \sum_{i=1}^{N_g} M_i \left(\frac{dN}{RD}\right) \tag{2.15}$$

where

$$C' = \sum_{j=1}^{N} \sum_{i=1}^{j} \left[1 - \frac{2(i-1)}{N}\right] \tag{2.16}$$

or

$$V = \frac{\sum_{i=1}^{N_g} M_i}{c'\,(RD/dN)} \tag{2.17}$$

The difference between this expression for the multi-girder unit and the one for the two girder unit, Eq. 2.4, is the coefficient C' and N. Evaluation of the double summations in Eq. 2.16 gives:

$$C' = \tfrac{1}{2}(N+1)^2 - \tfrac{1}{6}(N+1)(2N+1) \tag{2.18}$$

Defining $C = C'/N$, Eq. 2.17 can be written as:

$$V = \frac{\sum_{i=1}^{N_g} M_i}{C\,(RD/d)} \tag{2.19}$$

Substituting $N = N_g - 1$ into Eq. 2.18 gives an expression for C in terms of the number of girders in the bridge unit :

$$C = \frac{1}{6}\frac{N_g\,(N_g + 1)}{N_g} - 1 \qquad (2.20)$$

A check of this expression for a two girder unit gives a value of C equal to 1.0. This is the same coefficient as found in the derivation of the two girder unit. Table 2.1 lists the value of C as a function of the number of girders, N_g. It is interesting to note that the previous work on the V-load did not present an expression for the constant C in Eq. 2.20.

The summation of girder moments in Eq. 2.19 can be approximately represented by the summation of primary girder moments as done for two girder units. Consequently, the V-load acting on the outer girder at the diaphragm locations is:

$$V = \frac{\sum_{i=1}^{N_g} M_{pi}}{C\,(RD/d)} \qquad (2.21)$$

The V-loads acting an the diaphragm locations of the other girders are given by Eq. 2.14, based on the assumption of linearly varying diaphragm shear.

Table 2.1 V-Load Coefficients

Number of Girders, N_g	C
2	1.0000
3	1.0000
4	1.1111
5	1.2500
6	1.4000
7	1.5556
8	1.7143

In summary, the first of two analyses for each equivalent straight girder gives the P-load moment, shear, and reaction responses, M_p, V_p and R_p, respectively. The second analysis gives the responses due to the V-loads. The expression for the V-load factor is dependent on the number of girders as derived above. The V-loads are assumed to be distributed linearly between the outer and inner girders and therefore the V-load on a girder is proportional to its distance from the bridge centerline.

2.4 Torsional Response of Girders

Because of the horizontal curvature of the bridge unit the girders must resist torsional forces. The two types of torsional stresses which can exist in wide flange sections are St. Venant's torsion and warping torsion. Assuming no bracing in the plate of the bottom flange, the St. Venant stiffness for wide flange girders is less than its warping stiffness. For this reason, St. Venant's stresses are generally much less than the warping stresses, so St. Venant's torsion is neglected in an approximate analysis of curved girder units without

bracing in the plane of the bottom flanges. All of the torsion is assumed to be resisted by warping of the girders. The approximate torsional response analysis follows Refs. 6 and 15.

The section of a girder twisted through an angle q, by a torque, T, is shown in Fig. 2.6. The torque creates flange shear forces, T/h, in the direction of the torque, where h is the depth of the plate girder section. These flange shears cause lateral bending moments, M_f, in the flange.

The effects of warping torsion can be approximated by applying lateral forces to a straight model of the bottom flange. Due to the horizontal curvature, radial forces develop on the flanges to establish equilibrium. The lateral load on the flange, F_r, varies along its length and in proportion to the bending moment as required for radial equilibrium:

$$F_r = \frac{M}{hR} \tag{2.22}$$

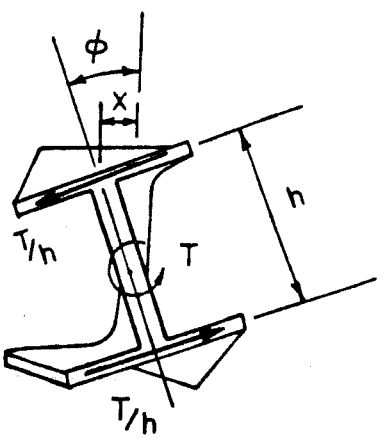

Figure 2.6 Girder section twisted by a torque.

where M is the total bending moment on the girder, h is the distance between flanges, and R is the radius of the girder. The distribution of these lateral flange loads is shown in Fig. 2.7. The diaphragms restrain lateral bending of the girders, acting as lateral supports for the flanges. In the approximation, the diaphragms are assumed to provide rigid supports against lateral bending.

The lateral bending moments in the flange resulting from this loading are the flange warping moments, M_f. The flange moments vary along the length of the flange. The normal warping stress at the flange tip is then given by:

$$\sigma_w = \frac{M_f}{S_f} \tag{2.23}$$

where S_f is the section modulus of the bottom flange for lateral bending. The longitudinal bending stress and warping stress distributions on a girder cross section are shown in Fig. 2.8. The summation of the stress due to bending, σ_b, and that due to warping, σ_w, gives the total stress at the tip of the flange, σ_t.

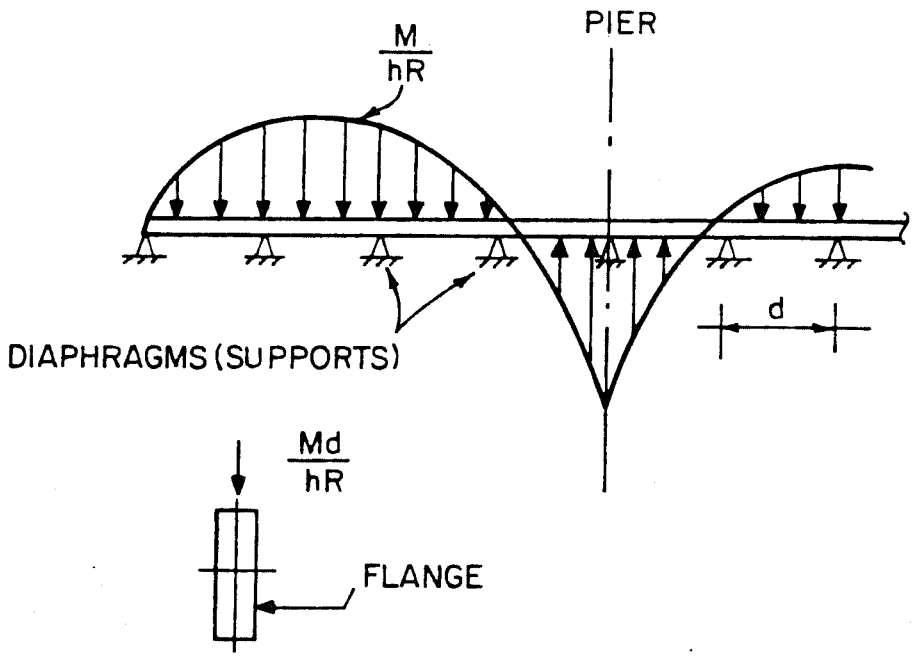

Figure 2.7 Distribution of lateral loads on flange.

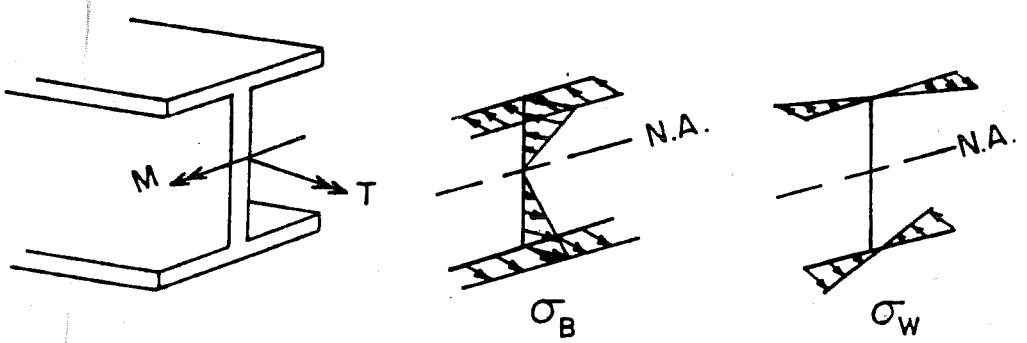

Figure 2.8 Bending and warping stress in girder cross section.

CHAPTER 3

ANALYSIS PROCEDURE

3.1 Introduction

There are two separate problems relevant to the analysis of curved bridge units. The first involves computing the moments, shears, longitudinal and warping stresses, and reactions that develop due to dead load and specified positions of live loads. A direct analysis of the structure with the prescribed loads can be performed to compute the responses. The second problem involves computing the envelope values of maximum and minimum moments and shears that can occur on the bridge due to moving live loads. Because of the complicated geometry of curved girder units, it is not possible a priori to determine the load positions producing maximum response, so a series of analyses is required, one for each live load position.

The approximate analysis procedure, based on the V-load method, presented in this chapter computes the response of multi- girder bridge units with variable radius of curvature and skew supports. The girders may be nonprismatic and include composite behavior of the steel girders and concrete slab. The loads acting on the bridge include the dead load, lane load and moving truck loads. Dead loads act on the bare girders, while the superimposed dead load and truck loads act on the composite girder.

The analysis procedure for horizontally curved bridges is based on the V-load method described in Chapter 2. Two analyses of the equivalent straight girders are performed for each load case. The applied loads on the girder are called P-loads, and analysis of the girders subjected to these loads results in P-load responses such as M_p, V_p, R_p, the bending moments, shears, and reactions, respectively. Because of the horizontal curvature of the unit, V-loads act on the girders. The girders are analyzed a second time with the V-loads applied at the diaphragm locations. The response due to these V-loads result in V-Load responses M_v, V_v, R_v, the bending moments, shears, and reactions, respectively. The response of the girders in the curved unit is the sum of the P-load and V-load responses.

The direct stiffness method is used to calculate the response of a girder to individual load cases. Each equivalent straight girder in the unit is modeled by an arbitrary number of prismatic beam elements (constant properties for each element) connected at nodes. The individual elements can have different section properties to represent the nonprismatic girders, including zones of composite and noncomposite behavior. The structural stiffness matrix is assembled from the element stiffness matrices. For a single load case, this structural stiffness matrix is factored and back-substituted with the load vector to determine displacements at the nodal points. Using these displacements the moments, shears, reactions, and stresses are computed in the beam elements.

The matrix stiffness method can be used efficiently in generating envelopes of minimum and maximum responses due to moving live loads. The structural stiffness matrix is independent of the loads; it can be assembled and factored once and used to obtain responses for the different load positions. To facilitate analysis of a unit for a large number of load positions, influence functions are introduced and used in the envelope procedure as described in Sec. 3.3.

An important requirement of the analysis is to compute the response values along the entire length of the girders, not just at the nodes. The more locations at which the response is computed, the better the resolution of the maximum and minimum response. The locations along the girders at which responses are computed are called grid points. The analysis procedure automatically generates grid points along each girder using the geometrical properties of the bridge unit and a desired level of response resolution. In computing the envelope values these grid points are used to locate the moving load. Each concentrated live load (e.g. due to a truck wheel) is placed at each grid point to assure that the maximum moment is found at all the grid points.

3.2 Analysis Procedure for Single Load Case

3.2.1 Model of Bridge Unit. The geometrical layout of the bridge unit is described by a reference line from which the locations of the girders are related. The reference line is represented by segments of constant curvature, possibly with tangent sections. The radii of the reference line segments are computed from its arclength and the corresponding angle of curvature. Each girder in the unit is located a constant radial distance from the reference line along the entire length of the bridge unit. Radial diaphragms between the girders are located arbitrarily along the reference line of the unit. Supports, which may be radial or skew, are located with respect to the reference line.

The analysis procedure allows nonprismatic girders. Each girder in the bridge is modeled independently by beam elements connected by nodes. A beam element is created wherever there is a change in section properties of the girder. Additional nodes are required at each support even if the section properties of the girder do not change across the support.

The grid points are the locations at which the response quantities are calculated and are used to position the moving load. The support locations (including skew) and diaphragm locations are used to generate the grid points along the girders. It is possible to specify additional grid points to increase the resolution of the responses.

3.2.2 Analysis of Girders for Single Load Case. The curved girders are separated, straightened and modeled by prismatic beam elements. The response of the girders is computed using the direct stiffness method by solution of the equilibrium equations:

$$K * U = P$$

for each girder, where K is the structural stiffness matrix assembled from beam element stiffness matrices, P is the load vector for the load case, and U is the vector of resulting displacements of the nodes. Displacements are computed for each degree of freedom of the girder. Each node has two degrees of freedom, a vertical translation and rotation. Vertical degrees of freedom at the support locations are deleted.

Because of the modeling of the girders by beam elements the stiffness matrix is banded, with a semi-bandwidth of four. A banded storage and equation solution procedure is used to minimize memory requirements and computation time in the equation solution procedure.

The nodal displacements of the girders are used to compute the internal forces at the ends of each element. The internal forces at all the grid points of the girders are computed accounting for concentrated or distributed loads on the elements. The reactions at the supports are computed from the shears on each side of a support.

3.2.3 Analysis of Bridge Unit For Single Load Case. The analysis of a bridge unit uses the procedure described in Sec. 3.2.2 for the response of each girder in the unit. The first load case is that of the P-loads which are applied to the unit; the resulting responses are denoted P-load responses. The moments, M_p, in the girders are summed at each diaphragm location and the V-loads are given by Eq. 2.21. These V-loads are applied to each girder at the diaphragm locations as a second load case. The response analysis described in Sec. 3.2.2 is again performed for each girder using the V-loads, and the responses computed are denoted as V-load responses. The total response of the bridge unit is then the sum of the P-load and V-load responses for each girder:

$$M_t = M_p + M_v$$
$$V_t = V_P + V_v$$
$$R_t = R_P + R_v$$

The analysis of a bridge unit for a single load case can be summarized as :

1. Determine P-loads

2. Perform single load case analysis of girders with P-loads for P-load responses

3. Compute V-loads

   3.1 Sum moments at the diaphragms

3.2 Compute V-loads at each diaphragm

4. Perform single load case analysis of girders with V-loads for V-load responses

5. Add the P-load and V-load responses for the total responses of the girders

3.3 Computation of Response Envelopes

The determination of the maximum and minimum response due to moving wheel loads requires analyses of the unit for numerous positions of the loads. Because each load case requires two analyses, P-load and V-load, for every girder, the number of solutions is very large. To improve the efficiency of the analysis for moving loads, influence functions for the girders are used to compute envelopes. Influence functions are responses in the beam elements due to a unit load at each degree of freedom in a girder. The influence functions are computed by placing a unit load on each degree of freedom and solving for the moments and shears in each beam element, and reactions at the supports.

To use the influence functions for the computation of response envelopes, the position of the truck loads on the unit is first determined. Once the load vector P is calculated for each wheel load position, it is multiplied directly by the influence functions to obtain the moments, shears, and the reactions for each girder due to the P-loads. The V-load responses are computed by multiplying the V-loads by the same influence functions for the girders. The responses are then computed at all grid points of the girders and the minimum and maximum values are saved. The truck loads are placed so that each concentrated load is placed on each grid point to produce maximum moment at that grid point. A slightly larger moment may be produced with the center cycle between grid points.

The procedure to compute the response envelopes can be summarized as:

1. Determine the influence functions
   - 1.1 Assemble the banded structural stiffness matrix from the element stiffness matrices
   - 1.2 Factor the stiffness matrix
   - 1.3 For each of two degrees of freedom per node :
     - 1.3.1 Apply a unit force at the node
     - 1.3.2 Back substitute for displacements
     - 1.3.3 Calculate member end forces
     - 1.3.4 Form influence functions for moment, shears, and reactions

2. Determine the position of the moving load along the reference line so that each load acts at each grid point

3. Multiply the load vector by the influence functions to obtain the moments, shears, and reactions due to the P-loads for each girder

4. Compute the V-loads

5. Multiply the V-loads by the influence functions to obtain V-load moments, shears, and reactions for each girder

6. Sum P-load and V-load response for the total response

7. Determine minimum/maximum response quantities at grid points

8. Repeat steps 2 through 7 until moving load is no longer on the bridge unit

3.4 Computation of Flange Warping Stresses

As described in Chapter 2, the flanges of the girders are subjected to warping due to the torsion induced by the horizontal curvature of the bridge unit. In composite girders the concrete slab acts together with the top flange to resist the warping moment. The section modulus for lateral bending of the top flange and slab is much larger than for the bottom flange resulting in smaller warping stresses. Generally only the warping of the bottom flange is important in composite systems.

In the approximate analysis procedure, the bottom flanges of the girders are straightened and modeled as individual flange elements supported at each diaphragm location. The curvature of the flanges is the same as that of the girders. Support locations, coordinates, and grid points are generated for the flanges as described in Sec. 3.2.1.

Using the model of the bottom flanges an analysis of the lateral bending can be performed after the loads are specified. As described in Chapter 2, the lateral bending of the flanges is caused by the radial flange forces which develop due to the horizontal curvature. The forces which act on the flange are computed using Eq. 2.22 in Chapter 2 and vary along the bridge in proportion to the total bending moment in the girders. To compute lateral bending stresses in the flange, the lateral force on the flange is applied to the flange model using equivalent concentrated loads at the grid points of the original girder. The lateral force at a grid point is considered to be an average of lateral loads between adjacent grid points. These forces are used to compute the bottom flange warping moments, M_f, by the same single load case analysis procedure used for the girders. Because the moment used to determine the lateral forces on the flanges is the sum of M_v and M_p, a separate V-load analysis of the flange is not required.

The flange warping moments act about the strong axis of the flange. The stress at the tip of the flange is given by $\sigma_w = M_f / S_f$ where S_f is the section modulus of the

flange. The sign of the stress as in tension or compression depends on the sign of the moment and which tip of the flange is under consideration. Figure 2.8 shows the distribution of warping stresses and bending stresses on a girder. The maximum total stress in the flange is then the combination of the warping stress and the longitudinal bending stress that gives the largest value.

CHAPTER 4

RESPONSE OF CURVED GIRDER BRIDGE UNITS

4.1 Introduction

This chapter presents the response of several idealized bridge units and compares the results of the approximate V-load analysis with the results from a finite element analysis procedure developed for horizontally curved bridges [7]. To evaluate the accuracy of the V-load analysis and the important parameters on the response of bridge units, several bridge schemes are analyzed. A single span two girder curved bridge unit is analyzed in the first set of comparisons. In the second set of comparisons, a three span, four girder bridge unit is analyzed. In the study of this second set, the radii of curvature, diaphragm spacing, and the support orientation are varied.

In the finite element analysis the bridge unit is divided into three-dimensional substructures modeled by one- and two-dimensional finite elements. Reference 7 gives details of the finite element model and analysis techniques used for curved bridge units. Diaphragms are modeled as beam elements connected to the top and bottom flanges of the girders. The concrete slab is modeled as two dimensional plate elements connected to the girders by rigid beam elements. The properties of the plate elements may be different in the transverse and longitudinal directions. When the concrete is considered ineffective, as in the negative moment regions, the slab can still transmit forces transversely to the girders. In this case, the elastic modulus in the longitudinal direction is small, but the modulus in the transverse direction is unaffected by the negative moments. In the finite element method the loads are represented by equivalent concentrated forces placed at the nodes of the mesh.

For the purpose of evaluating the approximate V-load analysis, the bridge models used in the V-load and finite element analyses were matched as close as possible. The curvature and span lengths of each bridge model are identical, as are the locations of the radial diaphragms. The girder section properties were modified in the V-load analysis to correspond to the model used in the finite element analysis. The dead load used in the V-load analysis was computed from the tributary slab weight and the girder weight.

A major difference in the two models is the representation of composite behavior of the bridge unit. In the finite element analysis the torsional stiffness of the slab is represented by the plate elements. The torsional stiffness of the slab is not accounted for in the V-load analysis, although composite behavior in the longitudinal direction is recognized. The difference in modeling the torsional behavior of the curved bridge unit will be apparent in the comparisons of the V-load and finite element response results.

4.2 Two Girder, Simple Span Bridge Unit

To evaluate the accuracy of the V-load method, a two girder bridge unit with simple spans is analyzed. Comparisons of the longitudinal bending stresses, warping, and total stresses are made for dead load, live load, and combined dead and live load for four variations of important parameters.

A plan view of the bridge is shown in Fig. 4.1a, cross section A-A of the bridge unit is shown in Fig. 4.1b. The table in Fig. 4.1 lists the parameters R, θ, and d defining Schemes A, B, C, and D that are studied in this section. The reference line along the centerline of the unit has an arclength of 100 feet. The diaphragms and end supports are radial and the girders are spaced 6 feet apart. The concrete deck slab is 7-1/2 inches thick and the modular ratio of the concrete to steel is eight. The noncomposite and composite moments of inertia for each girder are 12,626 in^4 and 35,874 in^4, respectively.

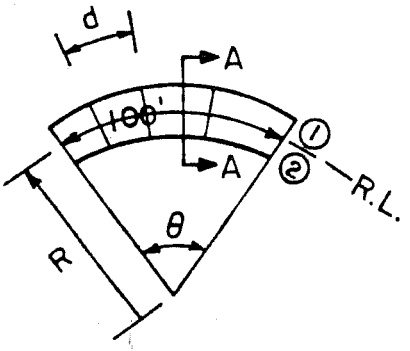

SCHEME	RADIUS R	ANGLE θ (°)	D.SPNG d
A	1000'	5.73	20'
B	1000'	5.73	10'
C	500'	11.46	20'
D	500'	11.46	10'

(a)

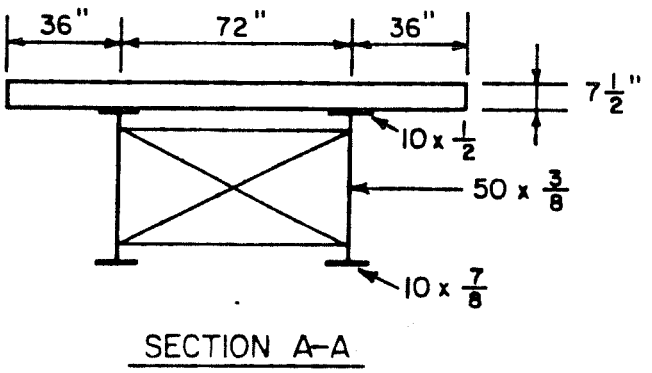

(b)

Figure 4.1 Two girder, single-span bridge unit showing (a) plan view and (b) cross section.

The girders were designed for noncomposite action under dead loads and composite action under live load. The dead load for each girder consists of the weight of the steel, 0.111 k/ft, and the concrete deck slab, 0.563 k/ft. The live load is a standard AASHTO HS20-44 truck [1], placed as shown in Fig. 4.2, with the spacing between the axles set at 14 feet. The wheels of the truck are placed directly on each girder so no transverse distribution factors are used. This is done to facilitate direct comparison of the V-load and finite element response results.

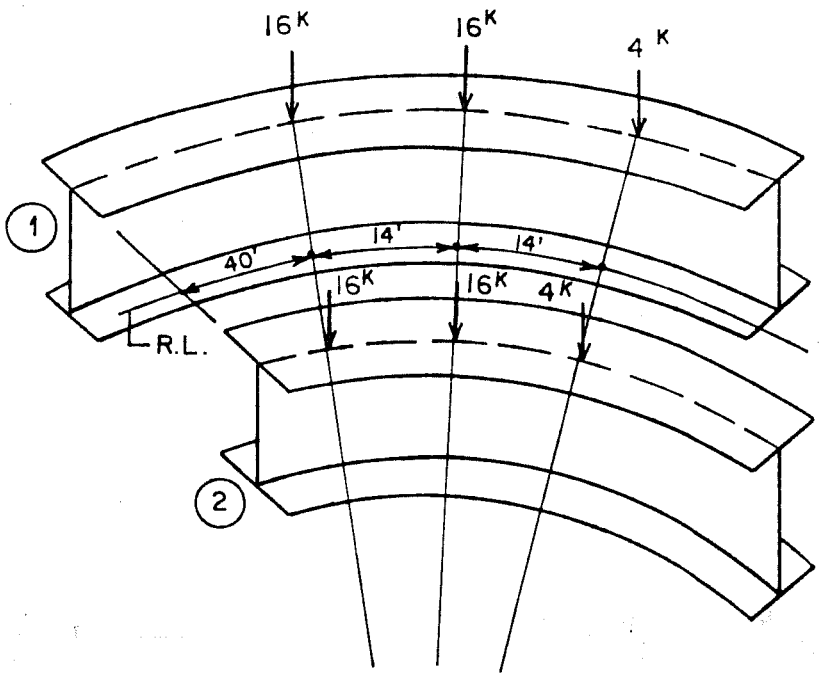

Figure 4.2 Location of wheel loads on two girder, simple-span bridge unit.

The placement of the truck shown in Fig. 4.2 produces maximum moments and bending stresses in the girders. This location was found using the V-load envelope procedure described in Chapter 3. The location of wheel loads to produce maximum moments for the four schemes is approximately the same, so the location of wheel loads shown in Fig. 4.2 is used for each scheme.

4.2.1 Response Comparisons. The response obtained from the V-load and finite element analyses are compared for dead load, live load, and combined dead and live load cases. The values listed are the stresses at midway through the bottom flange thickness at locations of approximately maximum bending stress, near midspan, unless otherwise noted. The percentage difference between the V-load and finite element results is calculated by:

$$\%D = \left(\frac{V\text{-}Load - FEM}{FEM} \right) * 100$$

4.2.1.1 Dead Load. The dead load stresses are computed by applying the dead load to the noncomposite steel girders. Comparison of the maximum longitudinal bending stresses for the four schemes is shown in Table 4.1a. The maximum stress in girder 1 is much larger than the stress in girder 2. The V-load maximum stress for girder 1 is within 4.1% of the finite element stress. All V-load stresses for girder 1 are conservative. For girder 2 the V-load stresses are less than the finite element values by as much as 10.6%. The largest percent difference in stresses for both girders occurs in Scheme D which has the sharpest curvature. It is important to note that the magnitude of bending stress is not sensitive to the diaphragm spacing. Figure 4.3 shows the longitudinal bending stress on the girders due to dead load for Schemes B and D (10 ft diaphragm spacing). The results clearly demonstrate the shifting of load from inner to outer girder which occurs in a horizontally curved bridge unit. Both the magnitude of the load shift and the difference between the V-load and finite element results increases with a decreasing radius of curvature.

Figure 4.4 shows the warping stresses due to dead load for the units with 500 ft radius (Schemes C and D). Peak warping stresses occur at the diaphragm locations and decrease with decreasing diaphragm spacing. The V-load warping stresses are greater than the corresponding finite element warping stresses at the diaphragm locations and less than the finite element values at points between diaphragms. In the V-load method, large warping stress exists at the diaphragm locations because the diaphragms are assumed to be infinitely stiff and provide rigid supports for the flange. This assumption is not made in the finite element method, so the flanges can deflect laterally at the diaphragm locations.

As described in Chapter 2, the warping stress combined with the longitudinal bending stress gives the total stress at the tip of the bottom flange. Comparison of the warping plus bending stresses due to dead load is made in Table 4.2a. The stresses are compared near the point of maximum bending stress. This is done because of the difference in modeling the flanges for the warping stresses in the two analysis methods.

The V-load method underestimates the warping plus bending stresses due to dead load between 8.4% and 49.5% when compared to the finite element values. The V-load stresses of girder 1 are closer to the finite element results than the stresses of girder 2. The percent differences are larger than those computed for the longitudinal bending stresses in Table 4.1a.

Figure 4.5 shows the dead load longitudinal bending plus warping stress curves for the 500 ft radius units (Schemes C and D). Peak stresses again occur for the V-load values at diaphragm locations and the stresses for the 20 ft diaphragm spacing are greater than

Table 4.1 Maximum Longitudinal Bending Stress in Bottom Flange (ksi)

Scheme	Radius	D. Spacing	Girder 1			Girder 2		
			V-Load	FEM	% D	V-Load	FEM	% D
a. Dead Load								
A	1000 ′	20 ′	24.21	23.87	1.4	11.74	11.95	-1.8
B	1000 ′	10 ′	24.37	23.61	3.2	11.58	11.78	-1.7
C	500 ′	20 ′	30.51	29.92	2.0	5.56	6.02	-7.6
D	500 ′	10 ′	30.82	29.62	4.1	5.25	5.87	-10.6
b. Live Load								
A	1000 ′	20 ′	14.63	12.38	18.2	7.60	9.70	-21.6
B	1000 ′	10 ′	14.70	12.34	19.1	7.53	9.57	-21.3
C	500 ′	20 ′	18.17	13.72	32.4	4.11	8.41	-51.1
D	500 ′	10 ′	18.32	13.76	33.1	3.97	8.21	-51.6
c. Dead Plus Live Load								
A	1000 ′	20 ′	38.84	36.25	7.1	19.34	21.65	-10.7
B	1000 ′	10 ′	39.07	35.95	8.7	19.11	21.34	-10.4
C	500 ′	20 ′	48.68	43.64	11.5	9.67	14.43	-33.0
D	500 ′	10 ′	49.14	43.88	12.0	9.22	14.10	-34.6

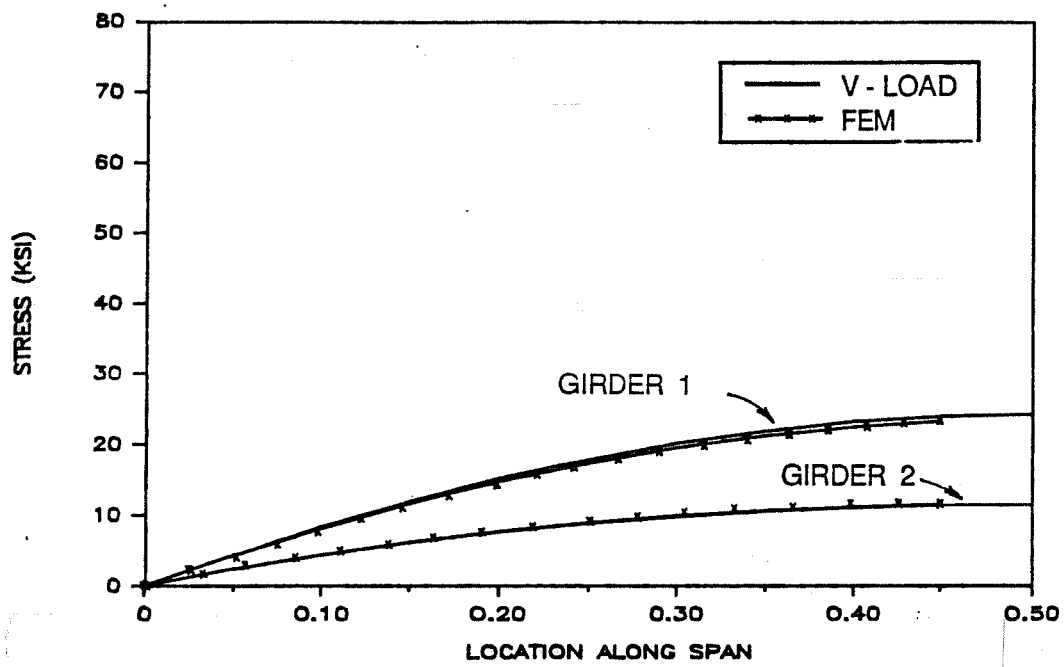

(a)

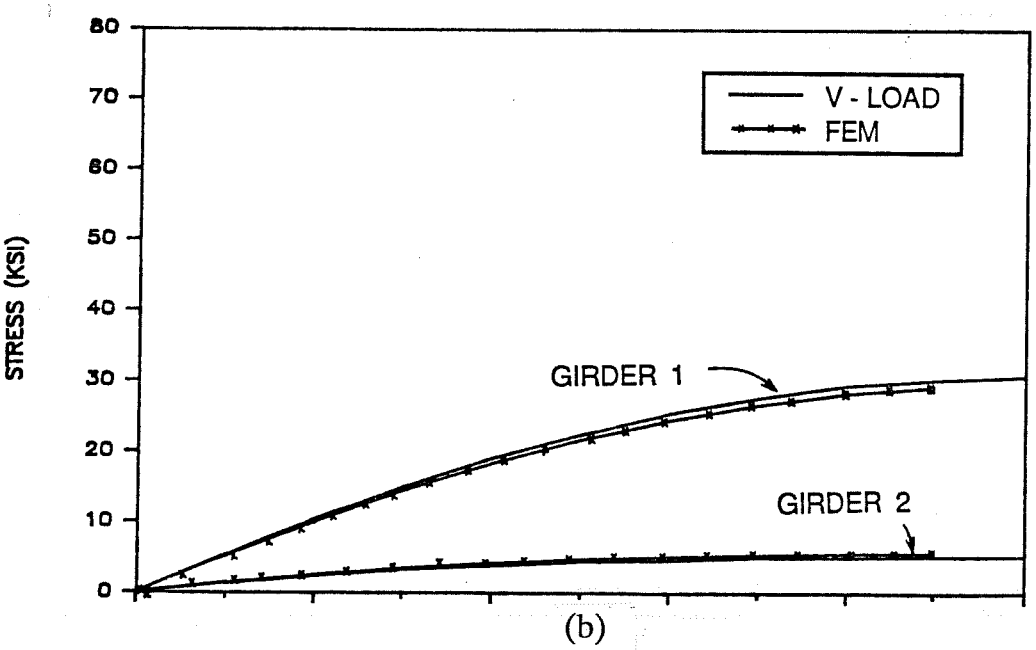

(b)

Figure 4.3 Longitudinal bending stress in bottom flange-dead load: (a) Scheme B; (b) Scheme D.

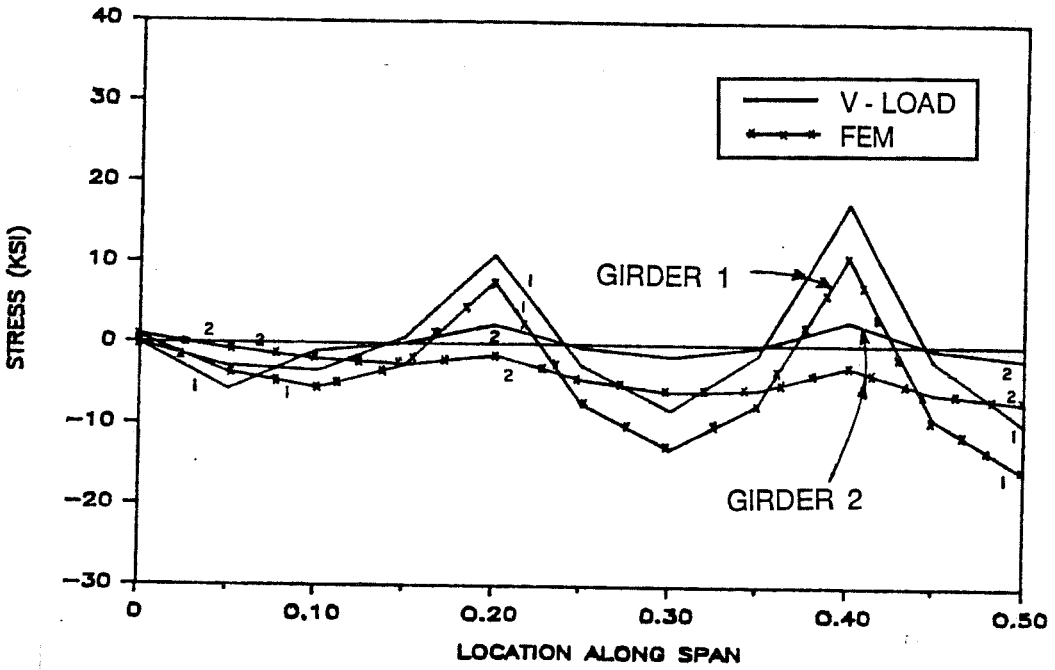

(a)

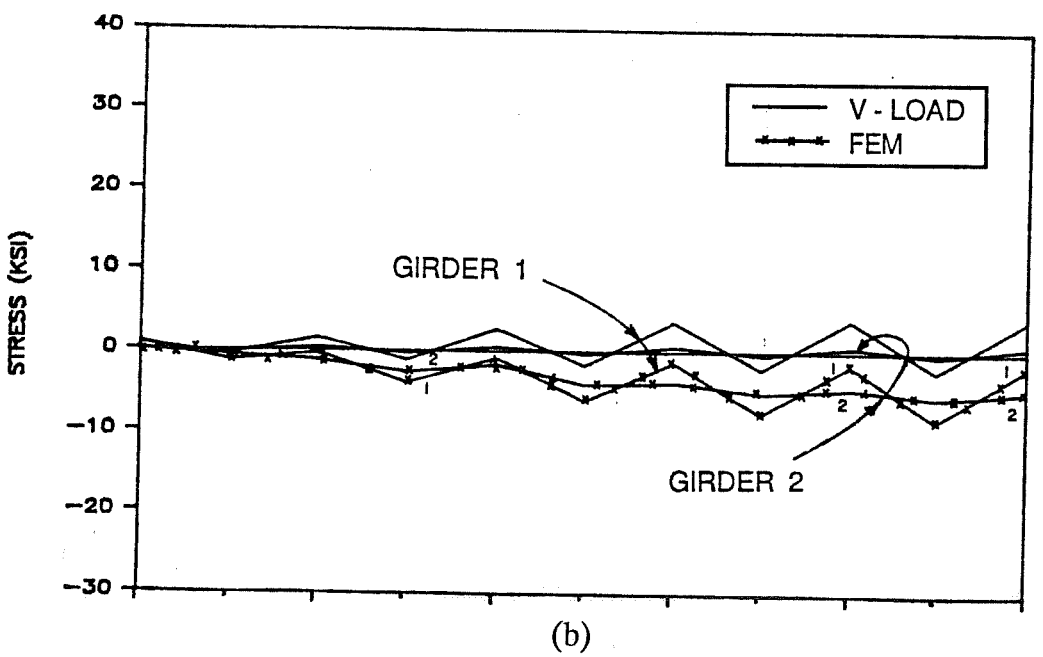

(b)

Figure 4.4 Warping stress in bottom flange - dead load: (a) Scheme C; (b) Scheme D.

Table 4.2 Bending and Warping Stress in Bottom Flange (ksi)

Scheme	Radius	D. Spacing	Location*	Girder 1			Girder 2		
				V-Load	FEM	% D	V-Load	FEM	% D
a. Dead Load									
A	1000 ′	20 ′	.5 L	28.06	30.82	-8.9	13.58	16.36	-17.0
B	1000 ′	10 ′	.45 L	24.96	27.26	-8.4	12.00	14.77	-18.7
C	500 ′	20 ′	.5 L	40.35	45.33	-11.0	7.27	13.09	-44.5
D	500 ′	10 ′	.45 L	32.71	32.71	-13.26	5.78	11.45	-49.5
b. Live Load									
A	1000 ′	20 ′	.5 L	18.17	15.69	15.8	9.48	12.36	-23.3
B	1000 ′	10 ′	.45 L	15.25	13.48	13.1	7.84	10.54	-25.6
C	500 ′	20 ′	.5 L	26.97	20.77	29.8	6.26	13.01	-51.9
D	500 ′	10 ′	.45 L	20.01	16.33	22.5	4.43	10.06	-56.0
c. Dead Plus Live Load									
A	1000 ′	20 ′	.5 L	46.23	46.51	-.6	23.06	28.72	-19.7
B	1000 ′	10 ′	.45 L	40.21	40.74	-1.3	19.83	25.31	-21.7
C	500 ′	20 ′	.5 L	67.32	66.10	1.8	13.53	26.10	-48.2
D	500 ′	10 ′	.45 L	52.72	54.04	-2.4	10.21	21.51	-52.5

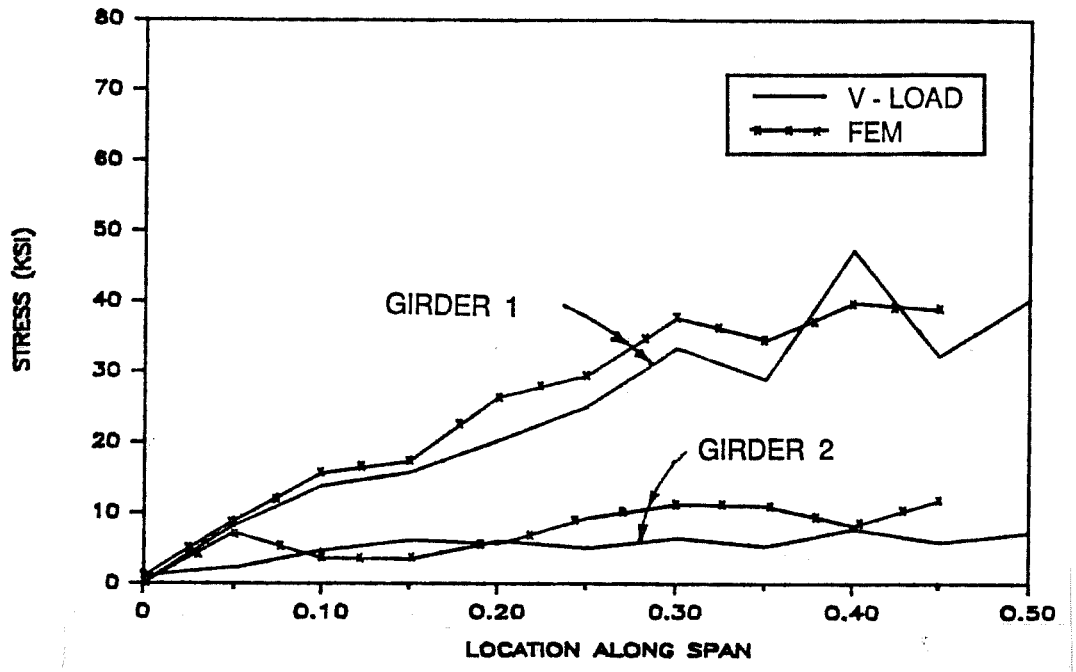

(a)

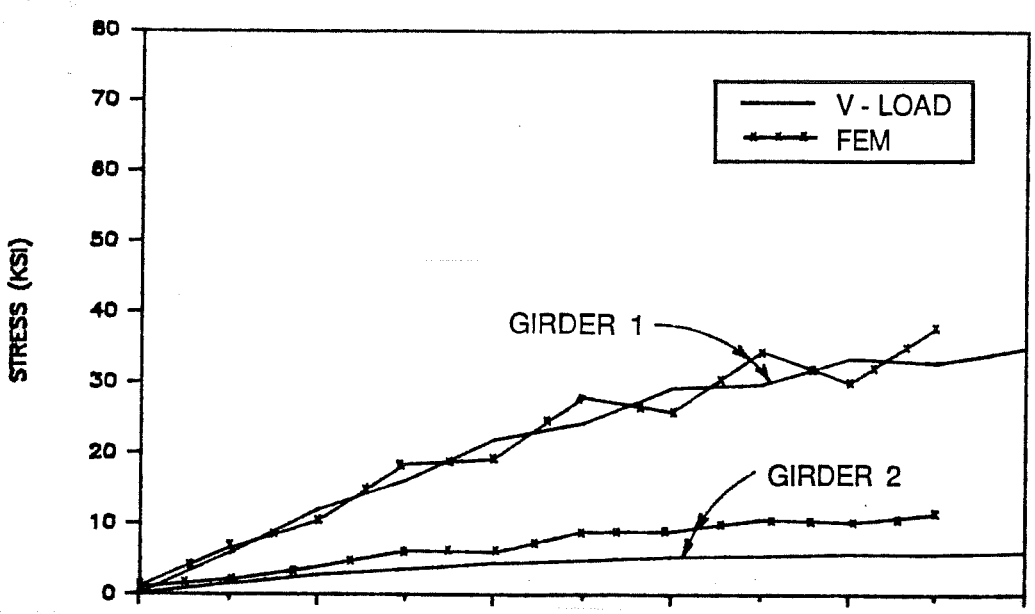

(b)

Figure 4.5 Longitudinal bending and warping stress in bottom flange - dead load: (a) Scheme C; (b) Scheme D.

for the 10 ft spacing. The V-load stresses are generally less than the finite element stresses for the 20 ft spacing but are only less between the diaphragms spaced at 10 ft.

In summary, the V-load analysis underestimates the torsional stiffness of the unit and consequently transfers too much load from the inner girder to the outer girder. This is evident by the conservative stress values for girders 1 and the unconservative values for girder 2 computed in the V-load analysis when compared to the more refined finite element analysis.

4.2.1.2 Live Load. The maximum longitudinal bending stresses due to live load alone on the composite girders are listed in Table 4.1b. The trends in the live load response are similar to the dead load response: bending stresses are not dependent on the diaphragm spacing and the error in the V-load analysis increases as the radius of curvature decreases. The percent difference between finite element and V-load stresses for live load is greater than for the dead load because the torsional stiffness of the slab is important in distributing the live loads to the girders. The V-load analysis transfers too much load from the inner to outer girder. The V-load stresses for girder 1 are conservative by up to 33%, while those for girder 2 are underestimated by up to 51%.

Table 4.2b lists the combined warping and longitudinal bending stresses from the V-load and finite element analyses due to live load. The addition of the warping stresses has little effect on the difference in live load stresses computed by the two analysis methods.

4.2.1.3 Dead Plus Live Load. The maximum longitudinal bending stress in the bottom flange due to dead plus live load is shown in Table 4.1c. Similar trends exist as in previous bending stress comparisons. The combined stress varies with the radius of curvature, not with the diaphragm spacing. The percent difference for the combined load lies between difference found in the dead load and live load cases.

Figure 4.6 shows the bending stress in the girders for the combined dead and live load case for a 10 ft diaphragm spacing (Schemes B and D). This figure is similar to Fig. 4.3 but has larger stresses and a greater difference between the finite element and the V-load results. The units with 500 ft radius shows a larger difference in stresses. The warping stresses for dead plus live load are shown in Fig. 4.7 for the Schemes C and D. The results are similar to those shown in Fig. 4.4, but the magnitude of the warping stresses is greater. Peak V-load warping stresses occur at diaphragm locations.

Combining the warping stresses in the flange with the longitudinal bending stresses results in the total stress for dead load plus live load as shown in Table 4.2c. The difference in total stresses for girder 1 is very small with the stresses in girder 2 underestimated by 20-50% by the V-load analysis. Combining dead and live load partially compensates for the poor correlation of values for the live load case for girder 1, but there is little change in the difference for girder 2. Figure 4.8 illustrates the combined warping and bending stresses

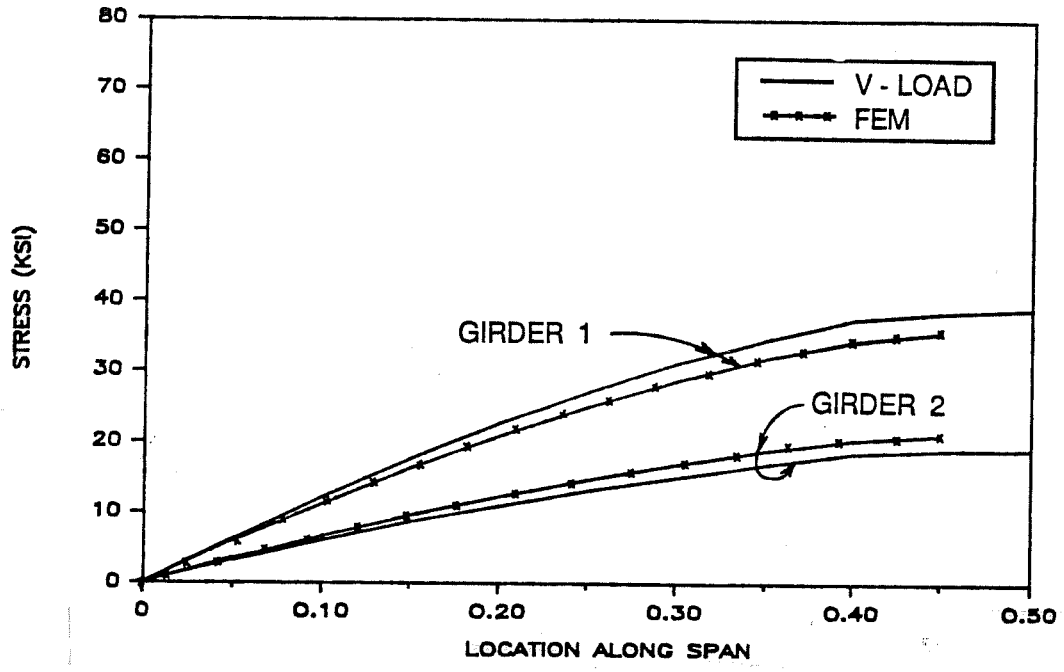

(a)

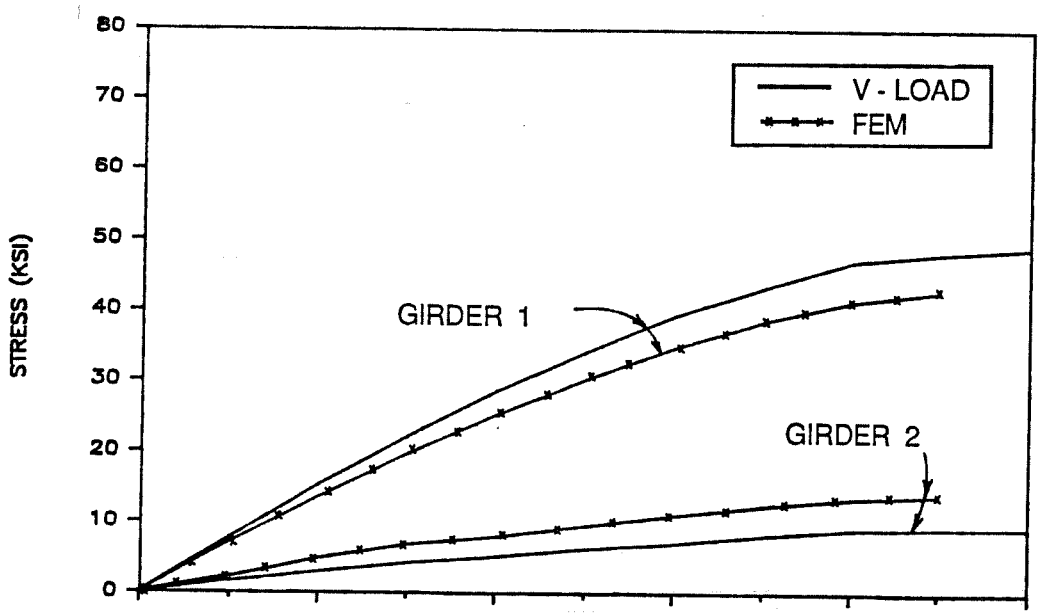

(b)

Figure 4.6 Longitudinal bending stress in bottom flange - dead plus live load: (a) Scheme B; (b) Scheme D.

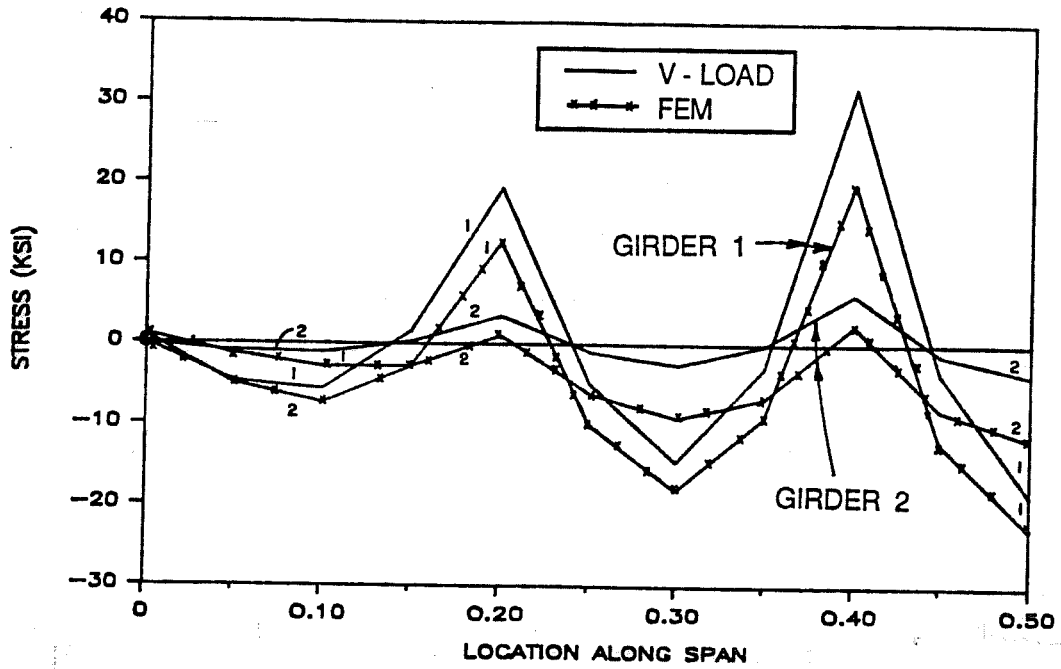

(a)

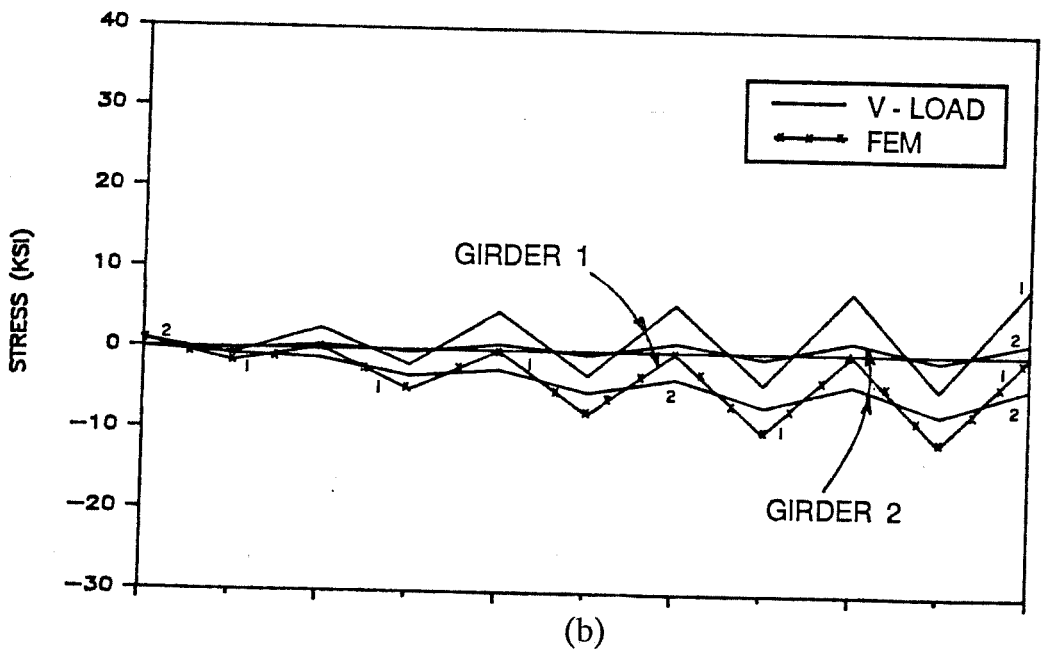

(b)

Figure 4.7 Warping stress in bottom flange - dead plus live load: (a) Scheme C; (b) Scheme D.

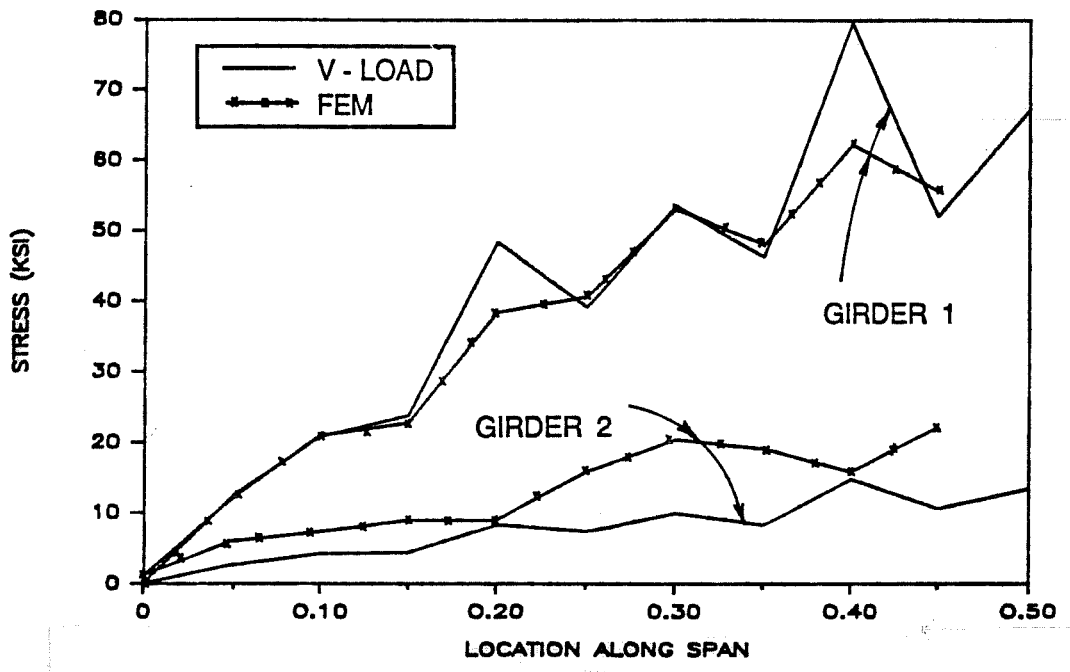

(a)

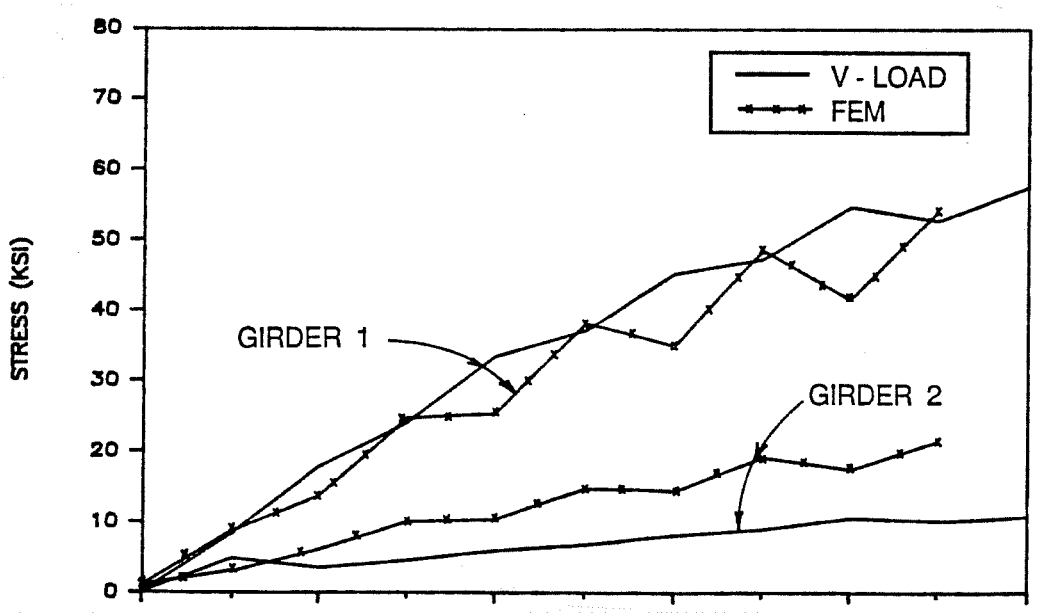

(b)

Figure 4.8 Longitudinal bending and warping stress in bottom flange - dead plus live load: (a) Scheme C; (b) Scheme D.

for the dead plus live load case. The same trend in values exists as previously noted for the combined warping and bending stress dead load case.

Reactions. The reactions due to dead load for Schemes A and C are listed in Table 4.3. The shifting of load from inner to outer girder is seen here. The difference between V-load and finite element reactions is fairly small. The error in the V- loads magnifies the difference in moments but not reactions. Summation of the V-loads gives more accurate reactions than multiplication of the V-loads by the moment arm to obtain the bending moments.

Table 4.3 Reactions (k) - Dead Load

Scheme	Radius	D. Spacing	Girder 1			Girder 2		
			V-Load	FEM	% D	V-Load	FEM	% D
A	1000′	20′	42.73	43.17	-1.0	24.60	24.22	1.6
C	500′	20′	51.80	52.71	-1.7	15.50	14.69	5.5

4.2.2 Summary. The responses for the two girder horizontally curved bridge shows important trends. The spacing of diaphragms has little effect on the longitudinal bending stresses but does affect the warping stresses. As the radius of curvature decreases the load carried by the outer girder increases, while the load carried by the inner girder decreases. However, the V-load analysis overestimates the shifting of the load from inner to outer girder. The slab contributes a significant torsional stiffness to the unit which is not accounted for in the V-load analysis for live load. Furthermore, in the V-loads analysis, the diaphragms do not contribute to the torsional stiffness of the bridge unit. The finite element analysis recognizes the contribution of the diaphragms to the torsional stiffness of the bridge unit. Because the transfer of forces between girders is related to the torsional stiffness of the bridge unit, the less torsional stiffness in the model, the greater is the shift of forces from the inner to the outer girders. Finally, the approximate method for computing lateral flange bending results in considerable error, particularly for widely spaced diaphragms.

4.3 Three Span, Continuous Bridge Unit

This section presents the analysis of a typical curved girder bridge unit to investigate further the accuracy of the approximate V-load method in determining the response to loads. The longitudinal bending and warping stresses due to several load cases will be computed for several different bridge configurations. The parameters considered in the

bridge configurations are diaphragm spacing, radius of curvature, and the support orientation.

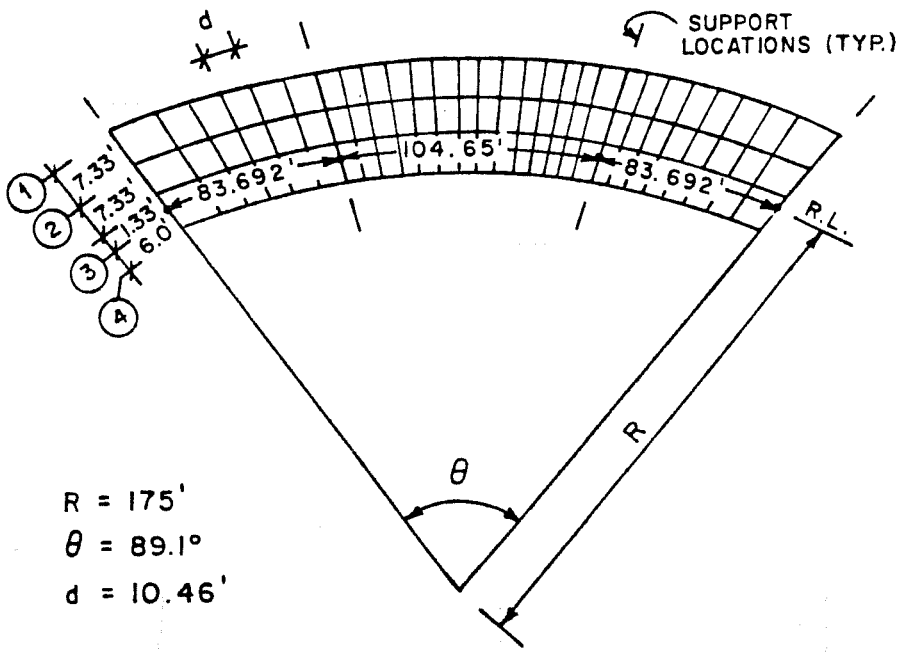

Figure 4.9 Plan view of four-girder, three-span bridge unit.

A plan of the unit is shown in Fig. 4.9. The standard bridge consists of three continuous spans with a total length of approximately 272 feet, a constant radius of curvature of 175 feet along the reference line, and radial supports. The girders are spaced at 7-ft 4-in. and numbered from outside to inside. The radial diaphragms are spaced a distance of 10.46 feet along the reference line. The concrete deck slab is 8 inches thick and the modular ratio for the concrete is eight. The slab overhangs the girders 1 and 4 by 3-ft 8-in.

The four, nonprismatic girders have the same cross section as shown in Fig. 4.10. The girders were designed for noncomposite action under dead load and composite action under live load. The noncomposite moment of inertia in negative and positive bending regions is 36,348 in^4 and 18,570 in^4, respectively. Under live load, composite action is assumed in positive moment regions and noncomposite action in negative moment regions. The composite moment of inertia in the positive moment region is 45,678 in^4. The positive and negative bending regions for all load cases were determined by the moment diagram for the bare girders under dead load.

To study the response of curved bridge units, variations of this standard bridge are examined. The bridge configurations studied are:

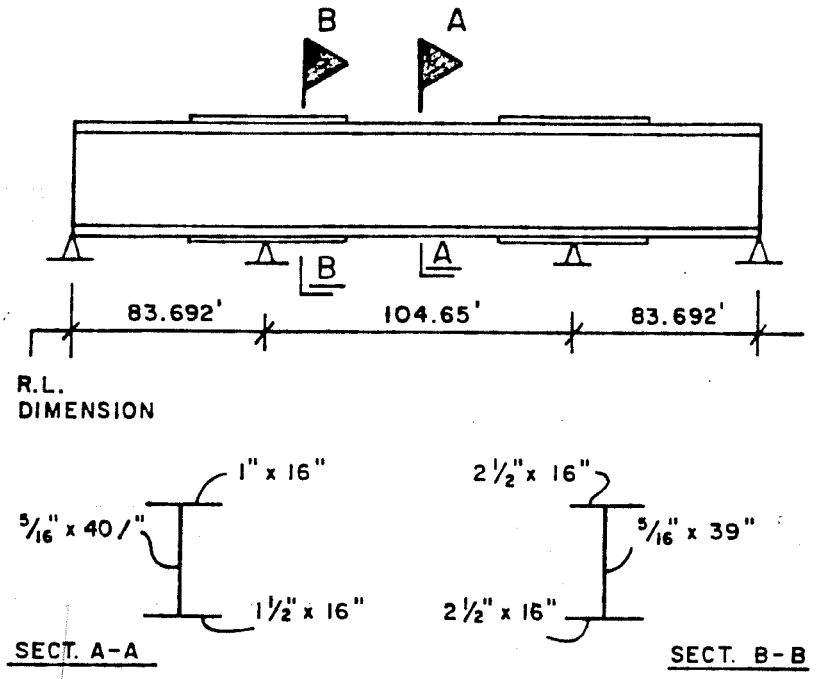

Figure 4.10 Cross section of typical girder in three-span bridge unit.

Bridge 1 - Standard Bridge with diaphragm spacing of 10.46 feet, radius of curvature of 175 feet, and radial supports.

Bridge 2 - Bridge 1 with the diaphragm spacing changed from 10.46 feet to 20.92 feet.

Bridge 3 - Bridge 1 with the radius of curvature changed from 175 feet to 350 feet.

Bridge 4 - Bridge 1 with the two interior supports skewed as shown in Fig. 4.11.

The dead load consists of the weight of the steel girders and the concrete deck slab. The concrete slab weight is 0.733 k/ft and the steel girders weight is 0.317 k/ft in the negative moment region and 0.179 k/ft in the positive moment region. The live load is a single AASHTO HS20-44 truck [1]. Lane loads were not considered for this study. The longitudinal placement of the truck on the unit to produce maximum stresses in girder 1 was determined using the V- load envelope procedure described in Chapter 3. The truck was placed at two different transverse locations on the bridge deck, an outer position and a middle position. Figure 4.12 shows the location of the wheel loads on the bridge for each placement. The finite element solution automatically accounts for the lateral distribution of load to the girders, whereas the V-load method requires specifying lateral distribution

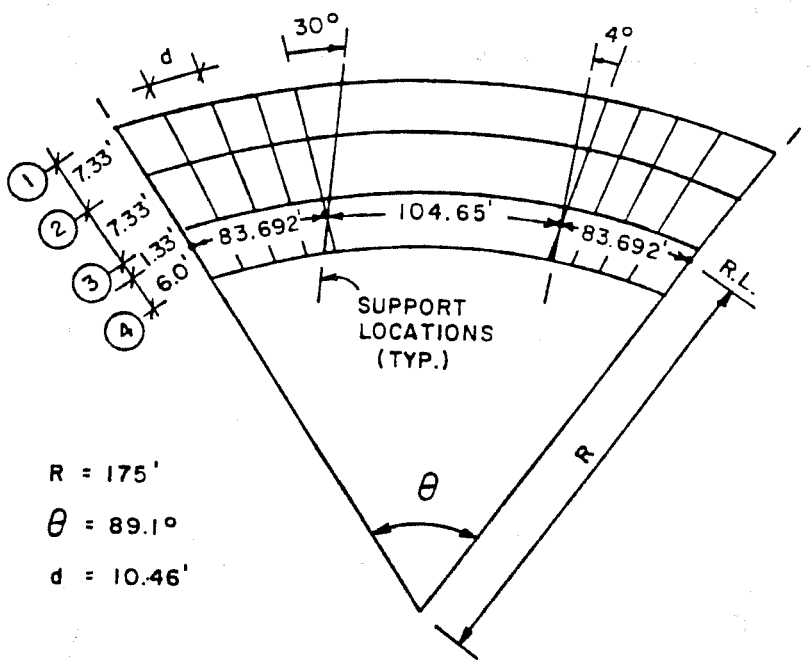

Figure 4.11 Plan view of bridge unit with skewed interior supports.

factors. To minimize the lateral distribution effects, the wheel loads are placed directly over the girders, as shown in Fig. 4.11. In reality, the slab and diaphragms act to transmit loads to all four girders, but the transverse distribution is neglected in the V-load analysis.

4.3.1 Effect of Curvature. Bridges 1 and 3 are compared to determine the importance of the radius of curvature on the responses of the unit. The reference line radius in Bridges 1 and 3 is 175 feet and 350 feet, respectively.

4.3.1.1 Dead Load. The longitudinal bending stresses due to dead load for Bridges 1 and 3 are listed in Table 4.4a. The stresses are given at two locations along each of the four girders, near the point of maximum bending stress. There is a large shift of load from girder 4 to girder 1 in Bridge 1, with the shift less for Bridge 3 with the larger radius of curvature.

The percent difference between finite element and V-load stresses, computed as for the simple span case, is also listed in Table 4.4a. The largest difference is 14.7% for any of the bending stresses of Bridges 1 and 3. Bending stresses in the negative moment regions are not predicted by the V-load method as accurately as in the positive moment regions. The results of the V-load analysis are conservative for Bridges 1 and 3. This contrasts with the analysis of for the simple span bridge unit (see Table 4.1a).

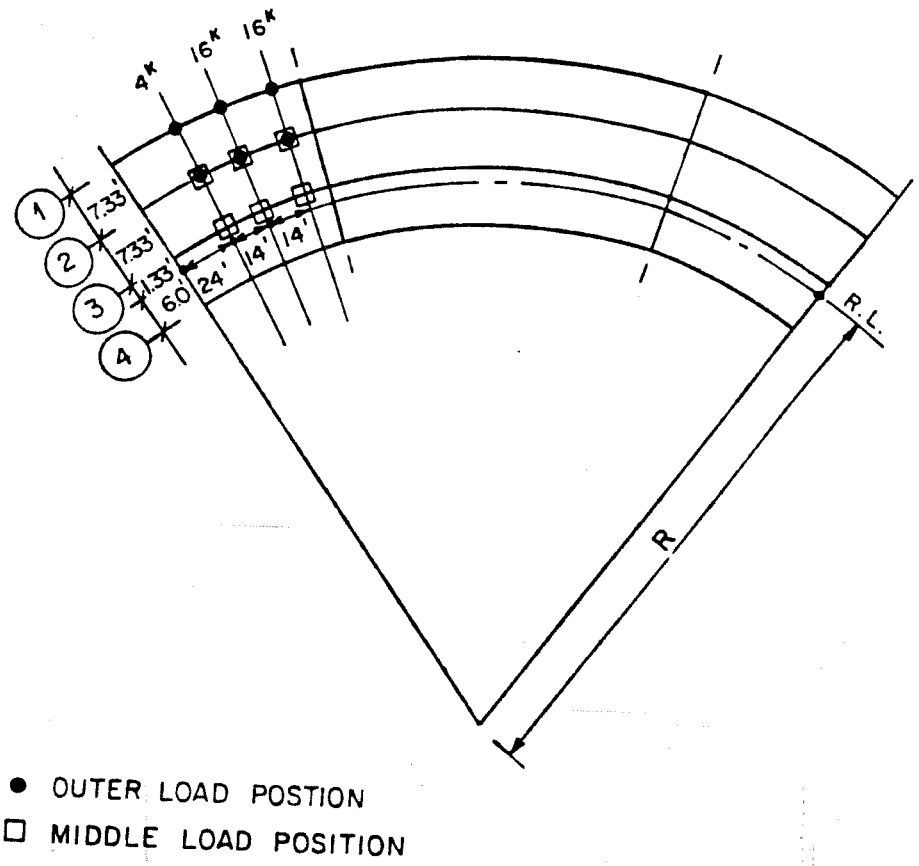

Figure 4.12 Locations of wheel placement for three-span, four-girder bridge units.

Figures 4.13 and 4.14 show plots of the dead load bending stresses in girders 1 and 4 of Bridges 1 and 3. The comparison between the stresses computed using the V-load method and finite element method is very good. The stresses in girder 1 of Bridge 1, are larger than those for Bridge 3; the opposite is true for girder 4. As the radius of curvature increases the difference between deadload bending stresses computed by the V-load and finite element methods decreases.

The warping stresses in the bottom flange of girders 1 and 4 of Bridges 1 and 3 due to dead load are listed in Table 4.5a. The warping stresses are given at two locations near the maximum positive and negative bending moment, but not at a diaphragm location, because of the difference in warping of the flanges in the two methods. The percent difference between the V-load and finite element warping stresses is large in the two bridges, although the values of the warping stresses are very small, with the largest value only 1.57 ksi.

Table 4.4 Longitudinal Bending Stress in Bottom Flage (ksi) - Dead Load

a) Dead Load

Bridge	R.L. Radius	D. Spacing	Skew	Location*	Girder 1			Girder 2			Girder 3			Girder 4		
					V-Load	FEM	% D	V-Load	FEM	% D	V-Load	FEM	% D	V-Load	FEM	% D
1	175 '	10.46 '	NO	.115 L	7.20	6.52	9.4	5.56	5.24	6.1	4.03	5.24	3.3	2.61	2.31	13.0
				.307 L	-8.71	-7.47	14.2	-7.57	-6.90	9.7	-6.50	-6.90	6.2	-5.49	-5.29	3.8
2	175 '	20.92 '	NO	.115 L	7.04	6.48	8.6	5.46	5.03	8.5	3.99	3.95	1.0	2.62	2.34	12.0
				.307 L	-8.88	-8.38	6.0	-7.63	-6.64	14.9	-6.44	-5.71	12.8	-5.33	-4.79	11.3
3	350 '	10.46 '	NO	.115 L	5.78	5.57	3.8	5.02	4.88	2.9	4.28	4.20	1.9	3.57	3.45	3.5
				.307 L	-7.63	-6.65	14.7	-7.09	-6.36	11.5	-6.57	-5.88	11.7	-6.07	-5.47	11.0
4	175 '	10.46 '	2 to 30°	.115 L	9.98	8.45	18.1	6.89	6.33	8.8	3.95	3.99	-1.0	1.16	1.21	-4.1
			3 to -4°	.307 L	-5.42	-5.18	4.6	-5.80	-5.92	-2.0	-6.18	-5.10	21.2	-4.46	-4.15	7.5

b) Live Load, Outer Load Position

Bridge	R.L. Radius	D. Spacing	Skew	Location*	Girder 1			Girder 4		
					V-Load	FEM	% D	V-Load	FEM	% D
1	175 '	10.46 '	NO	.135 L	6.89	5.84	18.0	-1.31	-1.45	-9.7
				.327 L	-2.05	-1.84	11.4	.30	.18	66.7
2	175 '	20.92 '	NO	.135 L	6.81	5.37	26.8	-1.34	-1.18	13.6
				.327 L	-2.03	-1.87	8.6	.29	.12	141.7
3	350 '	10.46 '	NO	.135 L	5.87	5.27	11.4	.65	.80	-18.8
				.327 L	-1.79	-1.61	11.2	.15	.14	7.1
4	175 '	10.46 '	2 to 30°	.135 L	7.66	5.51	39.0	-1.44	-1.35	6.7
			3 to -4°	.327 L	-2.28	-.98	132.7	.32	.19	68.4

c) Live Load, Middle Load Position

Bridge	R.L. Radius	D. Spacing	Skew	Location*	Girder 1			Girder 4		
					V-Load	FEM	% D	V-Load	FEM	% D
1	175 '	10.46 '	NO	.135 L	1.43	3.33	-57.1	-1.26	.91	-238.5
				.327 L	-.32	-1.01	-68.3	.28	-.40	-171.0
2	175 '	20.92 '	NO	.135 L	1.46	2.99	-51.2	-1.29	.89	-244.9
				.327 L	-.31	-1.01	-69.3	.28	-.47	-160.0
3	350 '	10.46 '	NO	.135 L	.67	2.76	-75.7	-.64	1.53	-141.8
				.327 L	-.16	-.82	-80.5	.14	-.51	-127.5
4	175 '	10.46 '	2 to 30°	.135 L	1.57	3.18	-50.6	-1.30	.82	-258.5
			3 to -4°	.327 L	-.29	-.78	-62.8	.31	-.49	-163.3

* Location from first support, where L is girder length

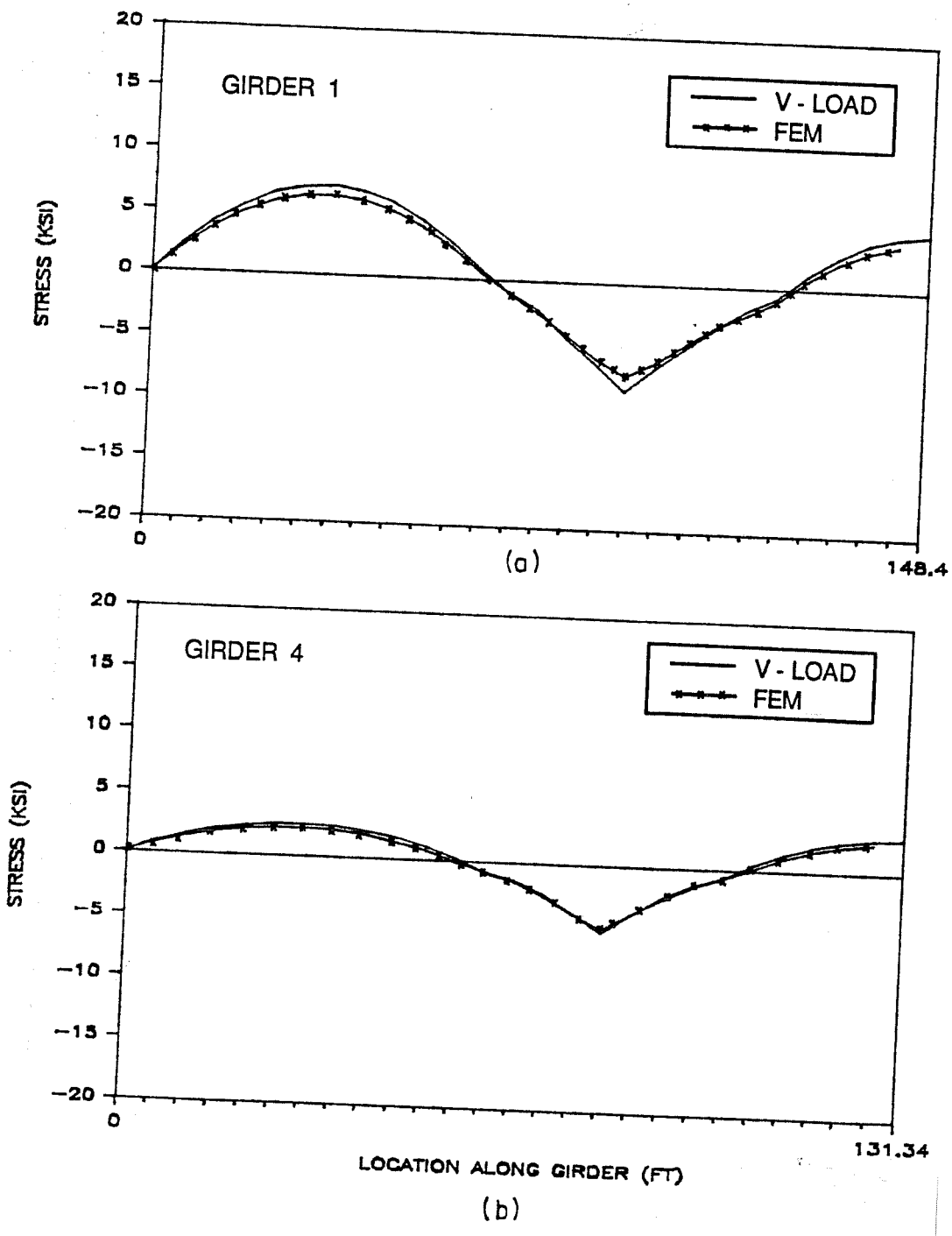

Figure 4.13 Longitudinal bending stress in bottom flange of Bridge 1 - dead load: (a) Girder 1; (b) Girder 4.

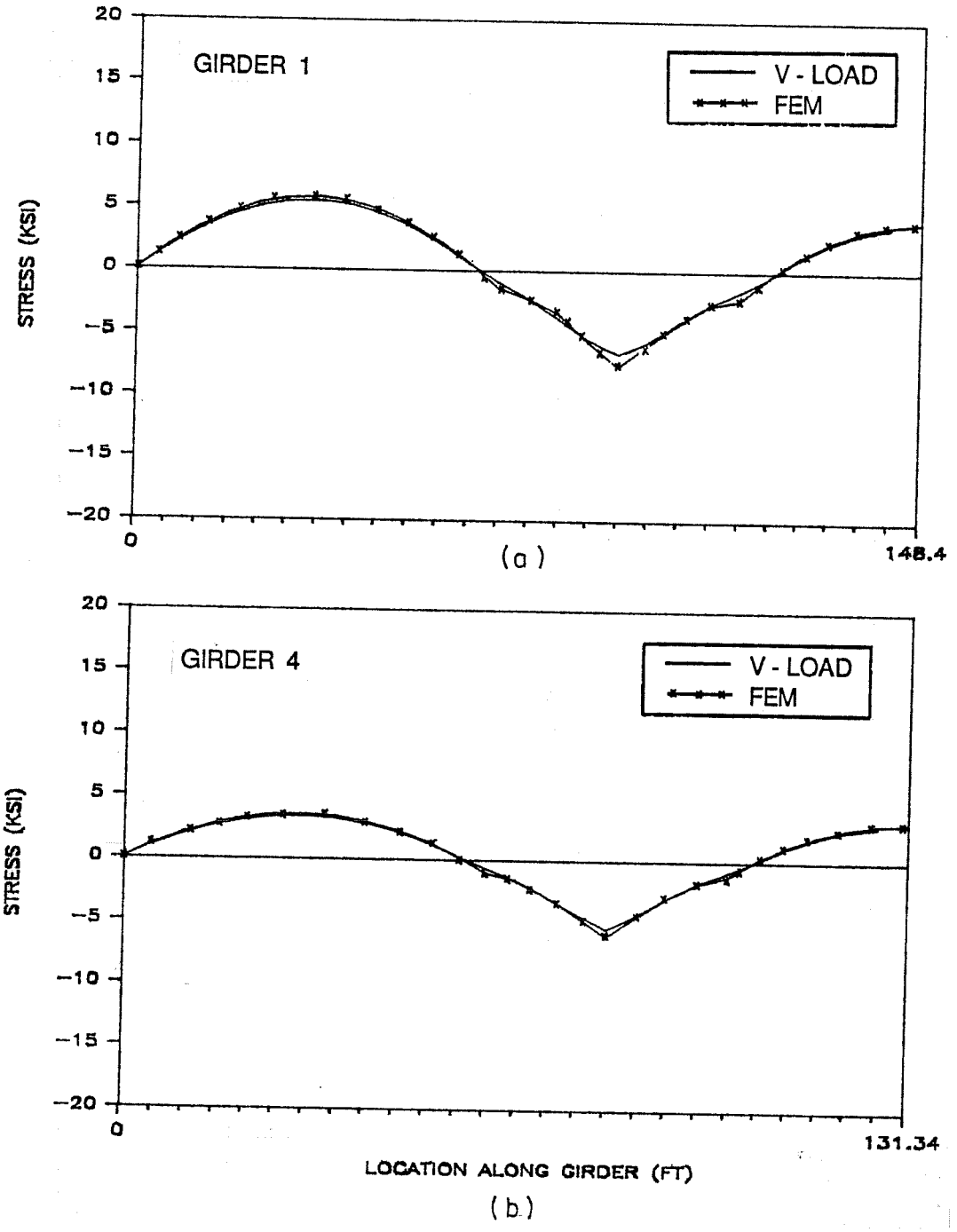

Figure 4.14 Longitudinal bending stress in bottom flange of Bridge 3 - dead load: (a) Girder 1; (b) Girder 4.

Table 4.5 Warping Stress in Bottom Flange (ksi)

a) Dead Load

Bridge	R.L. Radius	D. Spacing	Skew	Location*	Girder 1			Girder 4		
					V-Load	FEM	% D	V-Load	FEM	% D
1	175 '	10.46 '	NO	.096 L	-.89	-1.57	-43.3	-.29	-.73	-60.3
				.288 L	.87	1.37	-36.5	.46	.87	-47.1
2	175 '	20.92 '	NO	.096 L	-1.26	-1.30	-3.1	-.47	-.54	-12.9
				.288 L	2.62	2.38	10.1	1.38	1.52	-9.2
3	350 '	10.46 '	NO	.096 L	-.35	-.71	-50.7	-.20	-.45	-55.6
				.288 L	.36	.63	-42.9	.27	.49	-44.9
4	175 '	10.46 '	2 to 30°	.096 L	-1.17	-2.07	-43.5	-.15	-.80	-81.3
			3 to -4°	.288 L	-.44	-1.11	-60.4	-.65	-3.07	-78.8

b) Live Load, Outer Load Position

Bridge	R.L. Radius	D. Spacing	Skew	Location*	Girder 1			Girder 4		
					V-Load	FEM	% D	V-Load	FEM	% D
1	175 '	10.46 '	NO	.135 L	-1.04	-1.65	-37.0	.17	-.19	-189.5
				.327 L	.27	.52	-48.1	-.03	.16	-118.8
2	175 '	20.92 '	NO	.135 L	.69	-3.55	80.6	.14	.14	0
				.327 L	.52	1.16	-55.2	0.0	.08	-100.0
3	350 '	10.46 '	NO	.135 L	-.42	-.88	-52.3	.04	-.27	85.2
				.327 L	.11	.30	-63.3	-.01	.14	-107.1
4	175 '	10.46 '	2 to 30°	.135 L	-1.15	-1.56	-26.3	.18	-.19	-194.7
			3 to -4°	.327 L	.14	-.17	-182.4	-.07	.19	-136.8

c) Live Load, Middle Load Position

Bridge	R.L. Radius	D. Spacing	Skew	Location*	Girder 1			Girder 4		
					V-Load	FEM	% D	V-Load	FEM	% D
1	175 '	10.46 '	NO	.135 L	-.21	-.83	-74.7	.16	-.37	-143.2
				.327 L	.04	.25	-84.0	-.03	.13	-123.1
2	175 '	20.92 '	NO	.135 L	.84	-1.76	-147.7	.15	-.65	-123.1
				.327 L	-.06	.63	-109.5	0.0	.27	-100.0
3	350 '	10.46 '	NO	.135 L	-.05	-.34	-85.3	.04	-.26	-115.4
				.327 L	.01	.11	-90.9	-.01	.08	-112.5
4	175 '	10.46 '	2 to 30°	.135 L	-.22	-.79	-72.2	.16	-.35	-145.7
			3 to -4°	.327 L	.01	-.32	-103.1	-.04	.46	-108.7

* Location from first support, where L is girder length

Table 4.6 Bending and Warping Stress in Bottom Flange (ksi)

a) Dead Load

Bridge	R.L. Radius	D. Spacing	Skew	Location*	Girder 1			Girder 4		
					V-Load	FEM	% D	V-Load	FEM	% D
1	175 ′	10.46 ′	NO	.096 L	7.98	7.96	.3	2.87	3.01	-4.7
				.288 L	-7.41	-7.48	-.9	-4.36	-4.87	-10.5
2	175 ′	20.92 ′	NO	.096 L	8.30	4.89	69.7	2.00	1.66	20.5
				.288 L	-8.47	-7.84	8.0	-4.78	-5.03	-5.0
3	350 ′	10.46 ′	NO	.096 L	6.04	6.17	-2.1	3.72	3.84	-3.1
				.288 L	-6.03	-6.14	-1.8	-4.66	-4.77	-2.3
4	175 ′	10.46 ′	2 to 30°	.096 L	10.54	10.16	3.7	1.56	2.19	-28.8
			3 to -4°	.288 L	-1.89	-4.07	-53.6	-4.47	-7.09	-37.0

b) Live Load, Outer Load Position

Bridge	R.L. Radius	D. Spacing	Skew	Location*	Girder 1			Girder 4		
					V-Load	FEM	% D	V-Load	FEM	% D
1	175 ′	10.46 ′	NO	.135 L	7.93	7.49	5.9	-1.48	-1.64	-9.8
				.327 L	-2.32	-2.36	-1.7	.33	.34	-2.9
2	175 ′	20.92 ′	NO	.135 L	7.50	8.92	-15.9	-1.48	-1.32	12.1
				.327 L	-2.55	-3.03	-15.8	.29	.20	45.0
3	350 ′	10.46 ′	NO	.135 L	6.29	6.15	2.3	-.69	-1.07	-35.5
				.327 L	-1.90	-1.91	-.5	.16	.28	-42.9
4	175 ′	10.46 ′	2 to 30°	.135 L	8.81	7.07	24.6	-1.62	-1.54	5.2
			3 to -4°	.327 L	-2.42	-1.15	110.4	.39	.38	2.6

c) Live Load, Middle Load Position

Bridge	R.L. Radius	D. Spacing	Skew	Location*	Girder 1			Girder 4		
					V-Load	FEM	% D	V-Load	FEM	% D
1	175 ′	10.46 ′	NO	.135 L	1.64	4.16	-60.6	-1.42	1.28	-210.9
				.327 L	-.36	-1.26	-71.4	.31	-.53	-158.5
2	175 ′	20.92 ′	NO	.135 L	2.30	4.75	-51.6	-1.44	1.54	-193.5
				.327 L	-.37	-1.64	-77.4	.28	-.74	-137.8
3	350 ′	10.46 ′	NO	.135 L	.72	3.10	-76.8	-.68	1.79	-138.0
				.327 L	-.17	-.93	-81.7	.15	-.59	-125.4
4	175 ′	10.46 ′	2 to 30°	.135 L	1.79	3.97	-54.9	-1.46	1.17	-224.8
			3 to -4°	.327 L	-.30	-1.10	-72.7	.35	-.95	-136.8

* Location from first support, where L is girder length

The warping plus bending stress in girders 1 and 4 due to dead load are listed in Table 4.6a. For Bridges 1 and 3 the difference in V-load and finite element responses are within 10.5% and are much less than the warping stress differences found in Table 4.5a. In general, the V-load stresses are slightly smaller (2-5%) than the finite element stresses for Bridges 1 and 3.

Figures 4.15 and 4.16 show the dead load stresses due to bending and warping for girders 1 and 4 of Bridges 1 and 3. Again the results of the approximate V-load analysis are very good when compared to the finite element results. The stresses are increased with the addition of the warping stresses, which can be seen by comparing Figs. 4.15 and 4.16 with Figs. 4.13 and 4.14. The V-load method predicts larger warping stresses at diaphragms than does the finite element analysis because of the assumption that the flange is rigidly supported at the diaphragms. The peaks are more noticeable in Bridge 1 with the smaller radius of curvature particularly in the positive bending regions of the girders. Between diaphragms, the finite element warping stresses in the bottom flange are greater or very close to those predicted by V-load analysis.

4.3.1.2 Live Load. An AASHTO HS20-44 truck was placed on the bridge at two transverse locations, as shown in Fig. 4.12. In the outer load position, the wheel loads are placed directly on girders 1 and 2. In the middle load position, the wheel loads are placed directly on girders 2 and 3.

Tables 4.4b and 4.4c list the longitudinal bending stresses for girders 1 and 4 due to the two live load placements, respectively, on Bridges 1 and 3. The V-load stresses are conservative for girder 1 when the load is placed in the outer position.

For the middle load position, the bending stresses in Bridges 1 and 3 show poor correlation between analysis methods. For girder 1 the V-load stresses are as much as 80.5% less than the finite element stresses. The percent difference for girder 4 is even worse.

In Figure 4.17 are plotted the V-load and finite element stresses for girders 1 and 4 for the two live load placements on Bridge 1. The V-load and finite element curves in Fig. 4.17a and 4.17b for the outer load position are closer than those in Figs. 4.17c and 4.17d for the middle load position. For the first span of girder 4 for the middle load position, Fig. 4.17d shows a difference in sign between the V-load and finite element values in the bending stress.

The large difference in live load response as computed by the two analysis methods results from the transverse distribution of loads to the girders by the slab. The finite element analysis represent the torsional and transverse stiffness of the slab, whereas the V-load method does not account for transverse distribution of the load by the slab except by user defined transverse distribution factors. The outer live load position induces torque on the bridge unit. Because the V-load method does not include transverse distribution

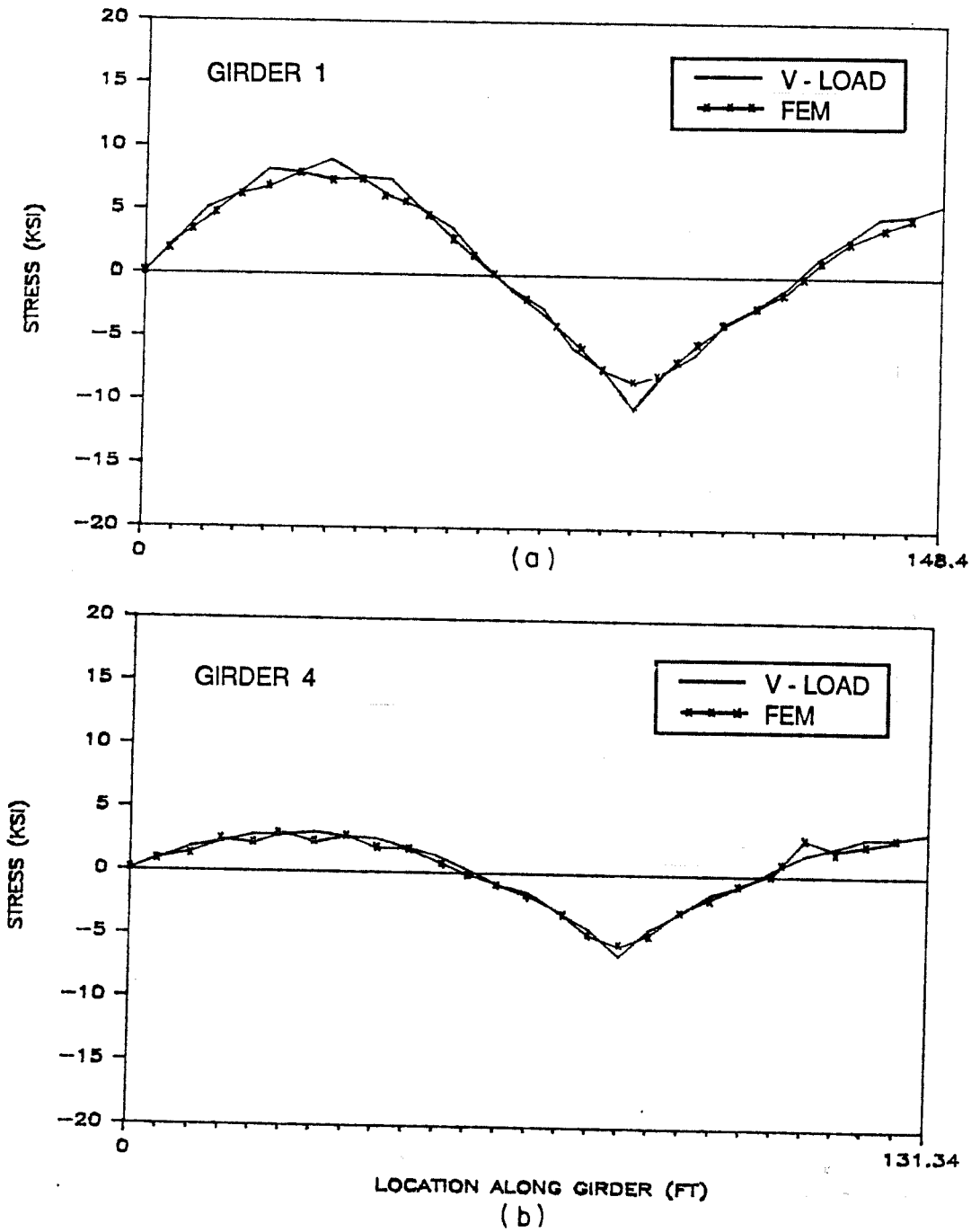

Figure 4.15 Longitudinal bending and warping stress in bottom flange of Bridge 1 - dead load: (a) Girder 1; (b) Girder 4.

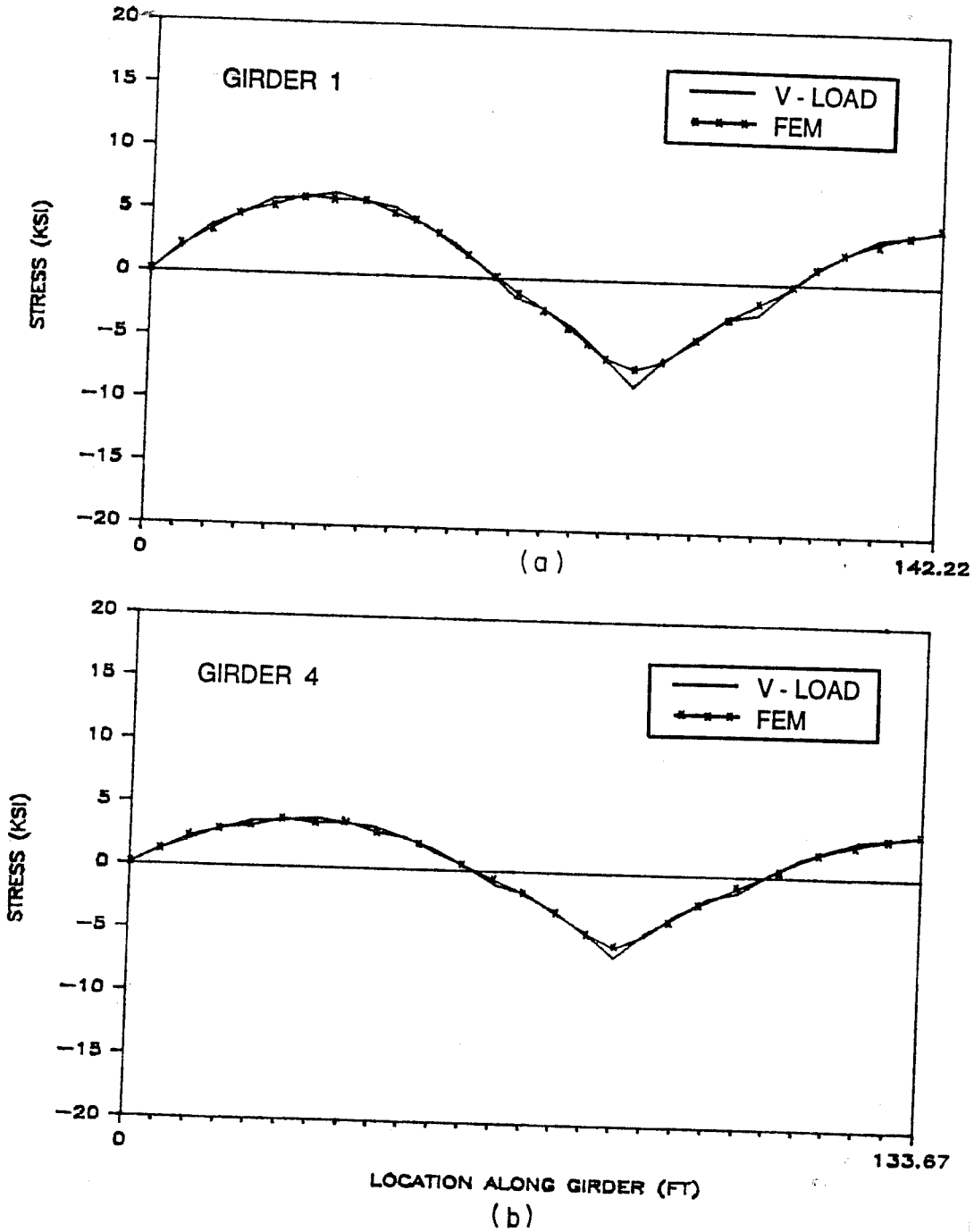

Figure 4.16 Longitudinal bending and warping stress in bottom flange of Bridge 3 - dead load: (a) Girder 1; (b) Girder 4.

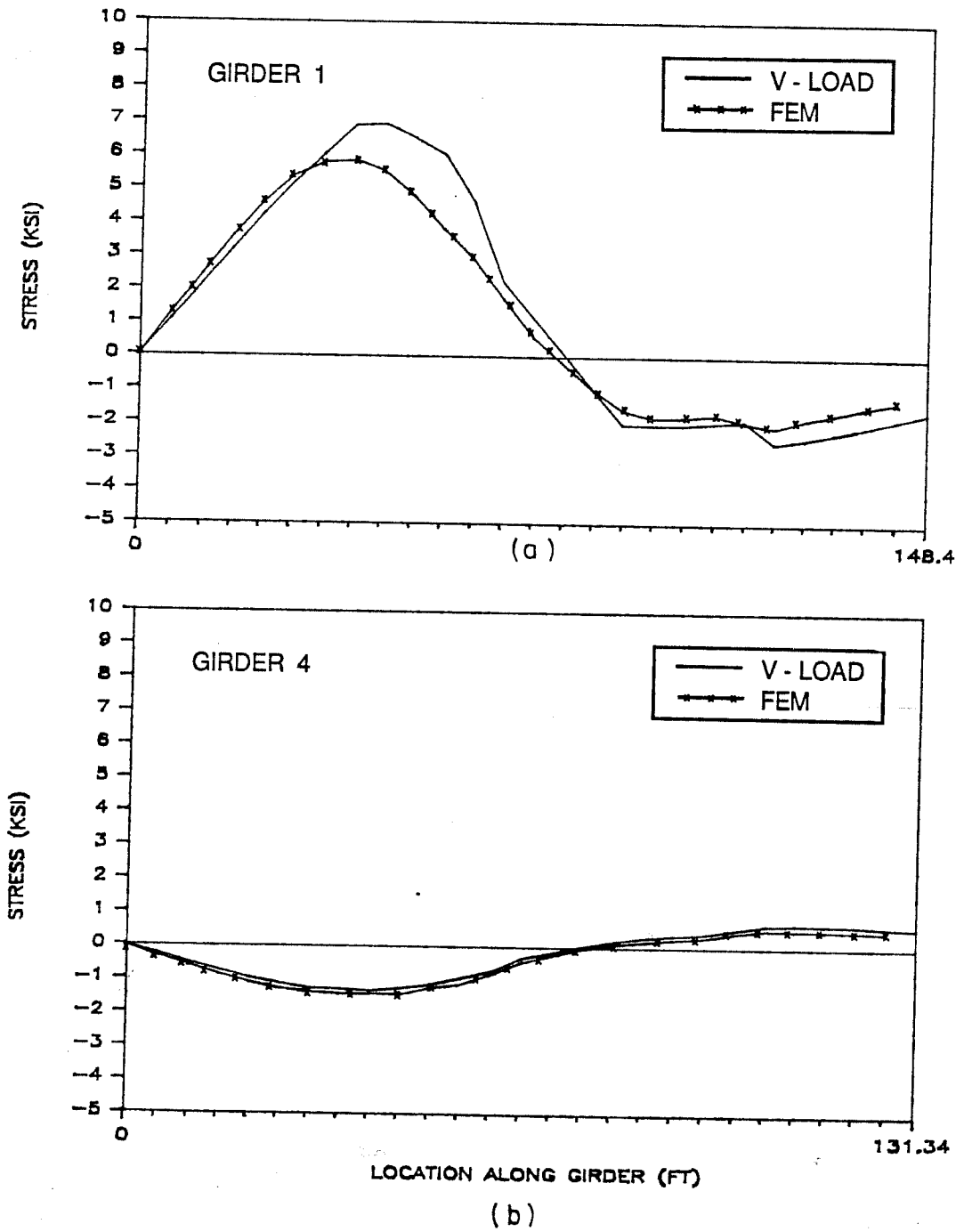

Figure 4.17 Longitudinal bending stress in bottom flange of Bridge 1 - outer live load: (a) Girder 1; (b) Girder 4.

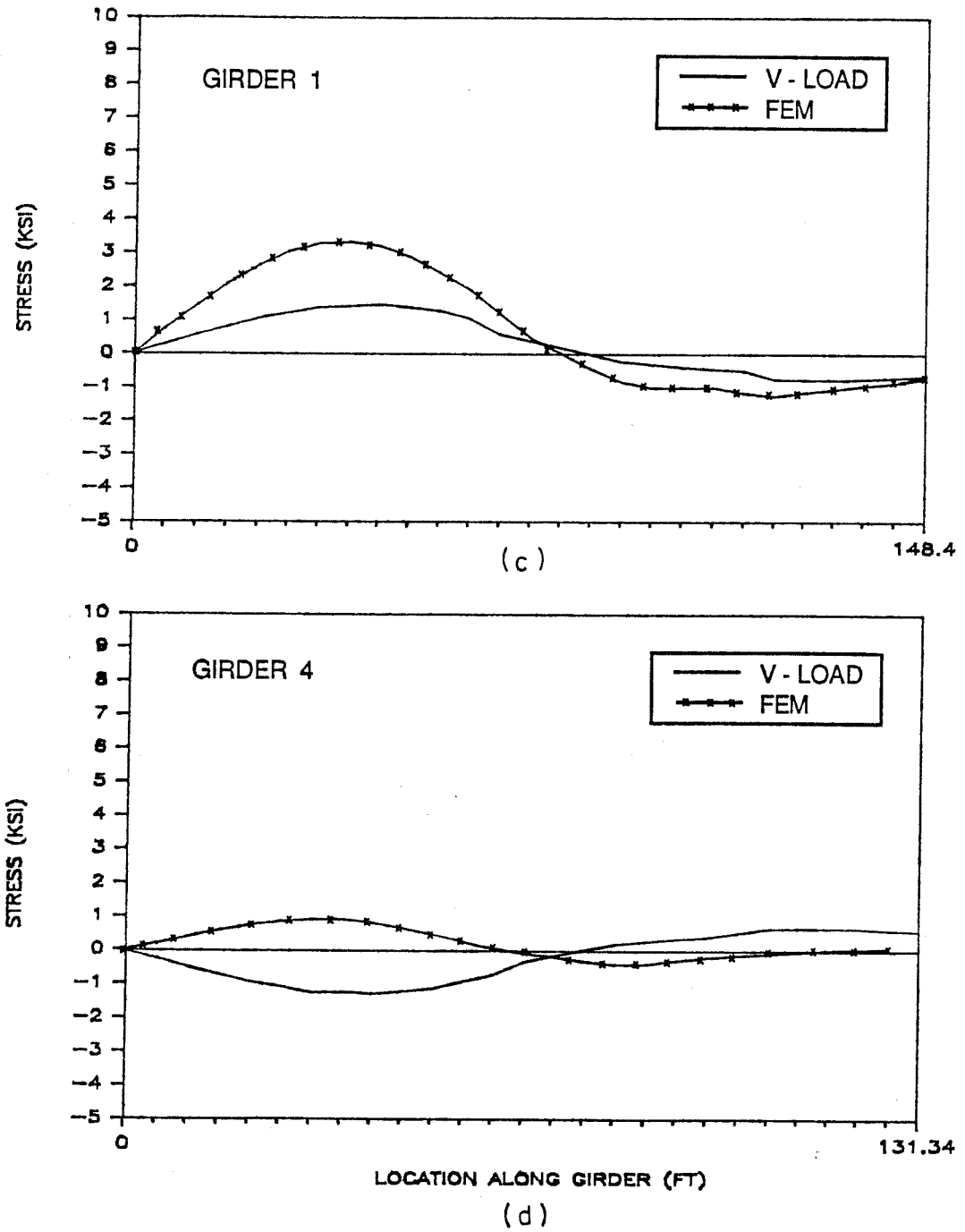

Figure 4.17 Longitudinal bending stress in bottom flange of Bridge 1 - middle live load: (c) Girder 1; (d) Girder 4.

and overestimates the torque due to curvature, the two effects cancel and the V-load stresses for outer live load position are close to the finite element stresses. In contrast, the middle live load position does not induce additional torque on the bridge unit, and consequently the V-load stresses are worse because the V-load methods overestimates the torque due to horizontal curvature. The differences in live load response are highlighted in this comparison because transverse distribution factors were not used in the V-load analysis. In practical application of the V-load method, approximate transverse distribution factors would be used to represent the effect of the slab. This is illustrated in Chapter 5 of the report.

The warping stresses in girders 1 and 4 due to live load are listed in Tables 4.5b and 4.5c. Because the live load bending stresses are in substantial error, it can be expected that warping stresses will be in greater error because they are computed from the live load bending moments. The maximum warping stress for the outer load position for girder 1 is approximately 1.65 ksi by the finite element analysis and 1.04 ksi by the V-load analysis for the outer load position. For the inner load position the maximum stress girder 1 and is 0.83 ksi from the finite element analysis and 0.21 ksi from the V-load analysis. The correlation of warping stresses between methods is very poor; the minimum difference is 37%, and the V-load warping stresses are unconservative.

Table 4.6b and 4.6c list bending plus warping stresses in the bottom flange for both live load placements. For the outer load position the difference for girder 1 of Bridges 1 and 3 is a maximum of 5.9%, while the difference for girder 4 is larger. The stresses in girder 4 are underestimated by the V-load method. The V-load and finite element stresses for the middle load placement are very poor again because the V-load method does not directly represent transverse distribution of live load.

The live load bending and warping stresses computed in the finite element and V-load analyses are shown in Fig. 4.18 for girder 1 and 4 of Bridge 1. The outer live load position gives closer V-load and finite element responses for reasons discussed above.

4.3.1.3 Dead Plus Live Load. Figure 4.19 shows the bending plus warping stresses due to combined dead and live load on girders 1 and 4 of Bridge 1 for both load placements. For the combined load the agreement between the V-load and finite element stresses in girder 1 is good, regardless of the load placement. The magnitude of the stress in girder 1 is slightly larger for the outer load position, as expected. The peak stresses at diaphragms are less noticeable in the V-load results of girder 4, (Figs. 4.19b and 4.19d). The V-load stresses are conservative for both girders of the outer load position but not for the middle live load position. Combining the dead and live load stresses reduces the difference between V-load and finite element results seen in the live load stresses of Figs. 4.17 and 4.18 because the relatively large dead load stresses are accurately predicted by the V-load method.

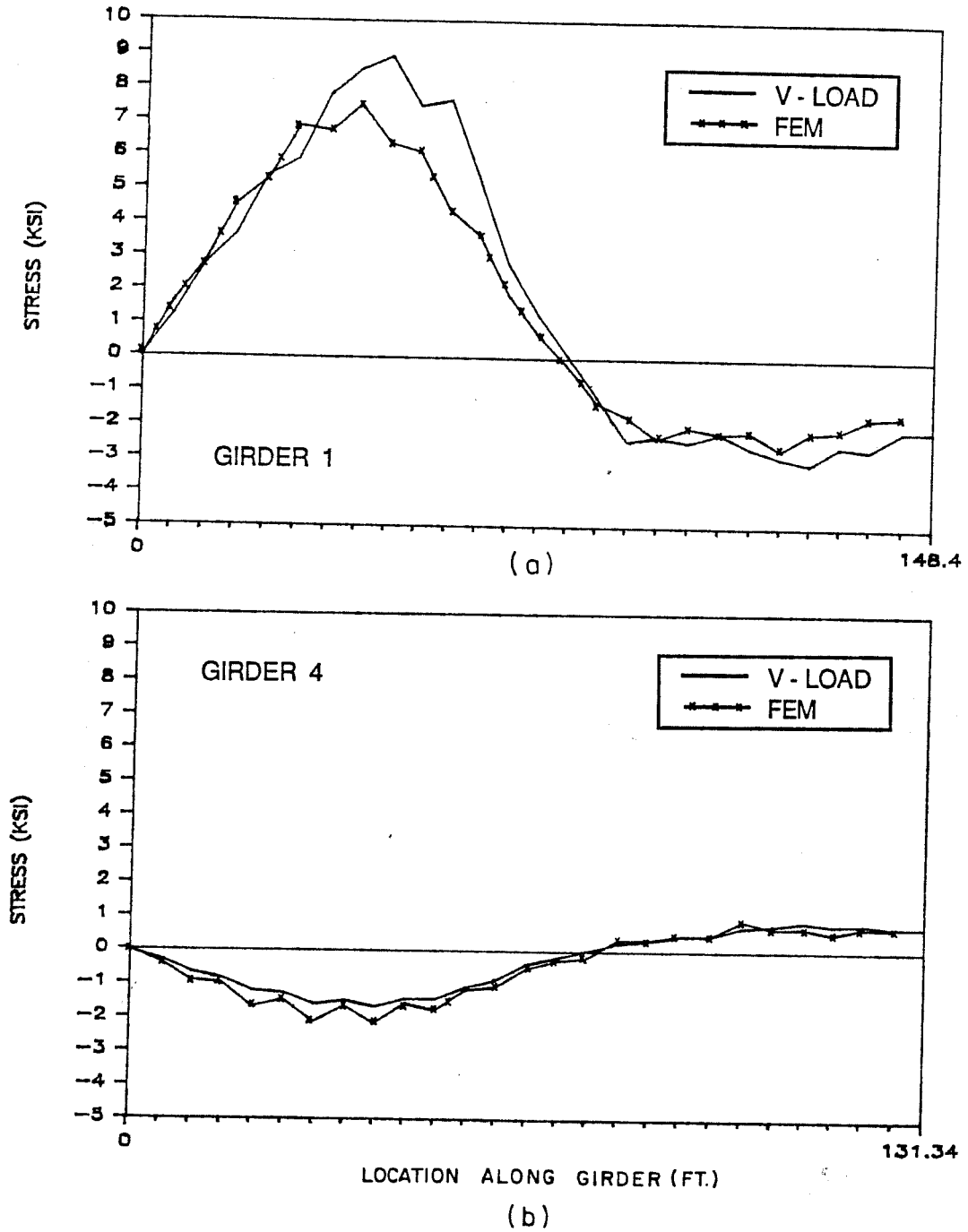

Figure 4.18 Longitudinal bending and warping stress in bottom flange of Bridge 1 - outer live load: (a) Girder 1; (b) Girder 4.

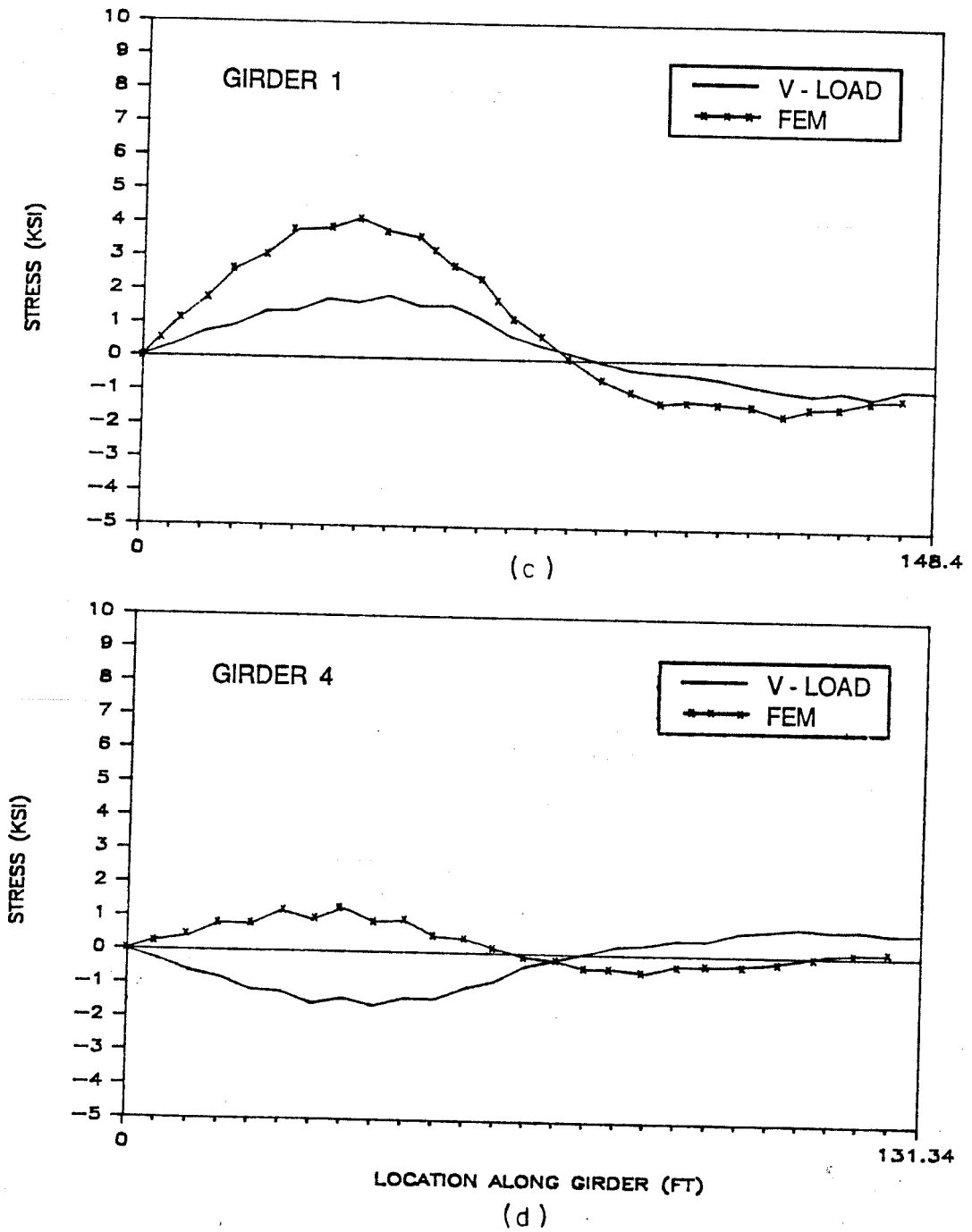

Figure 4.18 Longitudinal bending and warping stress in bottom flange of Bridge 1 - middle live load: (c) Girder 1; (d) Girder 4.

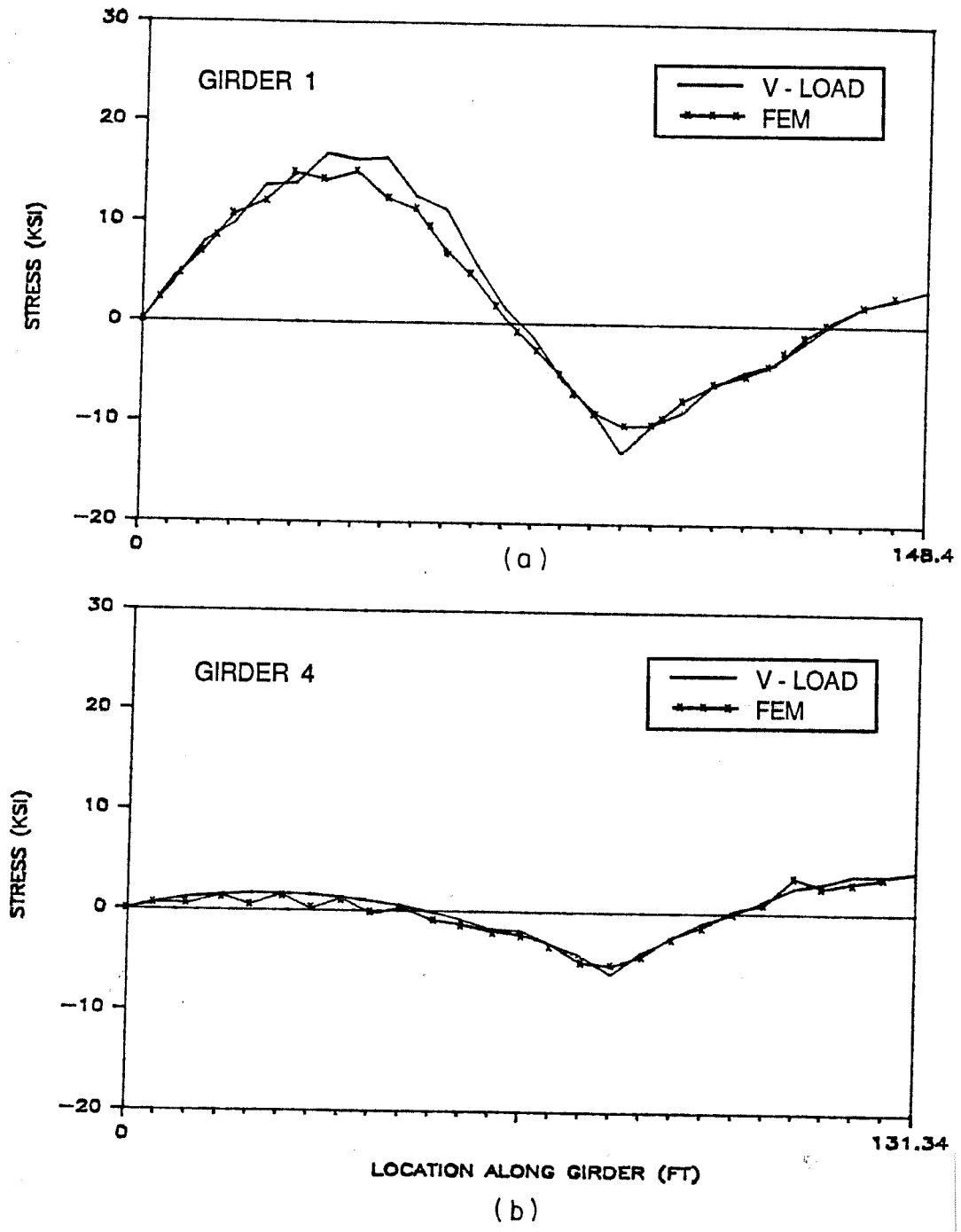

Figure 4.19 Longitudinal bending and warping stress in bottom flange of Bridge 1 - dead plus outer live load: (a) Girder 1; (b) Girder 2.

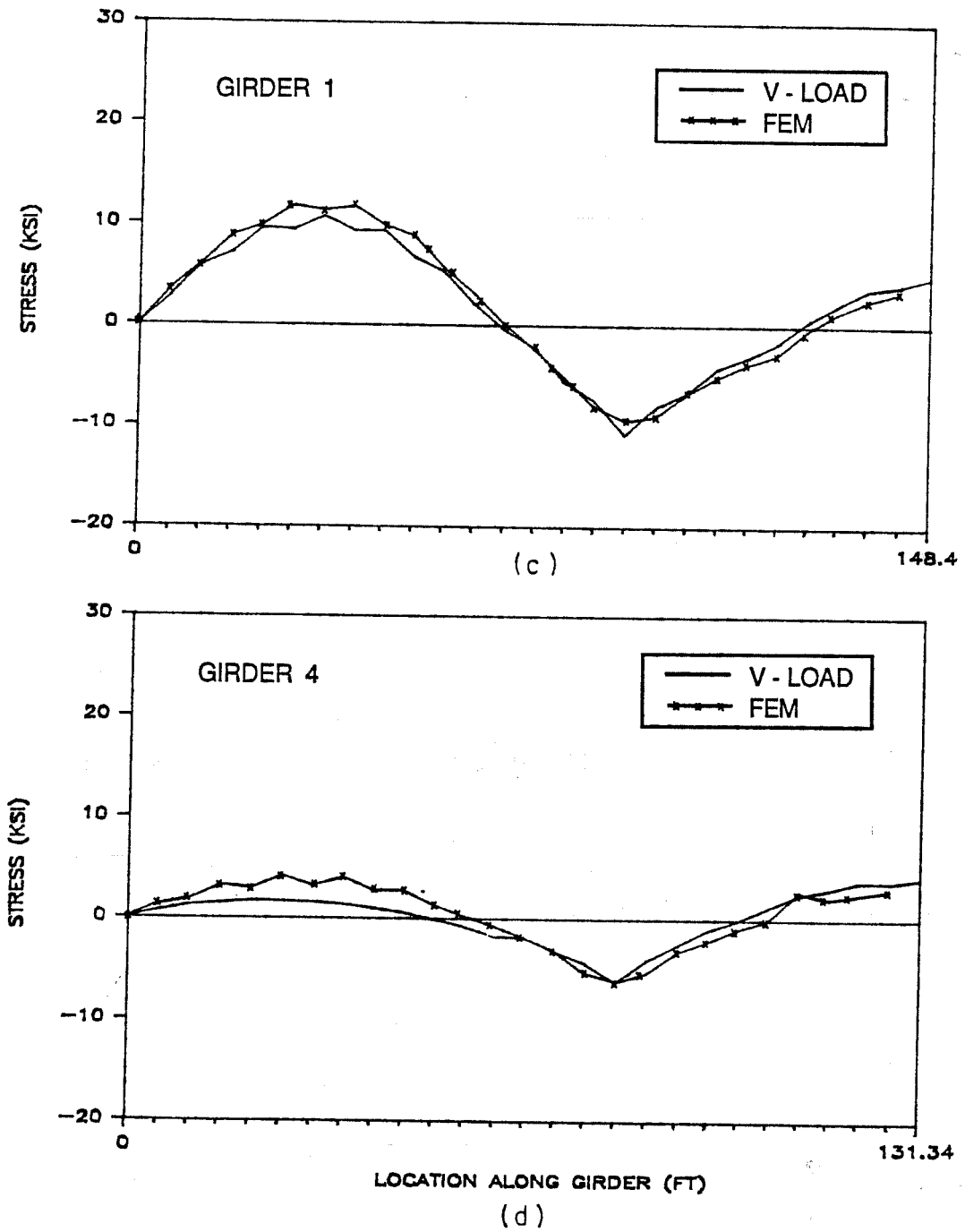

Figure 4.19 Longitudinal bending and warping stress in bottom flange of Bridge 1 - dead plus middle live load: (c) Girder 1; (d) Girder 4.

4.3.2 Effect of Diaphragm Spacing. The effect of the diaphragm spacing on the stresses in a horizontally curved bridge unit can be seen by comparing the response of Bridges 1 and 2. Bridge 1 has a diaphragm spacing of 10.46 feet and Bridge 2 has a diaphragm spacing of 20.92 feet.

4.3.2.1 Dead Load. The longitudinal bending stresses in Bridges 1 and 2 due to dead load are given in Table 4.4a for all four girders. The V-load analysis overestimates both the positive and negative bending stresses in all the girders. The difference between the V-load and finite element values is a maximum of 14.9% for Bridge 2 and 14.2% for Bridge 1. The positive and negative bending stresses, computed in both analyses, are not affected by the diaphragm spacing, as was seen in the analysis of the simple span in Sec. 4.2.

The warping stresses in the bottom flange due to dead load are listed in Table 4.5a for girders 1 and 4. The magnitude of the warping stresses in the flange between the diaphragms increases with increasing diaphragm spacing. Also, as the diaphragm spacing increases, the difference between V-load and finite element warping stresses between the diaphragms slightly decreases.

Table 4.6a lists the warping plus bending dead load stresses in girders 1 and 4. As the diaphragm spacing of Bridge 1 is increased to 20.92 feet, the total stress computed by the V- load method increases slightly for girder 1 and decreases slightly for girder 4. The percent difference between the V- load and finite element stresses increase in Bridge 2, mainly near the end support where the boundary conditions are different in the two analyses.

The bending plus warping stresses due to dead load for Bridge 2 are shown in Fig. 4.20 for girders 1 and 4. The peak stresses that occur at the diaphragm locations are noticeable. The warping stresses have more effect on the total stress values for Bridge 2 than for Bridge 1 because an increase in diaphragm spacing produces larger warping stresses with little change in the longitudinal bending stresses.

4.3.2.2 Live Load. Tables 4.4b and 4.4c list the longitudinal bending stresses in girders 1 and 4 due to the outer and middle live load positions. As in the dead load bending comparison, the change in diaphragm spacing has little effect on the magnitude of the bending stress. As discussed previously, the difference between the V-load and finite element analysis results is large.

The warping stresses developed due to the live load, listed in Tables 4.5b and 4.5c, are affected by the diaphragm spacing. However, the difference between the V-load and finite element values are not very different in Bridge 1 than in Bridge 2. While the warping plus bending stresses computed by the V-load method change little with the change in diaphragm spacing, the difference between V-load and finite element stresses does change. For Bridge 2 the V-load stresses in girder 4 due to the outer placement are now

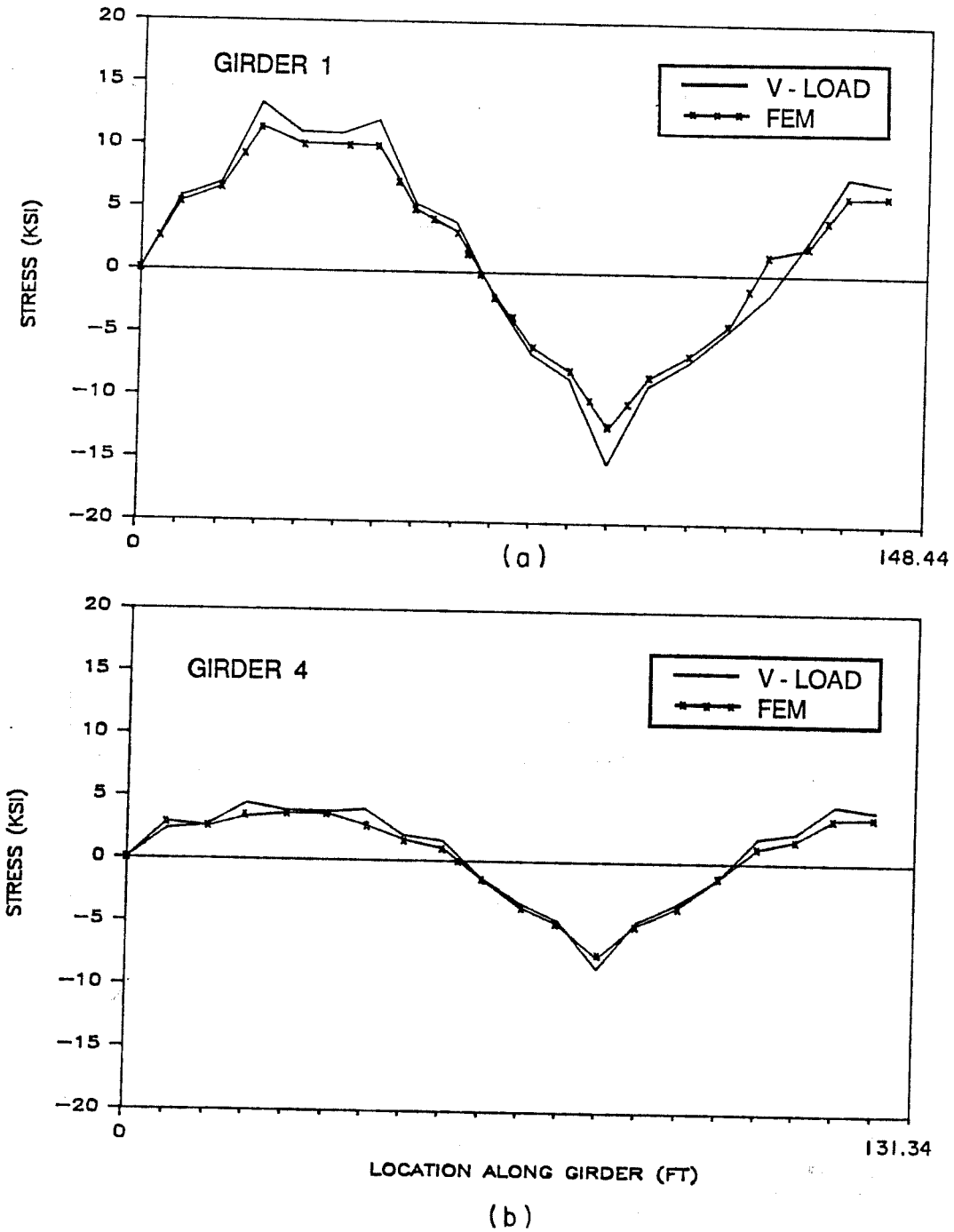

Figure 4.20 Longitudinal bending and warping stress in bottom flange of Bridge 2 - dead load: (a) Girder 1; (b) Girder 4.

conservative, although the magnitude of the stress is low. The correlation between the responses of the two methods is better for the outer live load position than for the middle live load position because of the difference in representing transverse distribution.

4.3.2.3 Dead Plus Live Load. The warping plus bending stresses for combined dead and live load for Bridge 2 are shown in Fig. 4.21. The V-load stresses for girder 1 are much larger for the outer load position than the middle load position but those for girder 4 do not vary much with the live load placement. Comparing Fig. 4.21 to Fig. 4.19, which shows the some stresses in Bridge 1, the effects of the larger diaphragm spacing in Bridge 2 are noticeable in the pronounced stress peaks. These peaks develop because of the larger warping stresses resulting from the larger diaphragm spacing, and the V-load assumption that diaphragms rigidly restrain lateral bending of the bottom flange.

4.3.3 Effect of Support Orientation. The effect of the orientation of the supports is investigated by comparing the results from the V-load and finite element analyses of Bridges 1 and 4. Bridge 1, as shown in Fig. 4.9 has four radial supports. Bridge 4 is the same as Bridge 1, but the two interior supports are skewed, one at 30O and the other at -4O with respect to the radial line (See Fig. 4.11). The girder lengths in Bridge 4 are slightly different four girders because of the change in support locations. The finite element model was changed at the first interior support in Bridge 4 by the removal of an adjacent diaphragm to allow for proper modeling of the bridge unit at that point.

4.3.3.1 Dead Load. Table 4.4a lists the longitudinal bending stresses due to dead load for the four girders. The positive bending stress in the first span of girder 1 increases with the introduction of the skew support because of the longer span length. The positive bending stresses in girders 1 and 2 and the negative bending stresses in girders 3 and 4 (skew) are not predicted as well using the V-load method in Bridge 4 as in Bridge 1 (no skew). Figure 4.22 shows the longitudinal bending stress due to dead load for girders 1 and 4 of Bridge 4. Comparing this with Fig. 4.13, the differences between the V-load and finite element results are largest in girder 1 for Bridge 4 and in girder 4 for Bridge 1.

The warping stresses in girders 1 and 4 due to dead load are listed in Table 4.5a. For Bridge 4 the warping stresses show a different sign at 0.288L compared to the same location in Bridge 1 because of the skewed support. The difference in warping stress from the two analysis is about 60.4% for Bridge 4 compared to 36.5% for Bridge 1. Combining the warping and bending stresses results in the stresses listed in Table 4.6a for dead load. The total stress in the positive region of girder 1 has increased in Bridge 4 while that in the negative region has decreased. For girder 4 the effects are the opposite. The difference between the V-load and finite element stresses is larger for the bridge with the skewed supports than the bridge with the radial supports.

Figure 4.23 shows the bending plus warping stresses due to dead load for girder 1 and girder 4 of Bridge 4. The change in span lengths, which corresponds to a change in bending moments and stresses, can be seen by comparison of Fig. 4.23 and Fig. 4.15. The

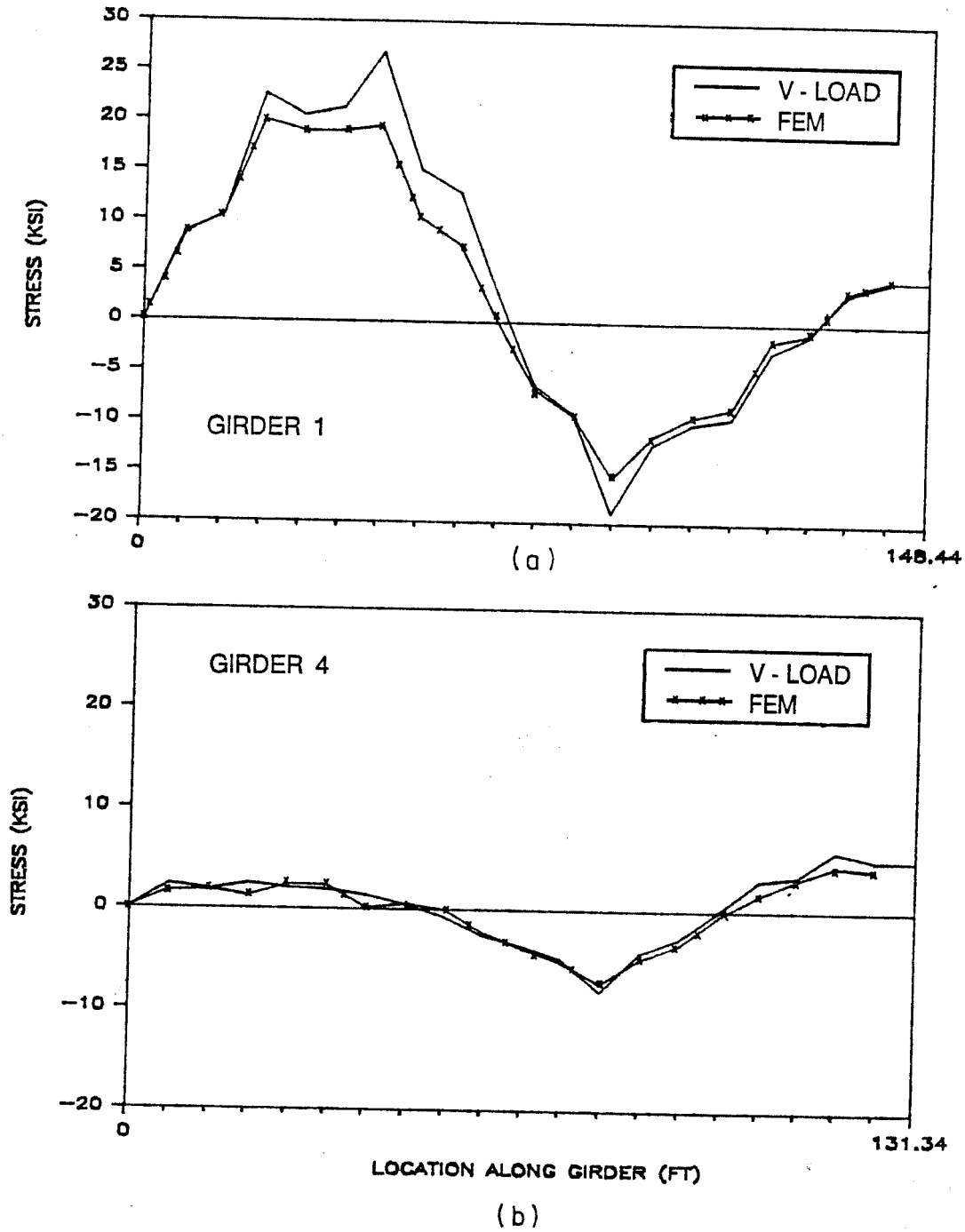

Figure 4.21 Longitudinal bending and warping stress in bottom flange of Bridge 2 - dead plus outer live load: (a) Girder 1; (b) Girder 4.

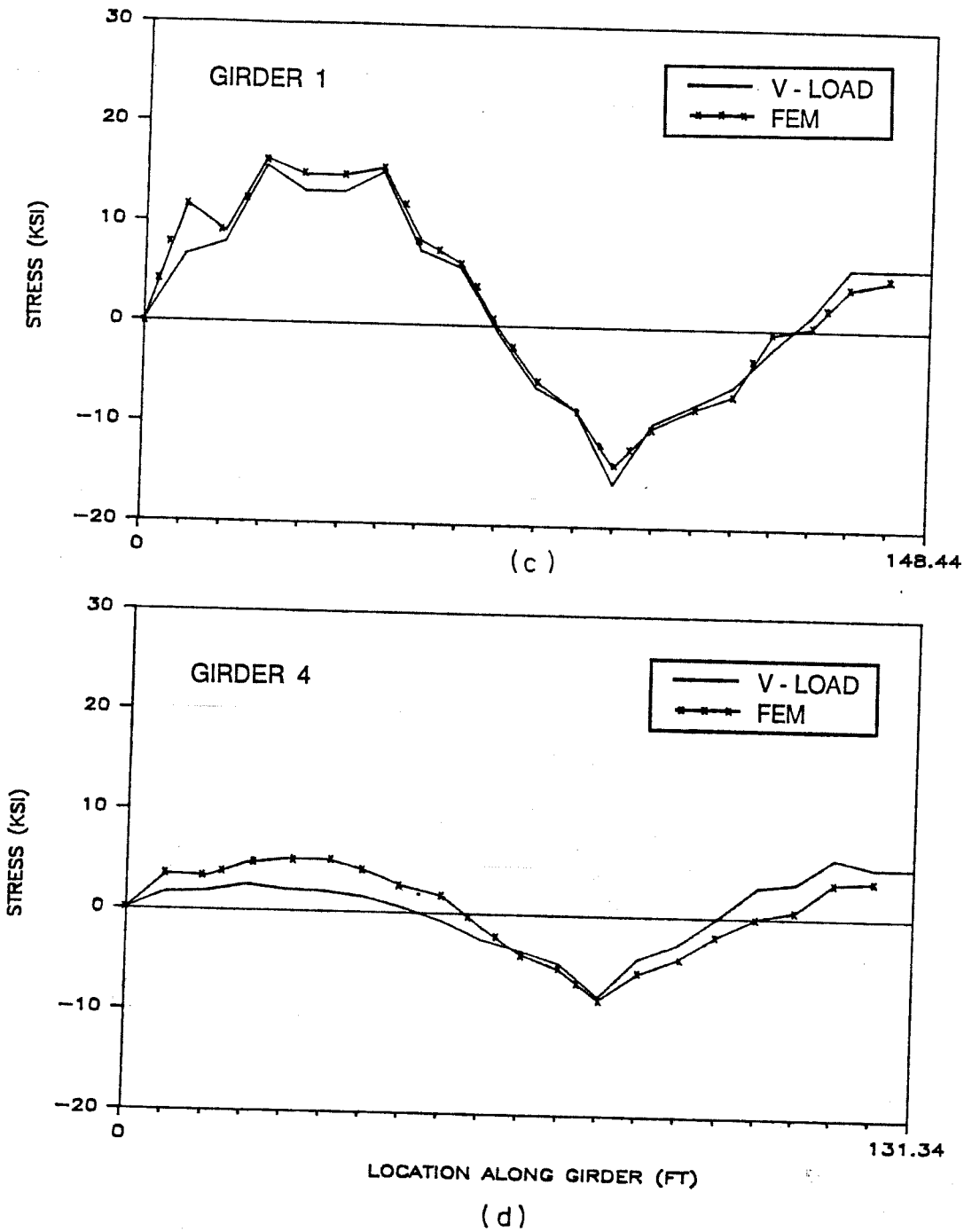

Figure 4.21 Longitudinal bending and warping stress in bottom flange of Bridge 2 - dead plus middle live load: (c) Girder 1; (d) Girder 4.

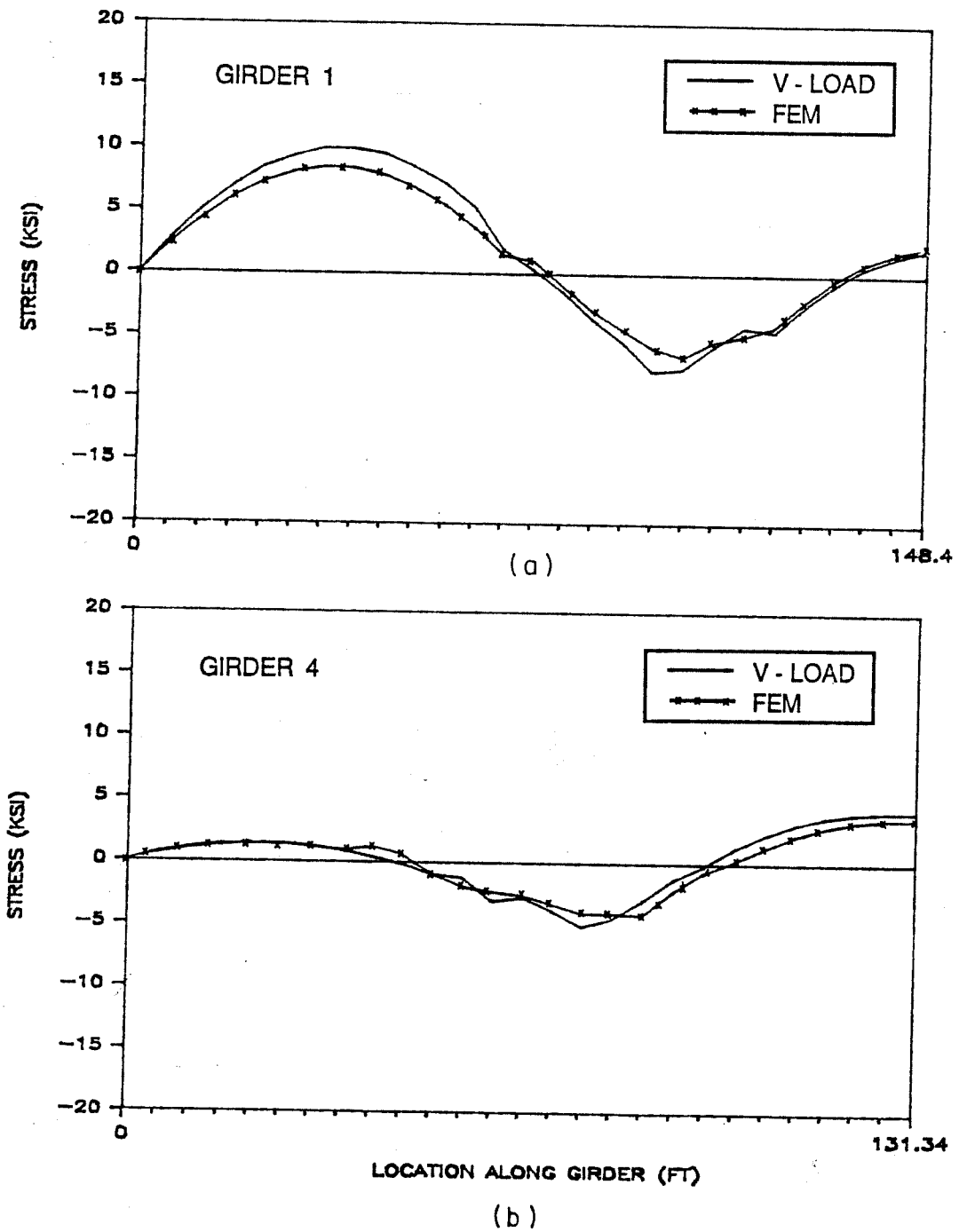

Figure 4.22 Longitudinal bending stress in bottom flange of Bridge 4 - dead load: (a) Girder 1; (b) Girder 4.

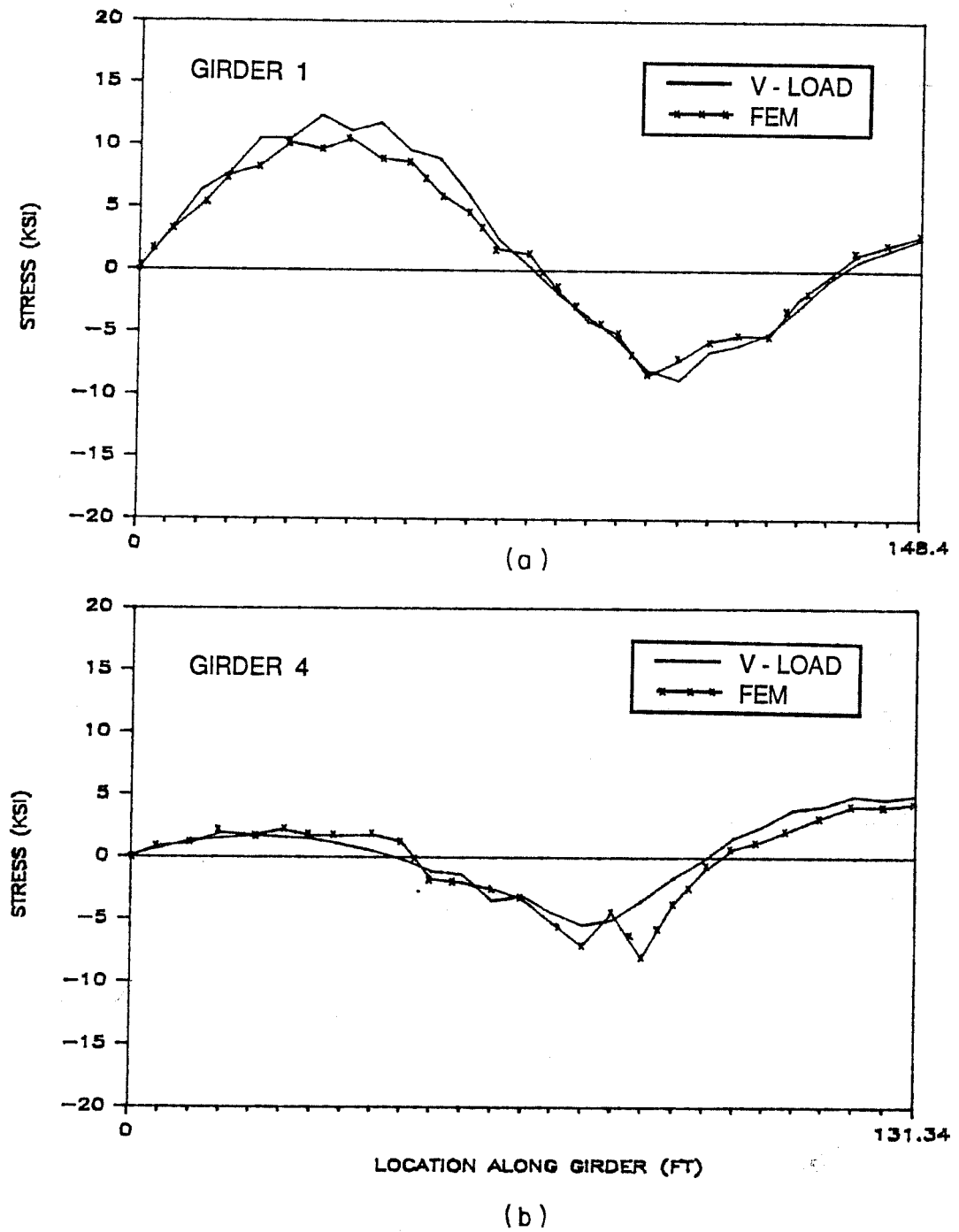

Figure 4.23 Longitudinal bending and warping stress in bottom flange of Bridge 4 - dead load: (a) Girder 1; (b) Girder 4.

removal of the diaphragm near the first interior support is evident by the peak in the finite element stress at that location for girder 4 (Fig. 4.23b).

4.3.3.2 Live Load. The bending stresses for girders 1 and 4 due to live load of the outer and middle positions are listed in Tables 4.4b and 4.4c. The skew affects the live load stresses near the interior supports of girder 1 for the outer live load placement. The percent difference between V-load and finite element responses also increases near the skew support. Because the diaphragm spacing is not altered in Bridge 4, except at the first interior support, the live load warping stresses are not affected except around that point. As with the previous comparisons, the outer live load placement results in better correlation between the V-load and the finite element results than does the middle live load position.

4.3.3.3 Dead Plus Live Load. Figure 4.24 shows the warping plus bending stresses in Bridge 4 due to combined dead and outer placement of live load. The results are very similar to those shown in Fig. 4.23 for warping plus bending stresses due to dead load. The longer span lengths produce larger positive stresses in the first span of girder 1 for Bridge 4 compared to the stresses of Bridge 1 in Fig. 4.19. The stresses in girder 4 show a complicated variation near the interior support, because of the skew.

4.3.4 Summary. The responses of the four curved girder bridge units show the effect of varying important parameters. As the radius of curvature decreases, the shift of load from the inner girders to the outermost girder increases. The diaphragm spacing does not affect the bending stresses, but it does affect the warping stresses. The larger the distance between diaphragms the greater the warping stresses at the diaphragm locations. Decreasing the diaphragm spacing decreases the magnitudes of the warping stresses and also decreases their influence on the warping plus bending stress values.

Skew supports affect the bending stresses responses because the span lengths are changed. As long as the diaphragm spacing does not change, the effect of skew supports on warping stresses is small.

The response of the unit to live load is particularly dependent on the distribution of load by the slab to the girders. The torsional stiffness of the slab is important in distributing the load. The V-load analysis makes no assumption on this torsional stiffness and does not include it in the approximate analysis, except through user defined transverse distribution factors.

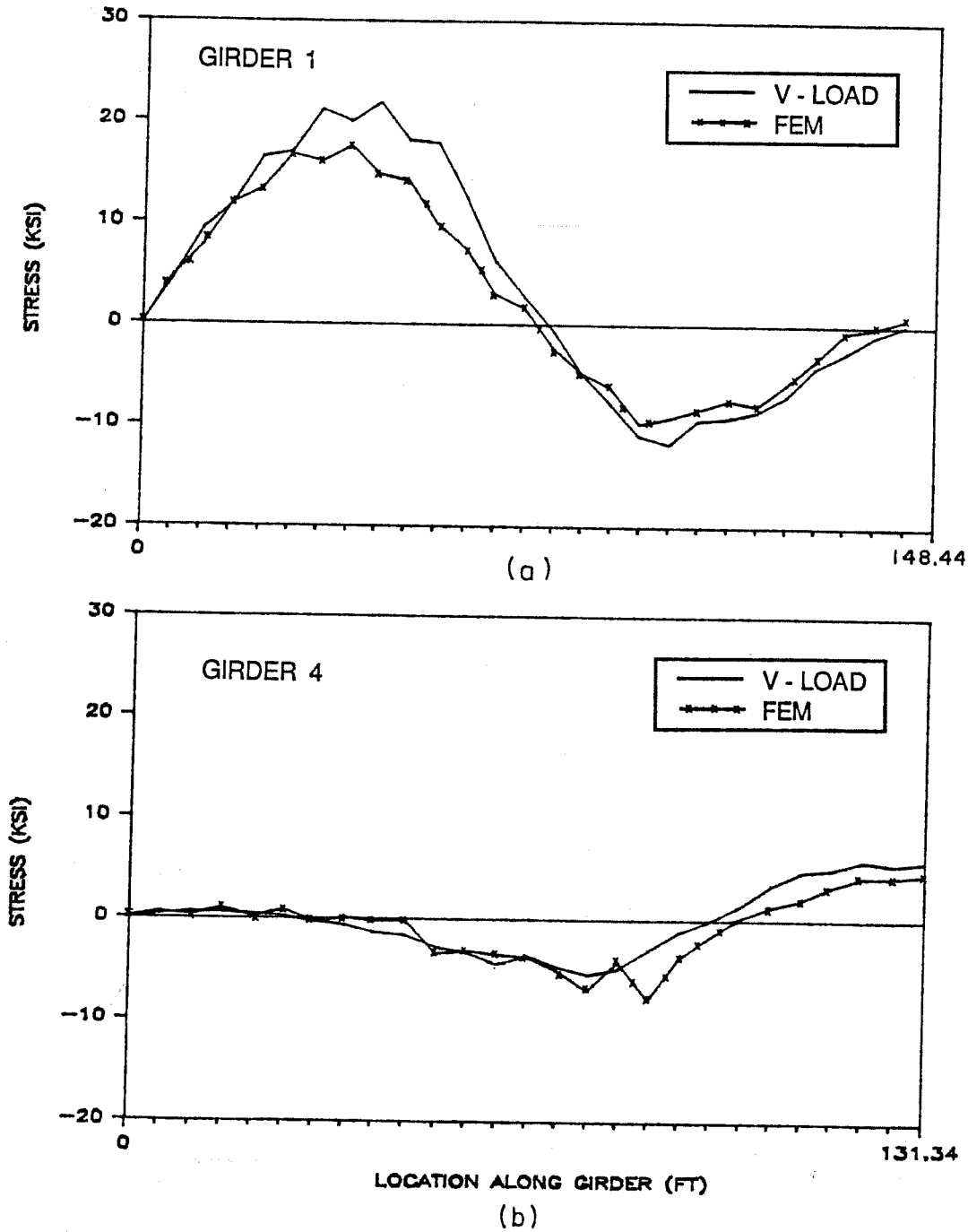

Figure 4.24 Longitudinal bending and warping stress in bottom flange of Bridge 4 - dead plus outer live load: (a) Girder 1; (b) Girder 4.

CHAPTER 5

RESPONSE ENVELOPES FOR MULTIGIRDER BRIDGE UNITS

5.1 Introduction

In design of multigirder bridges, the minimum and maximum responses due to a truck load moving over the bridge are needed to proportion the members. Envelopes for bending moment, shear force and reactions, as computed by the V-load method described in Chapter 3, are presented in this chapter for two curved bridge units.

To compute the live load responses, lateral distribution factors must be selected. The AASHTO straight girder live load distribution factors are used to compute the P-load, response of the girders to track loads [1]. The AASHTO factors are defined as the fraction of wheel load carried by each girder and are based on attaining maximum moment in each girder [15].

To compute the V-loads needed for the live load responses, a separate lateral distribution factor is required. Using the AASHTO live load lateral distribution factors for the V-load computation would result in too much load on the girders [15]. The V-loads depend on the summation of moments in the girders at a diaphragm location, not on the lateral placement of the load, and are maximum when all lanes are loaded. Because the V-loads act concurrently on the girders for a given live load position, the sum of the V-load distribution factors acting at a section should equal the number of wheel loads acting in the section [15]. Let NW be the number of wheel loads on a section, and NL the number of lanes loaded. For two wheel loads per lane, NL is equal to NW / 2. Consequently, the wheel load lateral distribution factor for NG girders, as computed in Reference 15, is::

$$DF = 2 * NL / NG$$

On the inner girder, the P-load and V-load moments are usually opposite in sign. As shown in the comparisons of Chapter 4, the total response of the interior girder due to live load is usually less than obtained from a finite element analysis. To correct this deficiency, it may be desirable to decrease the V-load applied to the inner girder. Reference 16 suggests that for the inner girder, NL in the above equation equal the number of loaded lanes applied to the inner girder. To compute the DF for the remaining girders NL would be the number of lanes of the bridge which are loaded.

5.2 Envelope Computation

The envelopes of bending moment and shear force for Bridges 1 and 4 from Sec. 4.3 are presented here. The live load is one AASHTO HS20-44 truck with constant axle spacing of 14 feet. For the bridge under consideration, the AASHTO wheel load distribution factors are 1.257 for the exterior girders 1 and 4, and 1.333 for the interior girders [1]. These distribution factors are applied to the truck wheel loads, P-loads, at each position to compute the P-load responses.

The V-load distribution factor is computed using the expression given in the previous section. One lane is loaded and there are four girders, so the V-load distribution factor is 0.5 for all girders. To compute the V-loads on a specific girder, the live load moments are summed about the diaphragms as described in Chapter 3. Because these moments are computed using the factored AASHTO live loads, the moments need to be multiplied by the ratio of the V-load distribution factor to the AASHTO factor. This multiplication adjusts the V-loads to have the distribution factor computed above. The ratio of the V-load distribution factor and AASHTO factor used in computing the live load V-loads are:

Girder 1 and 4 : .5 / 1.257 = .3978

Girder 2 and 3 : .5 / 1.333 = .3751

In this analysis the V-load distribution factor for the interior girder is not modified. As the truck moves across the bridge, from left to right, the moment and shear forces are computed at grid points along the girders, as described in Section 3.3. The minimum and maximum responses at each grid point are found by comparing responses due to each live load position.

Figures 5.1 through 5.4 show the minimum and maximum bending moments and shear forces for dead plus truck load for the girders in Bridge 1. The envelope curves have the same shape, but because of the V-loads the magnitude of the response decreases from girder 1 to girder 4. Figures 5.5 through 5.8 show the envelopes for the girders in Bridge 4, which has skew supports. Because of the skew supports the girders are not symmetric about the bridge centerline. The length of the first span in girders 1, 2, and 3, is slightly longer due to the support line being rotated clockwise from the radial position.

Table 5.1 lists the bending moments and shear forces at three locations of the girders of Bridges 1 and 4. By introducing a skew of 30 degrees, the length of the first span of girder 1 increases by approximately 8.5 feet. As expected the moment at 0.13L of girder 1 increases, by 23%, while the moment at the first interior support decreases, by 2.1% compared to the corresponding values of Bridge 1. The location 0.13L is near midpoint of span one. For girder 4 the moment in span one decreases by 23.1% and the moment at the support increases by 5.4% due to the shortening of span one. The presence of a skew support has no other noticeable effect on the response envelopes.

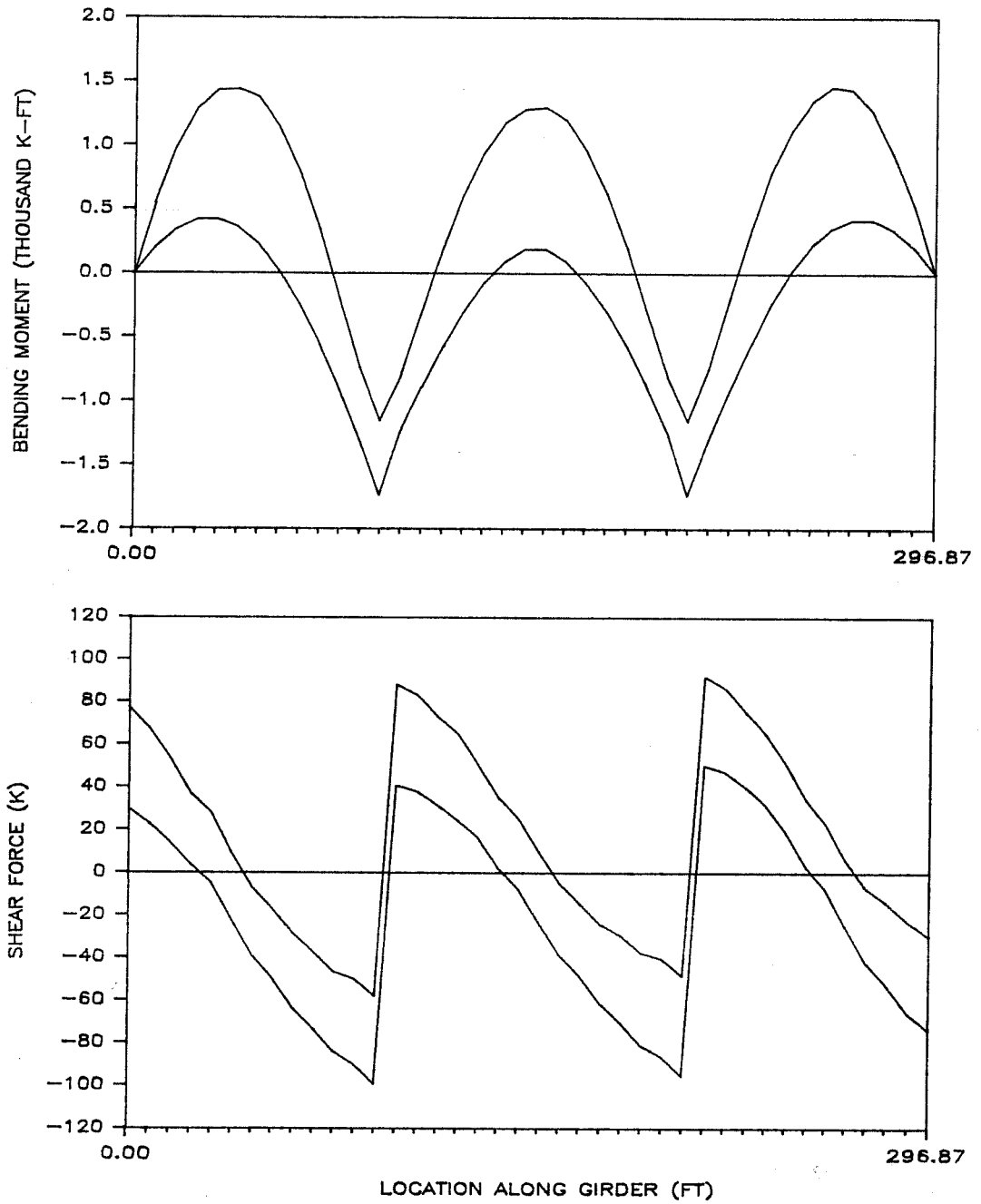

Figure 5.1 Bending moment and shear force envelopes of Bridge 1, Girder 1.

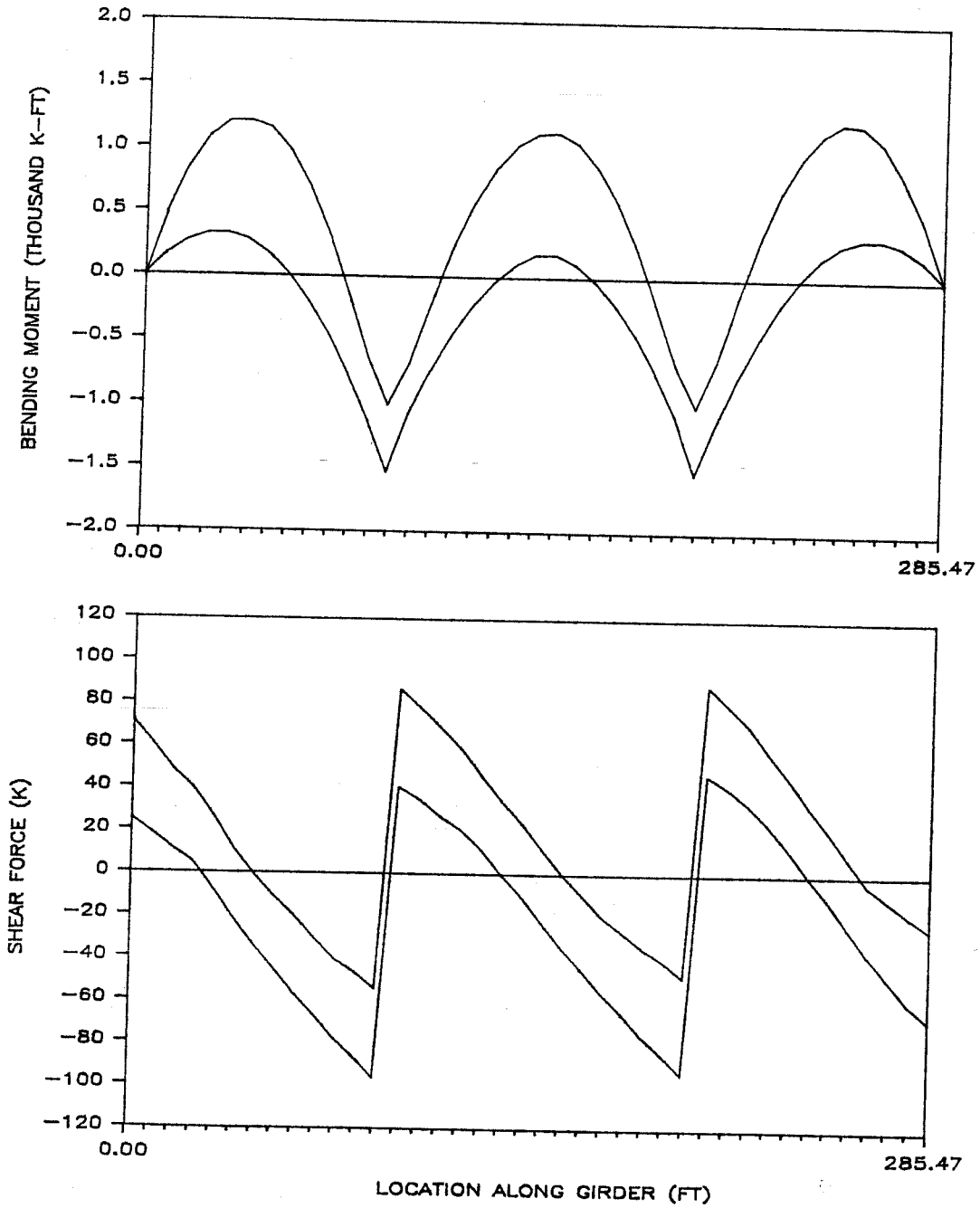

Figure 5.2 Bending moment and shear force envelopes of Bridge 1, Girder 2.

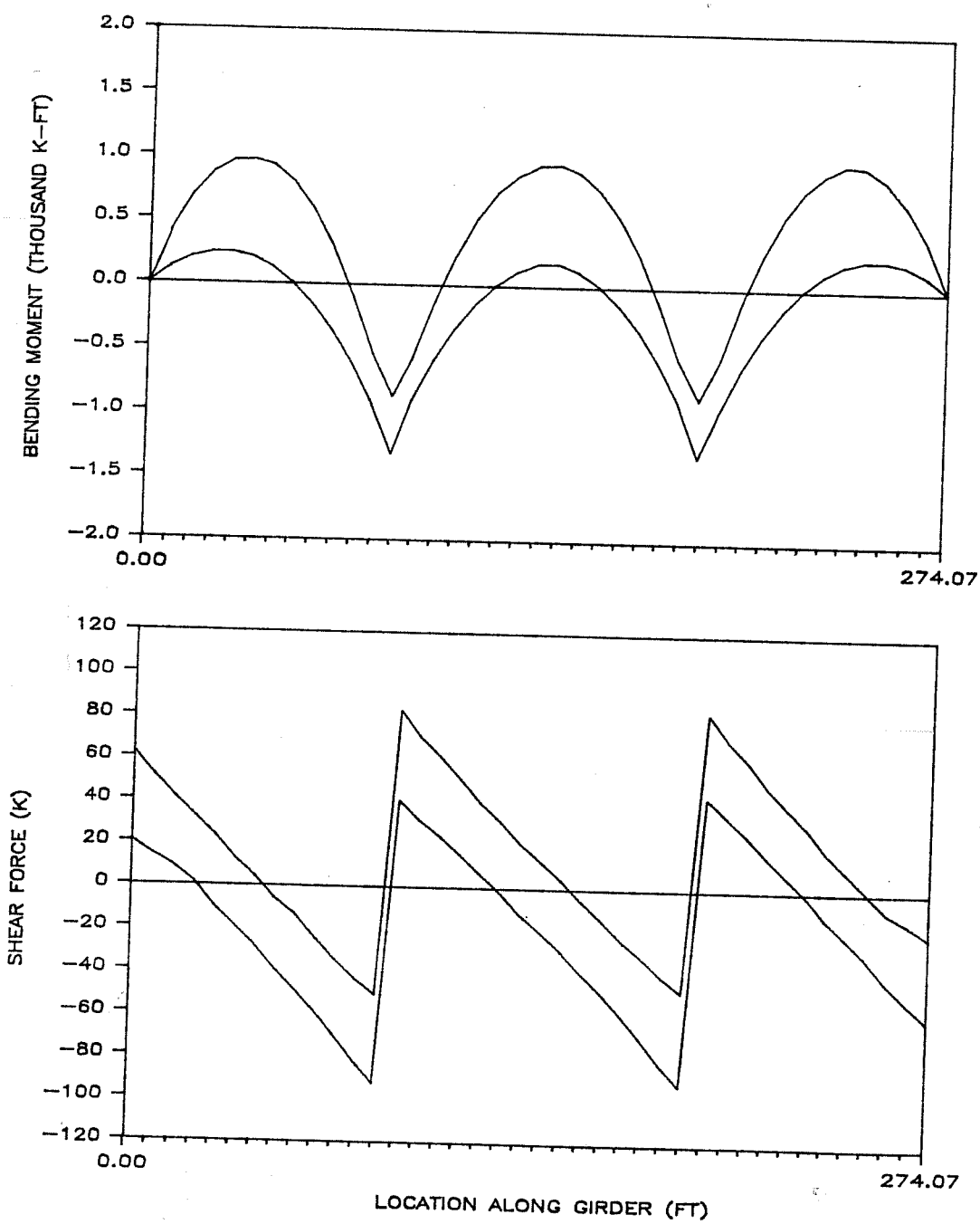

Figure 5.3 Bending moment and shear force envelopes of Bridge 1, Girder 3.

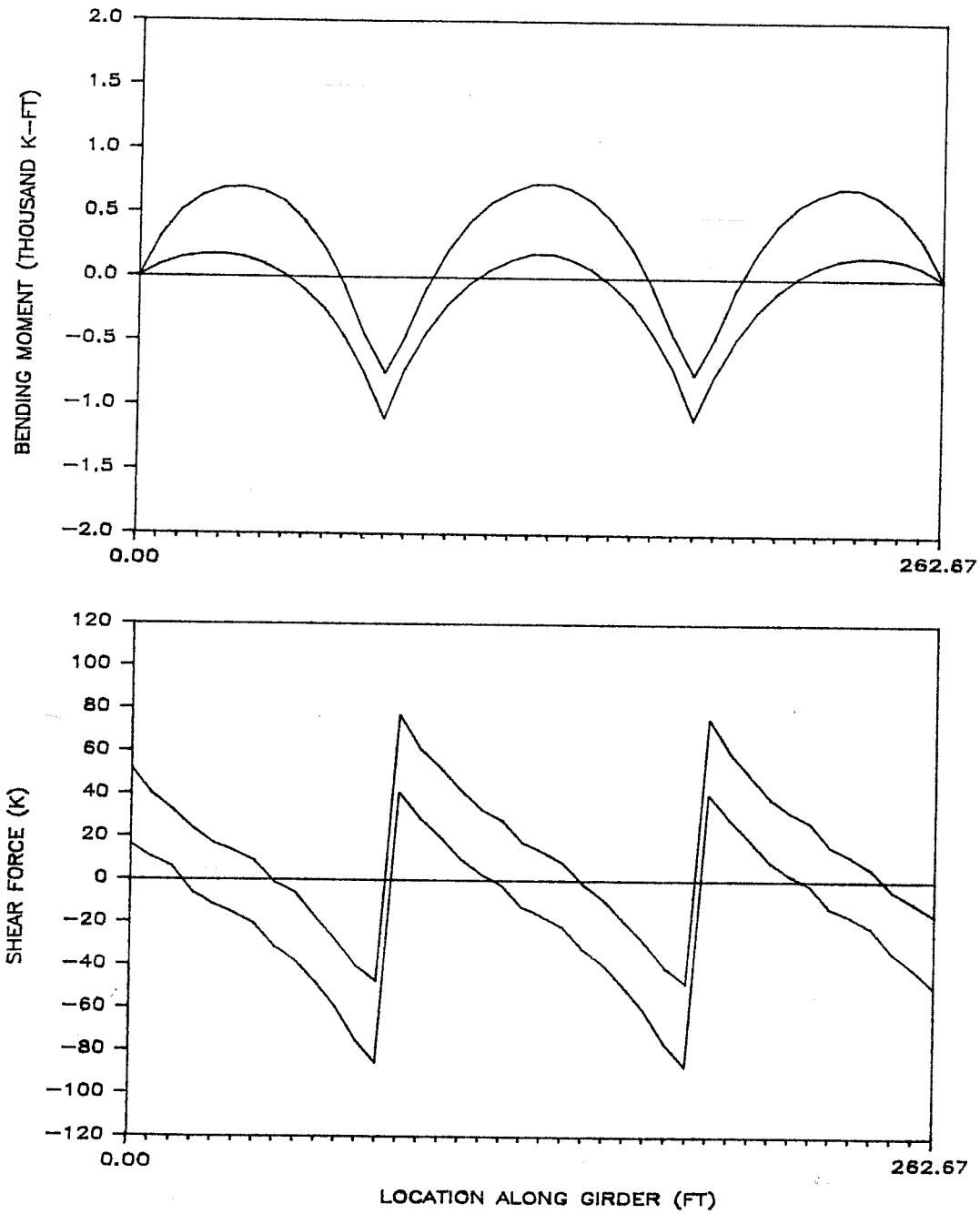

Figure 5.4 Bending moment and shear force envelopes of Bridge 1, Girder 4.

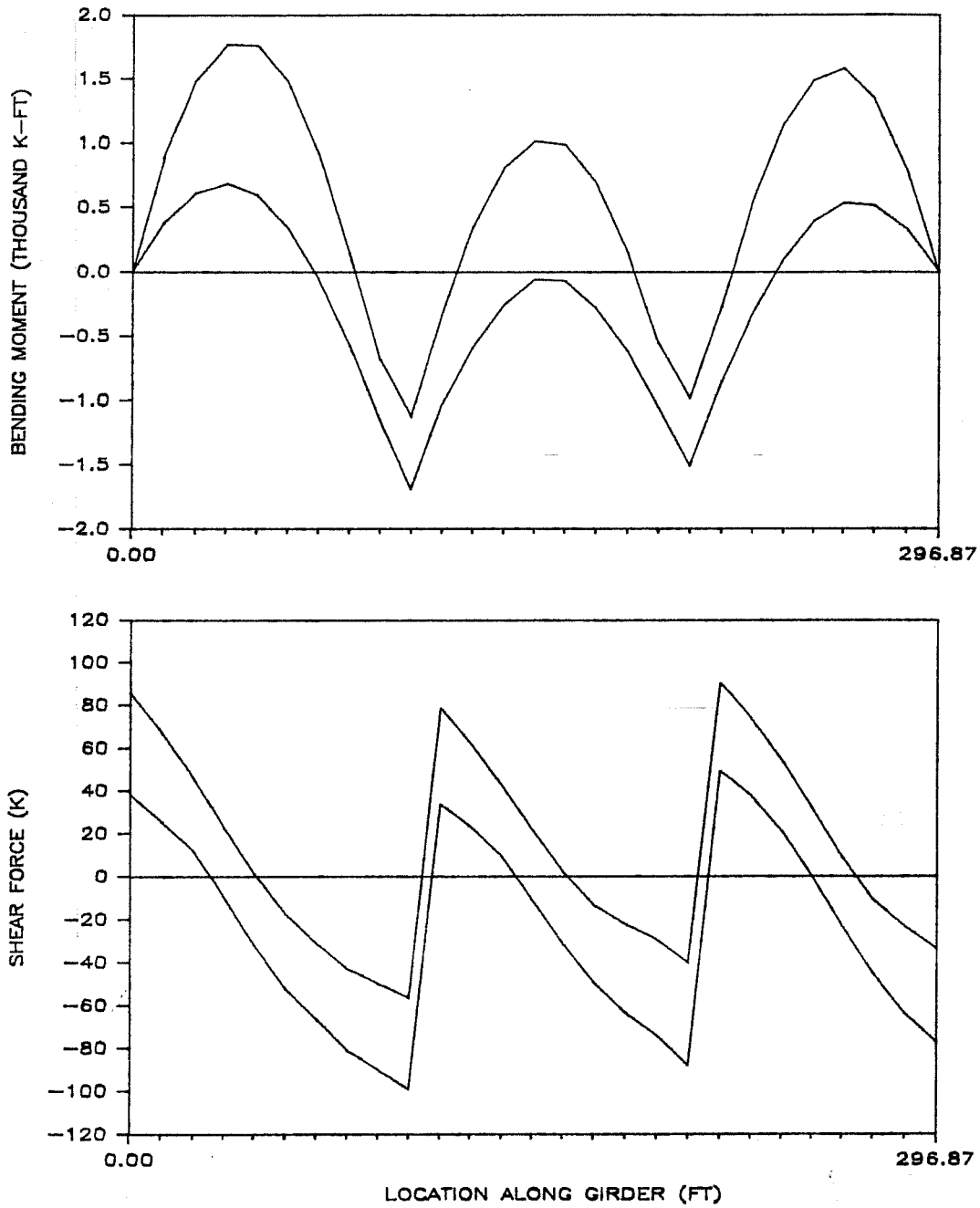

Figure 5.5 Bending moment and shear force envelopes of Bridge 4, Girder 1.

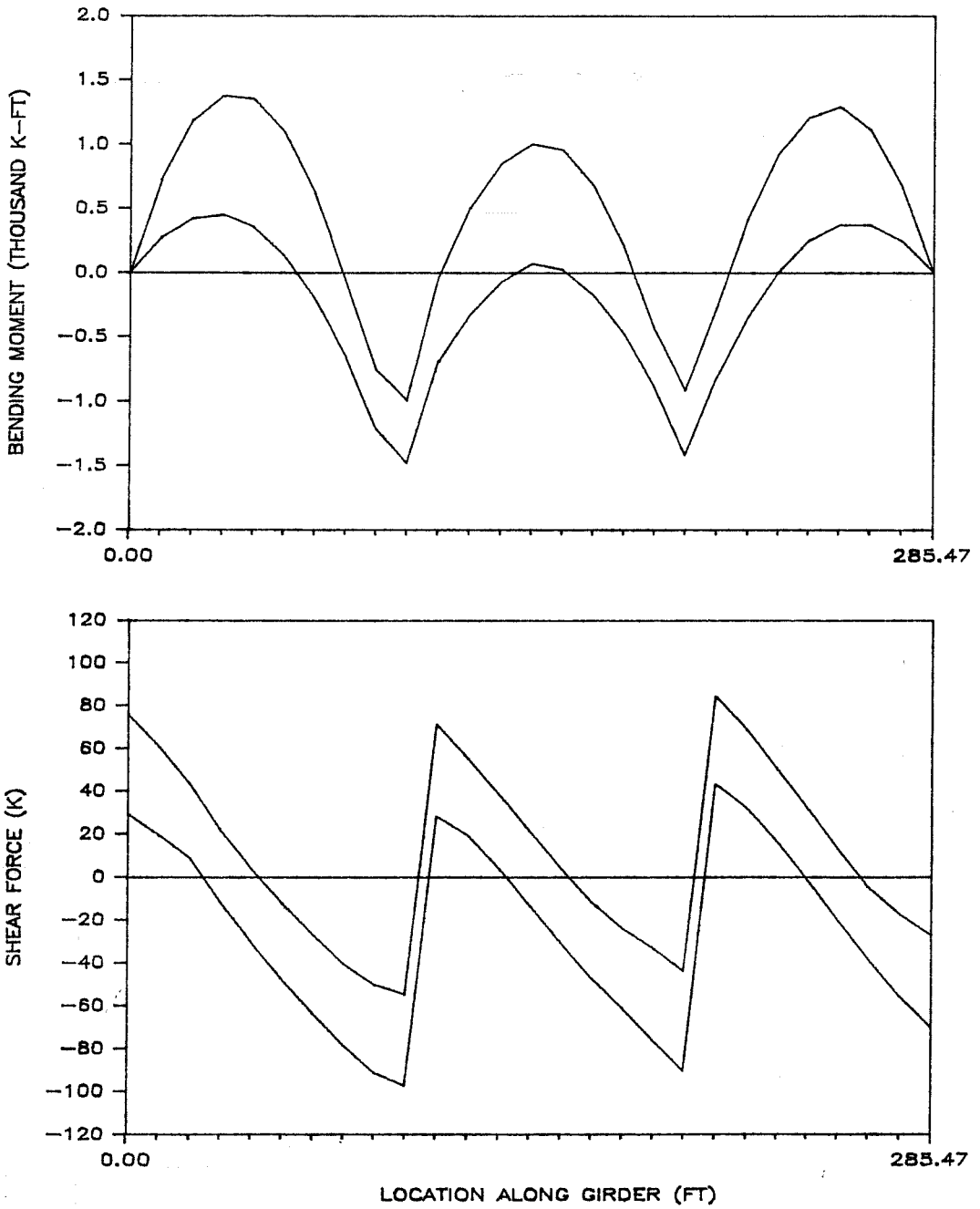

Figure 5.6 Bending moment and shear force envelopes of Bridge 4, Girder 2.

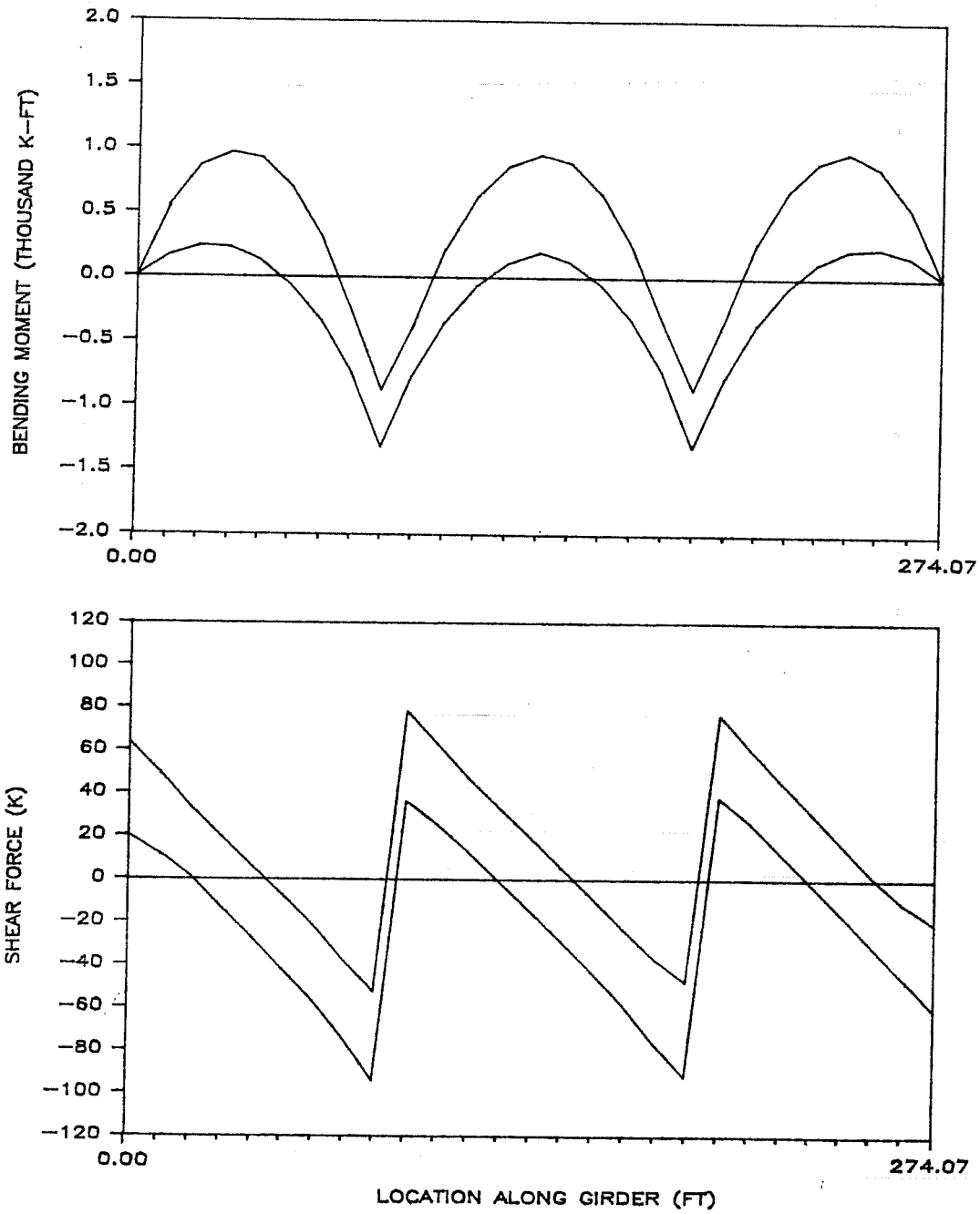

Figure 5.7 Bending moment and shear force envelopes of Bridge 4, Girder 3.

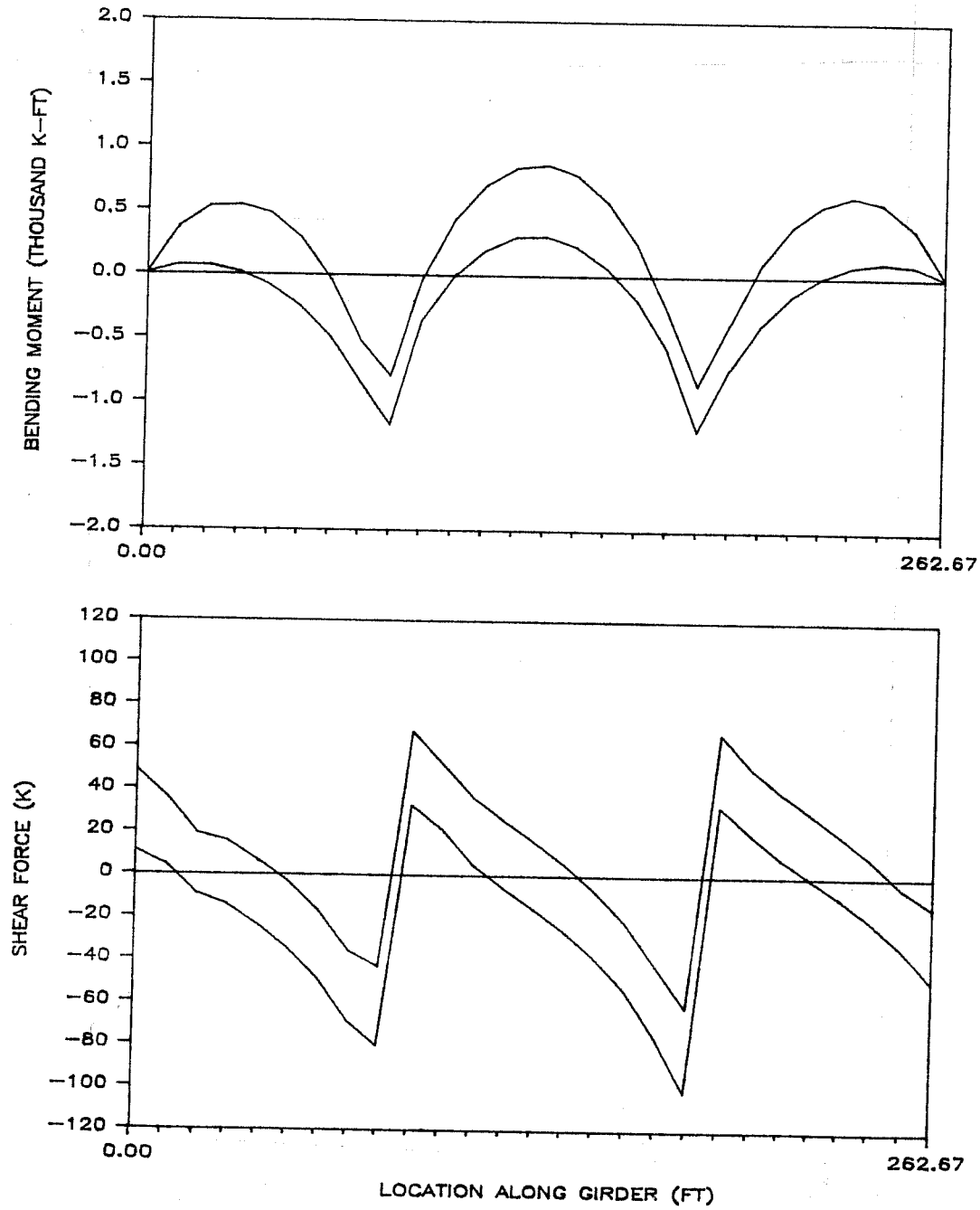

Figure 5.8 Bending moment and shear force envelopes of Bridge 4, Girder 4.

Table 5.1 Response Envelopes

Bridge	Skew	Location*	Girder 1		Girder 2		Girder 3		Girder 4	
			Minimum	Maximum	Minimum	Maximum	Minimum	Maximum	Minimum	Maximum
a) Moment (k-ft)										
1	NO	.13 L	357.4	1439.4	275.7	1211.2	204.3	969.4	150.0	700.1
		SUP. 2	-1734.6	-1154.9	-1534.7	-1009.2	-1326.2	-874.5	-1107.1	-753.5
		.5 L	192.0	1291.7	185.1	1133.5	182.0	951.7	189.1	734.5
4	YES	.13 L	667.5	1769.5	418.7	1374.1	197.4	967.5	-25.4	538.4
		SUP. 2	-1697.7	-1130.9	-1482.3	-995.2	-1322.3	-875.4	-1177.4	-794.5
		.5 L	-56.3	1017.8	72.1	1003.1	201.1	960.5	311.1	872.3
b) Shear (k)										
1	NO	.13 L	-22.4	8.8	-21.2	11.2	-19.1	12.6	-16.1	13.0
		SUP. 2	-99.3	-58.1	-96.5	-54.5	-92.4	-51.0	-86.0	-47.6
		.5 L	-15.7	17.3	-16.3	17.6	-16.0	17.0	-14.8	15.2
4	YES	.13 L	-15.4	17.1	-18.2	16.4	-19.8	13.7	-20.4	10.7
		SUP. 2	-99.3	-56.8	-97.6	-55.0	-94.2	-52.7	-80.4	-43.2
		.5 L	-11.3	21.7	-13.4	21.0	-14.9	19.0	-15.6	15.7

* Location from first support, where L is girder length.

Table 5.2 lists the minimum and maximum reactions resulting from a truck load moving across Bridges 1 and 4. For Bridge 1 the interior supports have the same minimum and maximum reactions. The interior support reactions for Bridge 4 are not identical, reflecting the unsymmetric configuration of Bridge 4. The orientation of the supports in the two bridge configurations do not greatly affect the reactions of the girders in the units.

Table 5.2 Envelopes of Reactions (k))

Bridge	Skew	Support	Girder 1		Girder 2		Girder 3		Girder 4	
			Minimum	Maximum	Minimum	Maximum	Minimum	Maximum	Minimum	Maximum
1	NO	1	30.0	78.8	25.3	73.2	20.7	65.3	16.5	55.0
		2	97.0	147.1	99.6	151.9	102.3	154.0	105.4	153.4
		3	97.0	147.1	99.6	151.9	102.3	154.0	105.4	153.4
		4	80.0	74.5	25.3	68.9	20.8	61.2	16.6	51.3
4	YES	1	38.5	86.5	29.	77.1	20.6	65.1	11.4	50.5
		2	97.8	148.7	99.6	152.2	101.5	153.1	103.5	151.3
		3	89.6	141.0	98.3	151.4	101.8	153.4	109.1	156.2
		4	33.9	77.1	27.3	69.5	20.6	59.8	14.1	47.6

CHAPTER 6

SUMMARY AND CONCLUSIONS

6.1 Summary

An approximate analysis of horizontally curved bridge units has been presented using equivalent straight girder analysis. Each girder is straightened and modeled as individual beam elements with constant properties. The individual girders are then analyzed using the direct stiffness method for the applied dead and live loads on the bridge, which are called P-loads.

The effects of the horizontal curvature of the unit are represented by a self-equilibrating vertical forces, V-loads, acting on the girders at diaphragm locations. The V-loads are derived from the summation of P-load moments in the girders at the diaphragm locations and geometrical properties of the bridge. The individual girders are then analyzed a second time for the V-loads. The response of the girders is the sum of the P-load and V-load responses at locations along each girder. The responses computed are the bending moments, shear forces, reactions, and bending and warping stresses.

Envelopes of the girder response due to a moving truck load along the bridge are computed using influence functions. The influence functions used in this analysis are the moments and shears in each element of the girders due to a unit load at every degree of freedom. The influence functions are multiplied by the applied truck loads to obtain the responses of the girders. This procedure is efficient because it eliminates the large number of substitutions of the equilibrium equations and force determinations for numerous positions of the loads.

Warping moments develop in the girders due to the horizontal curvature. The lateral bending of the bottom flanges is assumed to be proportional to the longitudinal bending moment on the girder. Loads are applied to the bottom flange of the girders which are straightened and modeled as individual beam elements with constant properties. The warping moments are converted to warping stresses using the section modulus for lateral bending of the flange. The warping stresses are combined with the longitudinal bending stresses to obtain the maximum stresses in the tip of the bottom flange.

The analysis techniques described were used to study the responses of two bridge systems, a two girder simple span unit and a four girder, three span unit. To evaluate the accuracy of the approximate method, the responses were compared with those from a finite element analysis of the bridges. Correlation between the V-load response and the finite element responses were made for the different bridge configurations for both dead and live loadings. Envelopes of minimum and maximum bending moment and shear force due to a truck load moving along the bridge were computed. The importance of certain bridge parameters; radius of curvature, diaphragm spacing, and support orientation, were also studied.

6.2 Conclusions

Shifting of load from the inner to outer girder is an important characteristic of horizontally curved bridges. The bending stress due to dead load computed in the V-load analysis for the two girder, simple span unit was found to be conservative for the outer girder but unconservative for the inner girder, compared to finite element results. For the four girder, three span unit the V-load responses are conservative for all girders compared to finite element responses. In general, the assumptions in the V-load method are valid for noncomposite girder systems, and lead to dead load responses of sufficient accuracy for design.

The difference between V-load and finite element responses are much greater for live load than for dead load. The torsional stiffness of the slab affects the distribution of live loads and the resulting live load stresses. The V-load method does not represent the torsional stiffness of the slab in distributing the forces due to the curvature. Consequently, the V-load method overestimates the shifting of load from the inner to outer girders. The actual distribution of primary and torsional loads to the girders and is only represented accurately in the finite element model of the unit. In a design application, the responses obtained from the V-load method for live load are only as good as the lateral distribution factors assumed in the V-load method. When the responses due to dead plus live load are computed the correlation between V-load and finite element responses is better than the live load only case because of the importance of dead load stresses in the units studied here.

The analysis conducted in this study showed the important characteristics in the response of curved girder bridge units. A decreasing radius of curvature of the bridge unit increases the longitudinal bending stress in the outer girder and decreases the bending stress in the innermost girder. The diaphragm spacing does not effect the longitudinal bending stress but does effect the warping stresses at the diaphragm locations. The larger the diaphragm spacing the larger are the warping stresses computed at the diaphragms. The presence of a skew support effects the bending moments and stresses by changing the span lengths of the girders. The error in the V-load method is greater for skew supports than radial supports, especially for live load.

In summary, the V-load method, as implemented in the analysis procedure described in this report, is suitable for preliminary design of curved girder bridge units. However, it is important that bridge engineers understand the limitations of the V-load method. The important limitations are: (1) the response is very dependent on transverse distribution factors; (2) the stresses in the inner girder tend to be underestimated; and (3) the effects of bracing in the plane of the bottom flanges is not included. Finally, the warping stresses in the bottom flange are subject to considerable error, particularly for widely spaced diaphragms. Given the limitations of the V-load method, it is recommended that a finite element analysis of the final design be performed and reviewed to assess the adequacy of the bridge.

REFERENCES

1. American Association of State Highway and Transportation Officials (AASHTO), Standard Specifications for Highway Bridges, AASHTO, Washington, D.C., Thirteenth Edition, 1983.

2. American Association of State Highway and Transportation Officials (AASHTO), Guide Specifications for Horizontally Curved Highway Bridges, AASHTO, Washington, D.C., 1980.

3. Culver, C., Brogan, D., and Bednar, D., " Analysis of Curved Girder Bridges," Engineering Journal, AISC, Vol. 7, No. 1, January 1970, p.10-15.

4. "Curved I-Girder Bridge Design Recommendations," Journal of the Structural Division, ASCE, Vol.10, No. 103, May 1977.

5. Gillespie, J.W., "Analysis of Horizontally Curved Bridges," Engineering Journal, AISC, Vol. 5, No. 4, October 1968, p.137-143.

6. Grubb, M.A., "Horizontally Curved I-Girder Bridge Analysis: V-Load Method," Transportation Research Record 982, p.26-36.

7. Hahn, K.H., Computer Program for the Analysis of Curved Girder Bridges, Thesis, Department of Civil Engineering, University of Texas at Austin, May 1987.

8. Heins, C.P., and Jin, J.O., "Live Load Distribution on Braced Curved I-Girders," Journal of the Stuctural Division, ASCE, Vol. 110, No. 3, March 1984, p.523-530.

9. Heins, C.P., and Siminou, J., "Preliminary Design of Curved Bridges," Engineering Journal, AISC, April 1970, p.50-61.

10. Heins, C.P., and Spates, K.R., " Behavior of Single Horizontally Curved Girder," Journal of the Structural Division, ASCE, Vol. 96, No. ST7, July 1970, p. 1511-1524.

11. Ketchek, K., " Another Approach to Simplified Design of a Curved Steel Girder, " Engineering Journal, AISC, Vol. 6, No. 4, October 1969, p.116-123.

12. McManus, P.F., and Nasir, G.A., "Horizontally Curved Girders-State of the Art," Journal of the Structural Division, ASCE, Vol.95, No. ST5, May 1969, p. 853 - 870.

13. Poellot, W.N., "Computer-aided Design of Horizontally Curved Girders by the V-load Method," Engineering Journal, AISC, First Quarter 1987.

14. Richardson, Gordon, & Associates, Consulting Engineers, "Analysis and Design of Horizontally Curved Steel Bridge Girders," United States Steel Structural Report, ADUSS 88- 6003-01, 1963.

15. United States Steel Corporation "V-Load Analysis, " USS Highway Structures Design Handbook, ADUSS 88-8535-01, Vol. 1, Chapter 12, July 1984.

16. USS Engineers & Consultants, Inc., "V-Load User Manual," May 1985.

17. Weaver, W. and Gere, J.M., Matrix Analysis of Framed Structures, Van Nostrand Reinhold Company Inc., New York, 1980.

18. Weissman, H. A., "Straight-Element Grid Analysis of Horizontally Curved Beam Systems," Engineering Journal, AISC, April 1970, p.41-49.